

---

**CHANNEL FORMATION, BINDING AND TRANSLOCATION  
PROPERTIES OF ANTHRAX, CDT AND RELATED TOXINS OF THE  
AB<sub>7</sub> TYPE**

---



**Dissertation**

zur Erlangung des naturwissenschaftlichen Doktorgrades  
der Fakultät für Biologie  
an der Bayerischen Julius-Maximilians-Universität Würzburg

vorgelegt von

**Angelika Kronhardt**

aus Lehrte

Betreuer der Arbeit: Prof. Dr. Dr. h.c. mult. Roland Benz

---

Würzburg, 2012



Eingereicht am .....

Mitglieder der Promotionskommission: Vorsitzender: Prof. Dr. ....

1. Gutachter: Prof. Dr. Dr. h.c. mult. Roland Benz

2. Gutachter: Prof. Dr. Roy Gross

Tag des Promotionskolloquiums: .....

Doktorurkunde ausgehändigt am: .....



Diese Dissertation wurde von mir selbständig und nur mit den  
angegebenen Quellen und Hilfsmitteln angefertigt.

Die von mir vorgelegte Dissertation hat noch in keinem früheren  
Prüfungsverfahren in ähnlicher oder gleicher Form vorgelegen.

Ich habe zu keinem früheren Zeitpunkt versucht,  
einen akademischen Grad zu erwerben.

Würzburg, .....



*„Der Fortgang der wissenschaftlichen Entwicklung ist im  
Endeffekt eine ständige Flucht vor dem Staunen.“*

*Albert Einstein*





Michael Leuber , Angelika Kronhardt, Fiorella Tonello, Federica Dal Molin and Roland Benz (2008) **Binding of N-terminal fragments of Anthrax edema factor (EF<sub>N</sub>) and lethal factor (LF<sub>N</sub>) to the protective antigen pore.** Published in *Biochimica et Biophysica Acta*.

Angelika Kronhardt\*, Christoph Beitzinger\*, Kerstin Duscha, György Hajos and Roland Benz (2011) **Interaction of Chloroquine-like 4-Aminoquinolines with Anthrax toxin Protective Antigen (PA).** Manuscript in preparation.

Angelika Kronhardt\*, Monica Rolando\*, Christoph Beitzinger, Caroline Stefani, Michael Leuber, Gilles Flatau, Michel R. Popoff, Roland Benz and Emanuel Lemichez (2011) **Cross-Reactivity of Anthrax and C2 Toxin: Protective Antigen Promotes the Uptake of Botulinum C2I Toxin into Human Endothelial Cells.** Published in *PLoS ONE*.

Christoph Beitzinger\*, Monica Rolando\*, Angelika Kronhardt, Caroline Stefani, Gilles Flatau, Emanuel Lemichez and Roland Benz (2011) **Anthrax toxin protective antigen promotes uptake of N-terminal His<sub>6</sub>-tag labeled polypeptides into cells in a voltage-dependent way.** Submitted to *PLoS ONE*.

Christoph Beitzinger\*, Angelika Kronhardt\* and Roland Benz (2011) **Binding partners of protective antigen from *Bacillus anthracis* share certain common motives.** E-book chapter published in *Toxins and Ion transfers*.

Angelika Kronhardt, Michel R. Popoff and Roland Benz (2011) ***Clostridium difficile* CDT toxin forms two different types of pores.** Manuscript in preparation.

\* these authors contribute to the paper equally

**All publications and manuscripts included in this thesis were used in agreement with the respecting journal and all participating authors.**



<b>Publications</b> .....	9
<b>Contents</b> .....	11
Preface – <b>Summary</b> .....	17
<b>Zusammenfassung</b> .....	19
Chapter 1 – <b>INTRODUCTION</b> .....	23
1.1 Bacterial toxins.....	23
1.1.1 Endotoxins .....	23
1.1.2 Exotoxins.....	24
1.1.2.1 Pore-forming toxins (PFTs).....	26
1.1.2.2 $\alpha$ -pore-forming toxins ( $\alpha$ -PFTs).....	27
1.1.2.3 $\beta$ -pore-forming toxins ( $\beta$ -PFTs).....	27
1.1.2.4 Cholesterol-dependent toxins (CDCs) .....	27
1.2 Binary toxins .....	28
1.2.1 Intoxication pathway of binary toxins.....	28
1.2.2 <i>Bacillus anthracis</i> Anthrax toxin .....	28
1.2.2.1 Protective antigen (PA).....	29
1.2.2.2 Edema factor (EF) .....	31
1.2.2.3 Lethal factor .....	31
1.2.3 <i>Clostridium botulinum</i> C2 toxin.....	31
1.2.3.1 C2II.....	31
1.2.3.2 C2I .....	32
1.2.4 <i>Clostridium difficile</i> CDT toxin.....	32
1.2.4.1 CDTb .....	32
1.2.4.2 CDTa.....	33
1.3 Aim of this work.....	34
Chapter 2 - <b>BINDING OF N-TERMINAL FRAGMENTS OF ANTHRAX EDEMA FACTOR (EF<sub>N</sub>) AND LETHAL FACTOR (LF<sub>N</sub>) TO THE PROTECTIVE ANTIGEN</b> .....	37
2.1 Introduction .....	37

2.2 Materials and methods.....	39
2.2.1 Anthrax Protective Antigen PA <sub>63</sub> .....	39
2.2.2 Cloning, expression and purification of truncated Anthrax Edema Factor (EF <sub>N</sub> ) and Lethal Factor (LF <sub>N</sub> ) .....	39
2.2.3 Lipid bilayer experiments .....	39
2.2.4 Titration experiments with EF <sub>N</sub> and LF <sub>N</sub> .....	40
2.3 Results.....	42
2.3.1 Evaluation of the stability constant of the binding of EF <sub>N</sub> or LF <sub>N</sub> to the PA <sub>63</sub> channel .....	42
2.3.2 His <sub>6</sub> -EF <sub>N</sub> and His <sub>6</sub> -LF <sub>N</sub> have a higher affinity for the PA <sub>63</sub> channel .....	42
2.3.3 EF <sub>N</sub> and LF <sub>N</sub> block PA <sub>63</sub> channels in a single hit process.....	44
2.3.4 EF <sub>N</sub> and LF <sub>N</sub> binding to PA <sub>63</sub> is ionic-strength dependent.....	45
2.3.5 Voltage increases binding affinity of EF <sub>N</sub> and LF <sub>N</sub> to the PA <sub>63</sub> channel .....	46
2.4 Discussion .....	50
<b>Chapter 3 - INTERACTION OF CHLOROQUINE-LIKE 4-AMINOQUINOLINES WITH         ANTHRAX TOXIN PROTECTIVE ANTIGEN.....</b>	<b>55</b>
3.1 Introduction.....	55
3.2 Materials and Methods .....	57
3.2.1 Materials.....	57
3.2.2 Lipid bilayer experiments .....	57
3.2.3 Titration experiments.....	57
3.2.4 Current-noise analysis.....	58
3.3 Results.....	59
3.3.1 Binding of blocker-substrates to the PA <sub>63</sub> channel .....	59
3.3.2 Substrate-induced current-noise-analysis of the PA <sub>63</sub> channel .....	61
3.4 Discussion .....	65
3.4.1 Half saturation constants emphasize the possibility to block PA <sub>63</sub> .....	65
3.4.2 Titration and noise data allow deeper insight in the chemical- group-dependent binding constants.....	65
<b>Chapter 4 - CROSS-REACTIVITY OF ANTHRAX AND C2 TOXIN: PROTECTIVE         ANTIGEN PROMOTES THE UPTAKE OF BOTULINUM C2I TOXIN INTO         HUMAN ENDOTHELIAL CELLS.....</b>	<b>71</b>
4.1 Introduction.....	71

---

4.2 Experimental procedures .....	74
4.2.1 Materials.....	74
4.2.2 Western Blots.....	74
4.2.3 Cell culture .....	75
4.2.4 Adenylate cyclase activity .....	75
4.2.5 ADP-ribosylation .....	75
4.2.6 Lipid bilayer experiments .....	75
4.2.7 Binding experiments .....	76
4.2.8 Statistics .....	76
4.3 Results.....	77
4.3.1 Interaction of PA <sub>63</sub> with C2I <i>in vitro</i> .....	77
4.3.2 Binding of C2II with EF and LF <i>in vitro</i> .....	77
4.3.3 PA <sub>63</sub> translocates C2I in cells.....	78
4.3.4 Interaction of C2II with LF and EF <i>in vivo</i> (cell-based assay) .....	81
4.4 Discussion .....	83
Chapter 5 - <b>ANTHRAX TOXIN PROTECTIVE ANTIGEN PROMOTES UPTAKE OF N-TERMINAL HIS<sub>6</sub>-TAG LABELED POLYPEPTIDES INTO CELLS IN A VOLTAGE-DEPENDENT WAY</b> .....	87
5.1 Introduction .....	87
5.2 Experimental procedures .....	90
5.2.1 Materials.....	90
5.2.2 Cell culture and biochemical products .....	90
5.2.3 Lipid bilayer experiments .....	91
5.2.4 Binding experiments .....	91
5.3 Results.....	93
5.3.1 Interaction of PA <sub>63</sub> pores with His <sub>6</sub> -C2I in artificial black lipid bilayer membranes .....	93
5.3.2 Addition of His <sub>6</sub> -tag to C2I potentiates its transfer via PA <sub>63</sub> .....	95
5.3.3 His <sub>6</sub> -tag does not facilitate binding of EF and LF to C2II channels.....	96
5.3.4 Binding of His <sub>6</sub> -gpJ and gpJ proteins to PA <sub>63</sub> and C2II channels.....	97
5.3.5 Binding of EDIN and His <sub>6</sub> -EDIN to PA <sub>63</sub> and C2II channels.....	97
5.3.6 His <sub>6</sub> -tag promotes EDIN internalization via PA <sub>63</sub> pores .....	98

---

5.3.7 The voltage dependency of PA <sub>63</sub> channels is changed when His <sub>6</sub> -EDIN is bound to the pore .....	99
5.4 Discussion .....	101
5.4.1 His <sub>6</sub> -tag addition to several bacterial factors increased the protein binding affinity to PA <sub>63</sub> but not to C2II channels.....	101
5.4.2 Influence of the His <sub>6</sub> -tag on uptake of EF, LF and C2I into cells.....	101
5.4.3 Bound (His <sub>6</sub> -)EDIN causes a difference in voltage-dependency of PA <sub>63</sub> pores .....	102
5.4.4 The PA <sub>63</sub> channel transports His <sub>6</sub> -C2I and His <sub>6</sub> -EDIN into HUVECs .....	103
<b>Chapter 6 - BINDING PARTNERS OF PROTECTIVE ANTIGEN FROM BACILLUS ANTHRACIS SHARE CERTAIN COMMON MOTIVES .....</b>	<b>107</b>
6.1 Introduction .....	107
6.2 Experimental procedure.....	108
6.2.1 Materials.....	108
6.2.2 Black lipid bilayer measurements .....	108
6.3 Results.....	110
6.3.1 Native effector proteins of protective antigen.....	110
6.3.1.1 Full length EF and LF .....	110
6.3.1.2 EF <sub>N</sub> and LF <sub>N</sub> .....	110
6.3.2 Cross-reactivity of Anthrax and C2 toxin .....	111
6.3.2.1 Binding of close related proteins.....	111
6.3.2.2 Binding of unrelated proteins is enabled by His <sub>6</sub> -tag.....	111
6.3.3 Small molecule inhibitors .....	112
6.3.3.1 Chloroquine and other 4-aminoquinolones block protective antigen.....	112
6.3.3.2 Cyclodextrin-complexes form a plug for the PA-pore .....	112
6.3.4 Binding of divalent and trivalent cations to protective antigen.....	113
6.4 Discussion .....	116
6.4.1 Binding substrates of protective antigen share common motives .....	116
6.4.1.1 Positive charges play a crucial role .....	116
6.4.1.2 Aromatic residues enhance affinities towards PA pores .....	116
6.4.2 Binding of charged substrates is voltage-dependent.....	117
6.4.3 Conclusion.....	117

---

Chapter 7 – <b><i>CLOSTRIDIUM DIFFICILE</i> CDT TOXIN FORMS TWO DIFFERENT TYPES OF PORES</b> .....	119
7.1 Introduction.....	119
7.2 Materials and Methods.....	121
7.2.1 CDTa and CDTb production and purification.....	121
7.2.2 Lipid bilayer experiments.....	121
7.2.2.1 Selectivity.....	121
7.2.2.2 Binding experiments.....	122
7.3 Results.....	124
7.3.1 Single channel measurements.....	124
7.3.1.1 Channel formation by activated CDTb.....	124
7.3.1.2 Channel formation by CDTb with cholesterol.....	125
7.3.2 Selectivity.....	126
7.3.2.1 Untreated CDTb channels are anion selective.....	126
7.3.2.2 CDTb channels preincubated with cholesterol are cation selective.....	126
7.3.3 Voltage-dependency.....	127
7.3.3.1 Untreated CDTb channels are highly voltage-dependent.....	127
7.3.3.2 CDTb channels preincubated with cholesterol are less voltage-dependent.....	127
7.3.4 Binding of CDTb channels to CDTa.....	128
7.3.4.1 Untreated CDTb does not bind CDTa.....	128
7.3.4.2 CDTb preincubated with cholesterol binds CDTa.....	129
7.3.4.3 CDTa blocks CDTb channels in a single hit process.....	129
7.4 Discussion.....	131
Chapter 8 – <b>CONCLUSION</b> .....	135
Appendix – <b>References</b> .....	139
<b>Curriculum Vitae</b> .....	148
<b>Danksagung</b> .....	150





## SUMMARY

The ability to produce toxins is spread among a huge variety of bacterial strains. A very prominent class of bacterial protein toxins is the family of binary AB toxins sharing a common mode of intoxication. A pore forming component B binds and translocates an enzymatic component A into the cytosol of target cells exhibiting a fatal mode of action. These components are supposed to be not toxic themselves but both required for cell toxicity.

Anthrax toxin produced by the Gram-positive bacteria *Bacillus anthracis* is the best studied binary toxin especially since its use as a biological weapon in the context of the attacks of 9/11 in 2001. In contrast to other binary toxins, Anthrax toxin possesses two different enzymatic components, edema factor (EF), a calcium- and calmodulin-dependent adenylat-cyclase and lethal factor (LF), a zinc-dependent metalloprotease. Protective antigen (PA) is the pore-forming component responsible for binding and translocation. *Clostridium botulinum* possesses in addition to the well known botulinum toxin (Botox) a variety of other toxins, such as the binary C2 toxin. C2 toxin is composed of the binding and translocation moiety C2II and the enzymatic moiety C2I acting as an actin-ADP-ribosyltransferase.

In this study, the mode of translocation and the binding kinetics to the enzymatic component were studied in a biophysical experimental setup. In chapter 2, the binding of the N-terminal fractions  $EF_N$  and  $LF_N$  to the PA channel are analyzed in artificial bilayer membranes revealing lower binding affinity compared to full-length EF and LF. Other biophysical properties like voltage-dependency and ionic-strength dependency are not influenced. The results suggest that additional forces are involved in the binding process, than those concerning the N-terminus exclusively, as it was supposed previously.

As the treatment of an Anthrax infection with antibiotics is often medicated very late due to the lack of early symptoms, tools to prevent intoxication are required. 4-aminoquinolones like chloroquine are known to block the PA channel, thereby inhibiting intoxication but they also lead to severe side-effects. In chapter 3 new promising agents are described that bind to PA in artificial bilayer systems, elucidating common motives and features which are necessary for binding to PA in general.

The possible interaction of Anthrax and C2 toxin is investigated by measuring the binding of one enzymatic component to the respective other toxin's pore (chapter 4). Interestingly, *in vitro* experiments using the black lipid bilayer assay show that PA is able to bind to C2I resulting in half saturation constants in the nanomolar range. Furthermore, *in vivo* this combination of toxin components exhibits cell toxicity in human cell lines. This is first-time evidence that a heterologous toxin combination is functional in *in vitro* and *in vivo* systems. In contrast, C2II is able to bind to EF as well as to LF *in vitro*, whereas in *in vivo* studies almost no toxic effect is detected. In the case of PA, an N-terminal His<sub>6</sub>-tag attached to the enzymatic subunit increased the binding affinity (chapter 5). A His<sub>6</sub>-tag attached to not related proteins also led to high binding affinities, providing the possibility to establish PA as a general cargo protein.

In chapter 6 a set of different molecules and proteins is summarized, which are either related or not related to binary toxins, PA is able to bind. In first line, the presence of positive charges is found to be responsible for binding to PA which is in accordance to the fact that PA is highly cation selective. Furthermore, we present evidence that different cationic electrolytes serve as a binding partner to the PA channel.

In the last decade another toxin has aroused public attention as it was found to be responsible for a rising number of nosocomial infections: *Clostridium difficile* CDT toxin. The mode of action of the enzymatic subunit CDTa is similar to C2I of C2 toxin, acting as an ADP-ribosylating toxin. The channel forming and binding properties of CDT toxin are studied in artificial bilayer membranes (chapter 7). We found that two different types of channels are formed by the B component CDTb. The first channel is similar to that of iota toxin's Ib of *Clostridium perfringens* with comparable single channel conductance, selectivity and binding properties to the enzymatic subunit CDTa. The formation of this type of channel is cholesterol-dependent, whereas in the absence of cholesterol another kind of channel is observed. This channel has a single channel conductance which is rather high compared to all other binary toxin channels known so far, it is anion selective and does not show any binding affinity to the enzymatic component CDTa. The results reveal completely new insights in channel formation properties and the flexibility of a pore-forming component. Additionally, these findings suggest further possibilities of toxicity of the pore forming component itself which is not known for any other binary toxin yet. Therefore, the pathogenic role of this feature has to be studied in detail.

## ZUSAMMENFASSUNG

Die Fähigkeit, Toxine zu produzieren, ist unter verschiedensten Bakterienstämmen sehr verbreitet. Zu diesen Toxinen zählt auch die Familie der binären AB-Toxine, die hauptsächlich von Bakterien der Gattung *Bacillus* und *Clostridium* gebildet werden. Charakteristisch für diese bakteriellen Proteintoxine ist der Wirkungsmechanismus der Zellintoxikation. Eine porenformende Untereinheit B bindet eine enzymatische Untereinheit A und transportiert diese in das Zytosol von Zielzellen, die dort tödliche Wirkung entfalten. Es wird angenommen, dass die einzelnen Komponenten an sich nicht toxisch sind, sondern nur in Kombination Zellvergiftung auslösen.

Anthrax-Toxin, das von dem Gram-positiven Bakterium *Bacillus anthracis* produziert wird, ist das bekannteste und am besten untersuchte binäre Toxin, besonders seit es im Jahr 2001 als Biowaffe eingesetzt wurde. Im Gegensatz zu anderen binären Toxinen besitzt das Anthrax-Toxin zwei enzymatische Komponenten: Edema Factor (EF), eine kalzium- und calmodulinabhängige Adenylatzyklase, und Lethal Factor (LF), eine zinkabhängige Metalloprotease. Protective Antigen (PA) ist die porenformende Komponente, die für die Binding und die Translokation der enzymatischen Untereinheiten verantwortlich ist. *Clostridium botulinum* produziert neben dem bekannten Botulinumtoxin (Botox) eine Reihe weiterer Toxine, unter anderem das binäre C2-Toxin. Dieses besteht aus der Binde- und Translokationskomponente C2II und der enzymatischen Komponente C2I, die als ADP-Ribosyltransferase fungiert.

Im Rahmen der vorliegenden Arbeit werden der Translokationsmechanismus und die kinetischen Bindeeigenschaften dieser Toxine biophysikalisch untersucht. In Kapitel 2 wird die Bindung der N-terminalen Fragmente  $EF_N$  und  $LF_N$  an den PA-Kanal in künstlichen Lipidmembranen analysiert. Obwohl die Spannungs- und Ionenstärkeabhängigkeit unverändert sind, weisen die verkürzten Proteine deutlich geringe Bindeaffinitäten zu PA im Vergleich zu den vollständigen Proteinen auf. Die Ergebnisse zeigen, dass, anders als bisher angenommen, weitere Kräfte als die zwischen dem N-Terminus und dem PA-Kanal eine Rolle für die Bindung der enzymatischen Komponente spielen.

Da bei einer Anthraxinfektion häufig keine frühen Symptome sichtbar sind, erfolgt die Behandlung mit Antibiotika in der Regel relativ spät. Daher werden neue Wirkstoffe benötigt, um einer Intoxikation vorzubeugen. Es ist bekannt, dass 4-Aminoquinolone, wie zum Beispiel Chloroquin, in der Lage sind, die PA-Pore zu blockieren und somit eine Zellvergiftung zu verhindern, allerdings haben diese Wirkstoffe starke Nebenwirkungen. In Kapitel 3 werden neue,

vielversprechende Wirkstoffe beschrieben, die an PA binden können und Aufklärung darüber geben, welche Eigenschaften für die Bindung an PA im Allgemeinen verantwortlich sind.

Des Weiteren wird untersucht, ob eine Kreuzreaktion zwischen den Komponenten des Anthrax- und C2-Toxins möglich ist (Kapitel 4). Dazu wird die Bindung einer enzymatischen Komponente an die Pore des entsprechenden anderen Toxins gemessen. Interessanterweise ergeben *in vitro* Experimente an künstlichen Lipidmembranen, dass PA an C2I bindet und *in vivo* Vergiftungen an humanen Zelllinien auslöst. Damit wird zum ersten Mal gezeigt, dass eine heterologe Toxinkombination sowohl *in vitro* als auch *in vivo* funktionell ist. C2II hingegen ist zwar in der Lage, EF und LF zu binden, die Transportrate in Zielzellen ist jedoch sehr gering. Im Fall von PA bewirkt ein N-terminaler His<sub>6</sub>-tag, der an die enzymatischen Einheiten gekoppelt ist, eine Erhöhung der Bindeaffinität, beschrieben in Kapitel 5. Dies ist sowohl für nah verwandte Proteine der Fall als auch für Proteine, die nicht im Zusammenhang mit binären Toxinen stehen. Somit eröffnet sich die Möglichkeit, PA als universelles Transportprotein zu nutzen.

In Kapitel 6 werden verschiedene Moleküle und Proteine beschrieben, die in der Lage sind, an PA zu binden. Vor allem positive Ladungen scheinen für die Bindung an PA-Kanäle verantwortlich zu sein, was mit der Tatsache, dass PA stark kationenselektiv ist, im Einklang steht. Des Weiteren wird zum ersten Mal beschrieben, dass verschiedene Kationen selbst als Bindepartner fungieren können.

Seit einigen Jahren ist ein weiteres Toxin in den Fokus der Öffentlichkeit gerückt, da es zunehmend für nosokomiale Infektionen verantwortlich gemacht wird: CDT-Toxin von *Clostridium difficile*. Wie das C2-Toxin besitzt CDT-Toxin ADP-Ribosyltransferaseaktivität, was zu irreversiblen Schäden des Aktin- Zytoskeletts und somit zum Zelltod führt. Die biophysikalischen Eigenschaften, betreffend Porenbildung und Bindeaffinität des CDT-Toxins werden in Kapitel 7 beschrieben. Wir zeigen, dass die B Komponente CDTb fähig ist, zwei unterschiedliche Kanäle zu bilden. Einer dieser Kanäle ist dem des Iota-Toxins von *Clostridium perfringens* ähnlich, die Einzelkanalleitfähigkeit, Selektivität und Bindeeigenschaften sind vergleichbar. Die Bildung dieses Kanals ist abhängig von Cholesterin, wohingegen in Abwesenheit von Cholesterin überwiegend ein anderer Kanal geformt wird. Dieser zeigt eine für einen binären Toxinkanal ungewöhnlich hohe Einzelkanalleitfähigkeit, der Kanal ist anionenselektiv und weist keinerlei Bindeaffinität zu der enzymatischen Komponente CDTa auf. Die Ergebnisse offenbaren neue Einblicke in die Formierung von Toxinkanälen und deuten darauf hin, dass dieses Toxin durch die Flexibilität der Kanalbildung möglicherweise zusätzliche Fähigkeiten besitzt, Zellintoxikation auszulösen. Dennoch ist die physiologische und pathogene Rolle dieser Eigenschaft noch weitestgehend ungeklärt und bedarf intensiver Untersuchung.





## INTRODUCTION

### 1.1 BACTERIAL TOXINS

The production of toxins is a feature spread among various species from prokaryotes to plants and animals in order to gain evolutionary advantages. In 1888 diphtheria toxin of *Corynebacterium diphtheriae* was the first bacterial toxin identified as a virulence factor causing severe disease (Roux and Yersin, 1888).

Nowadays, a lot of bacterial strains are known to possess the ability to produce bacterial protein toxins and the symptoms of many severe diseases like anthrax (*Bacillus anthracis*), cholera (*Vibrio cholera*) or whooping cough (*Bordetella pertussis*) can be attributed to these toxins. The purpose is the enhancement of bacterial survival, proliferation and spread. Damaging target cells, leading to cell death in worst case, the bacteria take benefit from the metabolism and resources provided by the host cells. Another feature of bacterial toxins is to manipulate the host's immune system in order to protect the pathogens from immune response.

During evolution, bacteria developed different modes of action to gain benefit from their hosts. Some destroy the permeability barrier of membranes. Others enter the cells and affect intracellular processes like signal transduction, actin polymerization or membrane trafficking (Schmitt *et al.*, 1999; Turk, 2007). Among them are bacterial toxins acting as enzymes which are highly toxic even in very low concentration (Rappuoli and Montecucco, 1997). The toxicity of bacterial proteins exceeds the potential of chemical agents by far. The LD<sub>50</sub> of botulinum neurotoxin A of *Clostridium botulinum* is 0.03 ng kg<sup>-1</sup> whereas the LD<sub>50</sub> of TCDD (dioxin) is 1 µg kg<sup>-1</sup>. Therefore, bacterial protein toxins belong to the most powerful poisons.

Bacterial toxins can be divided into two functional groups, the endo- and the exotoxins. Exotoxins are cell-associated whereas endotoxins are secreted by the bacteria (see Table 1.1).

#### 1.1.1 Endotoxins

Endotoxins are cell-associated structural components on the outer membrane of Gram-negative bacteria. As they do not act as enzymes, their mode of intoxication is often less specific and also less potent compared to exotoxins. Although these toxins are associated to the cell wall, growth,

autolysis or lysis as a result of host immune defense or antibiotics, small amounts can be released into the extracellular media. The term exotoxin refers typically to the lipopolysaccharide complex (LPS) in the outer membrane of Gram-negative bacteria such as *Escherichia coli*, *Neisseria*, *Shigella* or *Pseudomonas*. LPS itself consists of two different components, a polysaccharide and a lipid component A. The polysaccharide moiety is responsible for immunogenicity, whereas the lipid A causes toxic effects which lead to the secretion of proinflammatory cytokines and nitric oxides thereby implicating an endotoxic shock. Endotoxins are heat stable and cannot be converted into toxoids anticipating their application as vaccines (Trent *et al.*, 2006).

**Table 1.1. Comparison of Endo- and Exotoxins.**

<b>Feature</b>	<b>Endotoxin</b>	<b>Exotoxin</b>
<i>Chemical nature</i>	Lipopolysaccharide ~10 kDa	Protein > 20 kDa
<i>Bacteria</i>	Gram-negative	Gram-negative and Gram-positive
<i>Origin</i>	part of the outer membrane	extracellular, bacterial secretion
<i>Heat-stable</i>	yes	usually not
<i>Antigenic</i>	yes	yes
<i>Usage as toxoid</i>	no	yes
<i>Toxicity</i>	low	high
<i>Specificity</i>	low	high
<i>Enzymatic activity</i>	no	usually yes

modified from (Leuber, 2007)

### 1.1.2 Exotoxins

Unlike endotoxins, exotoxins are produced by Gram-negative as well as by Gram-positive bacterial strains and secreted as soluble proteins particularly during the exponential growth phase and during sporulation. In general exotoxins have enzymatic activity and share common features with enzymes such as denaturation by heat, acid or proteolysis. Accordingly, their efficiency can be characterized by enzymatic kinetic models and they share high specificity and a similar mode of action. The high specificity is not only related to their molecular mode in the cytosol of target cells, but also to specific cell types. Tetanus toxin of *Clostridium tetani* for instance exclusively



affects neurons. However, a variety of other toxins are able to target almost every kind of cells leading to necrosis, apoptosis and cell death. As exotoxins are sensitive to heat, strongly antigenic and can be transformed into toxoids, they are often used as targets for vaccine development (Table 1.2).

**Table 1.2. Examples for bacteria's enzymatic properties and their biological effect.**

<b>Toxin</b>	<b>Enzymatic activity</b>	<b>Biological effect</b>
<i>Cholera toxin</i>	ADP-ribosylates adenylatecyclase Gs regulatory protein	Activates adenylate-cyclase; increased cAMP promotes secretion of electrolytes and fluids in the intestine, leading to diarrhea
<i>Diphtheria toxin</i>	ADP-ribosylates elongation factor 2	Inhibition of protein synthesis and cell death
<i>Pertussis toxin</i>	ADP ribosylates adenylatecyclase Gi regulatory protein	Blocks inhibition of adenylatecyclase; increased levels of cAMP effect hormone activity
<i>Shiga toxin</i>	Glycosidase cleavage of ribosomal RNA (28s rRNA)	Inactivation of ribosomal 60s subunit, stopping protein synthesis and leading to cell death
<i>Botulinum neurotoxin A</i>	Zn <sup>2+</sup> -dependent protease acting on synaptobrevin at motor ganglioside	Inhibition of presynaptic acetylcholine release from peripheral cholinergic neurons resulting in flaccid paralysis
<i>Tetanus toxin</i>	Zn <sup>2+</sup> -dependent protease acting on synaptobrevin in the central nervous system	Inhibition of neurotransmitter release from inhibitory neurons in the central nervous system, resulting in spastic paralysis
<i>Anthrax lethal toxin</i>	Zn <sup>2+</sup> -dependent protease, cleaving MAPKK	Inhibition of MAPK pathway leading to cell death
<i>Anthrax edema toxin</i>	Ca <sup>2+</sup> - and calmodulindependent adenylate- cyclase	Increased intracellular cAMP interfering with cell signalling
<i>Large clostridial toxins</i>	Glycosylates small, monomeric G-proteins	Interference with small G-protein induced signaling pathways with effects on morphology and physiology
<i>Clostridium botulinum C2 toxin</i>	ADP-ribosylates G-actin at Arg177	Interference with the actinpolymerisation, disruption of the cytoskeleton
<i>Bordetella pertussis AC toxin</i>	Calmodulin-dependent adenylate-cyclase	Increased cAMP leading to inhibition of phagocytosis by neutrophils and macrophages; hemolysis or leukolysis

modified from(Leuber, 2007)

### 1.1.2.1 Pore-forming toxins (PFTs)

About 25% of all bacterial proteins toxins have the capability to form pores in membranes, hence these pore-forming toxins (PFTs) are an important class of exotoxins. The majority is secreted in the cell surrounding as water soluble monomers. Some of them require proteolytic cleavage to be activated meaning that they are able to assemble to oligomers inserting as a transmembrane channel. The transmembrane region can consist either of  $\alpha$ - helices ( $\alpha$ -PFTs) or of  $\beta$ -barrels ( $\beta$ -PFTs) (Table 1.3).

Table 1.3. Examples of  $\alpha$ - and  $\beta$ -PFTs.

Toxin	Organism	Structural characteristics
<b><math>\alpha</math>-PFT</b>		
Colicin	<i>Escherichia coli</i>	Globular pore-forming domain, ten $\alpha$ -helices including two hydrophobic helices
Diphtheria toxin	<i>Corynebacterium diphtheriae</i>	Two disulfide-linked chains resulting from cleavage of one protein, ten $\alpha$ -helices
Exotoxin A	<i>Pseudomonas aeruginosa</i>	Six $\alpha$ -helices, not predominantly hydrophobic
Cry toxins	<i>Bacillus thuringiensis</i>	Seven $\alpha$ -helices, five necessary for toxicity
<b><math>\beta</math>-PFT</b>		
$\alpha$ -Hemolysin	<i>Staphylococcus aureus</i>	Heptamer and prepore, 14-stranded transmembrane $\beta$ -barrel, mushroom shaped
Leucocidins	<i>Staphylococcus aureus</i>	Heterooctamer of LukF and LukS
Pneumolysin	<i>Streptococcus pneumoniae</i>	Ring of 30-50 subunits, two $\beta$ -strands per unit, cholesterol-dependent
Aerolysin	<i>Aeromonas hydrophila</i>	Heptameric pores without prepore formation
Anthrax toxin	<i>Bacillus anthracis</i>	Binary toxins see Chapter 1.2 for details
C2 toxin	<i>Clostridium botulinum</i>	
CDT toxin	<i>Clostridium difficile</i>	

modified from (Leuber, 2007)

### 1.1.2.2 $\alpha$ -pore-forming toxins ( $\alpha$ -PFTs)

The mechanism of oligomerization and pore formation of  $\alpha$ -PFTs is still not fully understood, however, some of these toxins are quite well studied. Colicin toxin of *Escherichia coli* for example is known to require a three step mechanism from monomers to functional pores including receptor binding, unfolding of the pore-forming domain release of hydrophobic helices (Zakharov *et al.*, 2004). Exotoxins A from *Pseudomonas aeruginosa* or Cry toxin from *Bacillus thuringiensis* in contrast do not possess a hydrophobic hairpin (Allured *et al.*, 1986; Boonserm *et al.*, 2005).

### 1.1.2.3 $\beta$ -pore-forming toxins ( $\beta$ -PFTs)

Compared to  $\alpha$ -PFTs much more is known about pore formation and membrane insertion of  $\beta$ -PFTs. In general, after secretion of water soluble monomers into the extracellular medium the monomer oligomerize and pore formation occurs closely linked to significant conformational changes. The  $\beta$ -strands of the subunits form a  $\beta$ -barrel that forms the transmembrane channel and spans the membrane. There are four classes of  $\beta$ -PFTs including the  $\alpha$ -hemolysin family (e.g. *Staphylococcus aureus*  $\alpha$ -hemolysin), aerolysin toxins (e.g. *Clostridium perfringens*  $\epsilon$ -toxin), cholesterol-dependent cytolysins (e.g. *Streptococcus pneumoniae* pneumolysin) and the binary toxins (e.g. *Bacillus anthracis* Anthrax toxin).

### 1.1.2.4 Cholesterol-dependent cytolysins (CDCs)

The family of cholesterol-dependent toxins comprises amongst others *Clostridium perfringens* perfringolysin, *Streptococcus intermedius* intermediolysin and *Streptococcus pneumoniae* pneumolysin. These toxins require cholesterol rich regions in the membrane where they can bind to and oligomerize to prepores consisting of 30 to 50 monomers, except in the case of intermediolysin which binds to the human cell receptor CD59. After conformational change, they form a functional pore of large size leading to cell lysis. Interestingly, although cholesterol is not necessary for oligomerization of intermediolysin, it is required for pore formation and membrane insertion (Heuck *et al.*, 2007). The role of cholesterol for the other toxins concerning pore formation and membrane insertion is not clarified so far but is supposed to have at least an impact.

## 1.2 BINARY TOXINS

Binary toxins are a class of  $\beta$ -PFTs exotoxins comprising amongst other Anthrax toxin of *Bacillus anthracis*, C2 toxin of *Clostridium botulinum*, CDT of *Clostridium difficile* and iota toxin of *Clostridium perfringens*. Characteristic for this type of AB toxins is that they consist of two different protein domains which are supposed to be non toxic themselves and both necessary for intoxication. These two domains can be either secreted separately like those mentioned above or be located on the same protein chain like diphtheria toxin of *Corynebacterium diphtheria* or the large clostridial toxins toxA and toxB of *Clostridium difficile* (Lemichez and Boquet, 2003; Egerer *et al.*, 2007). Component B is responsible for binding and translocation whereas component A exhibits enzymatic activity. They act inside the target cell's cytosol affecting the cytoskeleton or signal transduction pathways leading to apoptosis and cell death.

### 1.2.1 Intoxication pathway of binary toxins

Following secretion of the A and B component by the bacteria, the B component is activated by proteolytic digestion of a host enzyme which cleaves an about 20 kDa fragment from the N-terminus of the precursor. The activated B moiety forms prepores which are in general heptamers (in the case of Anthrax toxin also octamers were found) (Feld *et al.*, 2010) that bind to a cellular receptor on the target cell surface as well as to the enzymatic component. This complex is internalized by receptor-mediated and clathrin-dependent endocytosis in cholesterol rich regions of the membrane. Acidification of the endosome leads to structural changes converting the prepore into a membrane inserting  $\beta$ -barrel pore as well as to the unfolding of the enzymatic component that is translocated through the pore into the cell cytosol (Benson *et al.*, 1998; Nassi *et al.*, 2002; Young and Collier, 2007) where they exhibit their toxic effect (Figure 1.1).

### 1.2.2 *Bacillus anthracis* Anthrax toxin

Anthrax toxin is produced by the rod shaped, Gram-positive bacterium *Bacillus anthracis*. The spores are highly resistant and can survive in soil for decades causing infections when taken up by a host (Dixon *et al.*, 1999; Mock and Fouet, 2001).

The mode of infection depends on the way of spore incorporation. Uptake via skin abrasion leads to cutaneous infection and lesions that can form black eschar. Gastrointestinal infection causes bloody vomiting, severe diarrhea and inflammation of the intestinal tract. The highest mortality rate is due to infection of the pulmonary system which leads to respiratory collapse.

Anthrax toxin consists of the binding and translocation component protective antigen (PA) which is able to form pores in cell membranes. Unlike other binary toxins, Anthrax possesses two different A components called edema factor (EF) and lethal factor (LF) with different enzymatic properties. Both enter the target cell cytosol via translocation through the PA pore (Figure 1.1).

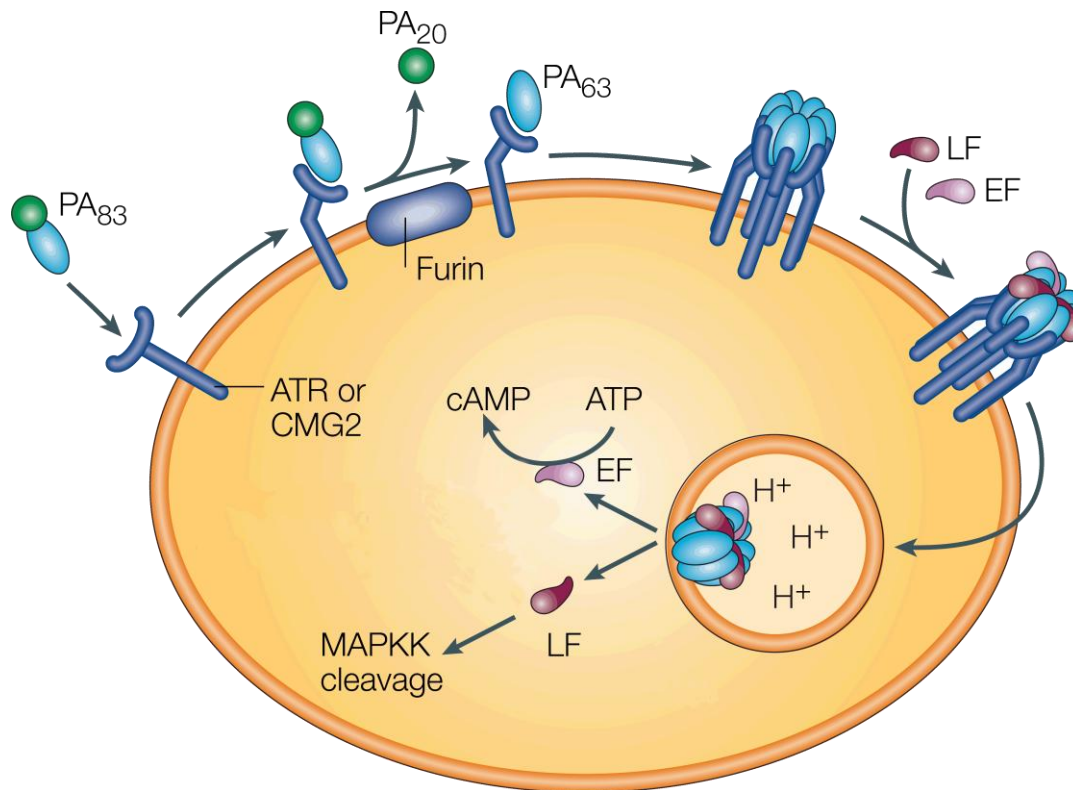


**Figure 1.1. Intoxication pathway of *Bacillus anthracis* Anthrax toxin.** A precursor (PA<sub>83</sub>) binds to a cellular receptor. Proteolytically activated PA<sub>63</sub> forms a heptameric prepore, which is able to bind up to 3 enzymatic components EF and/or LF. After clathrin-dependent endocytosis, acidification of the endosome leads to prepore-to-pore conversion of the PA heptamer and subsequent translocation of the enzymatic components into the cytosol. EF causes an increase of cAMP while LF cleaves MAPKKs. Modified from (Rainey and Young, 2004).

### 1.2.2.1 Protective antigen (PA)

Protective antigen (PA) is the binding and translocation component of the Anthrax toxin. Its name refers to its use as a vaccine against anthrax infection. PA is secreted as an 83 kDa protein and consists of four functional domains. The cleavage site for proteolytic activation is located in domain I, domain II harbors the ability of membrane insertion, domain III is responsible for oligomerization and domain IV is the region of receptor binding (Petosa *et al.*, 1997; Lacy and Collier, 2002). Two cell-associated receptors PA is able to bind to are known: Anthrax toxin receptor (ATR) (Bradley *et al.*, 2001; Liu and Leppla, 2003) and tumor endothelial marker 8

(TEM8) (Carson-Walter *et al.*, 2001). Activation of PA<sub>83</sub> is accomplished by proteolytic cleavage of a N-terminal 20 kDa fragment by a furin-like protease resulting in a 63 kDa PA monomer able to form oligomers. The exact structure of the membrane spanning PA heptamer is not solved yet, but a model of the channel can be derived from the structure of the water soluble heptameric prepore (Figure 1.2) (Petosa *et al.*, 1997; Nguyen, 2004) on the basis of the related mushroom-shaped pore of *Staphylococcus aureus*  $\alpha$ -hemolysin (Song *et al.*, 1996). According to this model, formation of the  $\beta$ -barrel requires  $\beta$ -hairpins derived from the unfolding of a greek-key motif as well as the association of the seven  $\beta$ -hairpins to a 14-stranded  $\beta$ -barrel (Benson *et al.*, 1998; Nassi *et al.*, 2002). This prepore-to-pore conversion is triggered by acidification of the endosome (Krantz *et al.*, 2004; Krantz *et al.*, 2005).

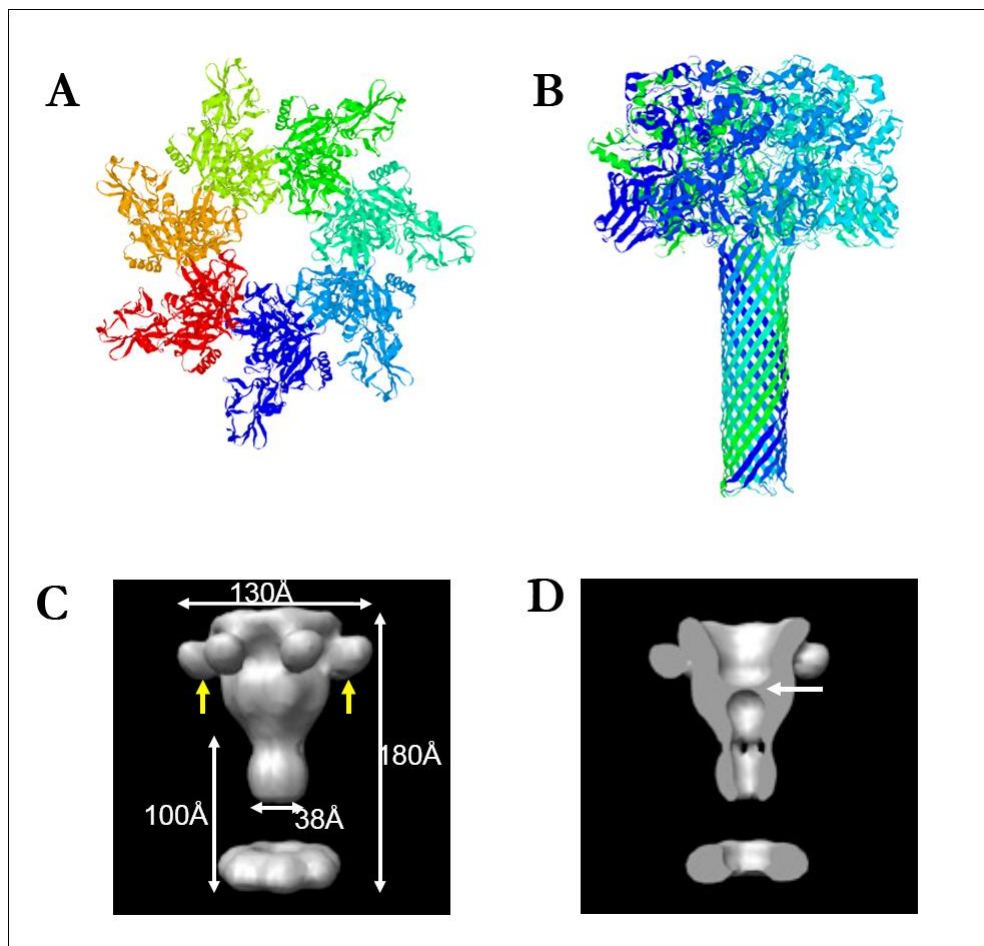


**Figure 1.2. Structure of the heptameric PA<sub>63</sub> pore.** (A) Top view of the heptameric prepore (Petosa *et al.*, 1997). (B) Hypothetical model of membrane-inserted PA heptamer with membrane-spanning  $\beta$ -barrel. (Nguyen, 2004). (C, D) Three-dimension reconstitution of the PA surface incorporated in nanodiscs and central cut of the interior structure reconstruction (Katayama *et al.*, 2010).

### 1.2.2.2 Edema factor (EF)

Edema factor (EF) is one of the enzymatic components of Anthrax toxin. The 89 kDa protein is a calcium- and calmodulin-dependent adenylate cyclase. In the cytosol of target cells it accumulates cyclic AMP interfering with water homeostasis and cell signaling pathways (Dixon *et al.*, 1999; Mock and Fouet, 2001; Young and Collier, 2007). EF impairs neutrophil functions and is supposed to be responsible for edema infection in cutaneous anthrax.

### 1.2.2.3 Lethal factor (LF)

Lethal factor (LF) is the second enzymatic component of Anthrax toxin. LF (90 kDa) is a highly specific zinc-dependent metalloprotease acting as a mitogen-activated protein kinase kinases (MAPKKs) leading to a blockage of this signaling pathway and apoptosis (Turk, 2007). In macrophages LF prevents a rapid activation of the immune system by inhibiting the release of cytokines and chemokines such as tumor necrosis factor alpha (TNF- $\alpha$ ) and interleukin-1 $\beta$  (IL-1 $\beta$ ) (Pellizzari *et al.*, 1999). As dendritic cells and T-cells are inhibited as well, early infection symptoms are missing. Therefore, application of penicillin and doxycyclin *B. anthracis* is sensitive to takes place quite late in general (Lacy and Collier, 2002).

## 1.2.3 *Clostridium botulinum* C2 toxin

*Clostridium botulinum*, an anaerobic, spore-forming, Gram-positive bacterium, produces various highly potent neurotoxins such as botulinum neurotoxins (BoNT). These toxins cause botulism by blocking exocytosis of acetylcholine in neuromuscular junctions (Johnson, 1999; Szule and Coorssen, 2003). Additional to BoNTs, *C. botulinum* strains C and D also secrete the binary toxin C2 (Aktories *et al.*, 1987) which is an actin-ADP-ribosylating toxin. It causes necrotic and hemorrhagic lesions in the intestine, increasing blood pressure and inducing edema (Simpson *et al.*, 1988; Considine and Simpson, 1991). Like the closely related Anthrax toxin, C2 toxin is a binary toxin of the AB-type with a B component named C2II forming channels consisting of  $\beta$ -PFTs and an enzymatic A component C2I.

### 1.2.3.1 C2II

The binding and translocation component C2II (80 kDa) is highly homologous to Anthrax toxin's protective antigen, mainly in the three domains responsible for pore formation, oligomerization and binding of the enzymatic compound. The crystal structure of the water-

soluble prepore is solved and a model of the heptameric channel could be derived according to these data (Petosa *et al.*, 1997; Schleberger *et al.*, 2006).

### 1.2.3.2 C2I

The 49 kDa C2I is the enzymatic component of the C2 toxin (Aktories *et al.*, 1986b; Fujii *et al.*, 1996) acting as an ADP-ribosyltransferase (Simpson, 1984) that modifies G-actin into F-actin at position Arg177. This leads to the disassembly of existing actin filaments (Aktories *et al.*, 1986a; Wegner and Aktories, 1988), the destruction of the target cell's actin cytoskeleton and finally to rounding and death of the cells.

### 1.2.4 *Clostridium difficile* CDT toxin

*Clostridium difficile* is an anaerobic, rod-shaped, spore-forming, Gram-positive bacterium. The pathogenicity is mainly due to the exotoxins Toxin A and Toxin B (TcdA and TcdB) belonging to the class of large clostridial toxins (LCTs). These toxins cause mucosal inflammation and diarrhea after treatment with antibiotics in hospitals. Because of that CDT toxin poses an increasing challenge concerning nosocomial infections. Hypervirulent strains of *C. difficile* additionally produce the binary *Clostridium difficile* transferase (CDT) toxin (McDonald *et al.*, 2006) which is a member of the binary AB type of toxins acting as an actin-ADP-ribosylating toxins closely related to *Clostridium botulinum* C2 toxin, *Clostridium perfringens* iota toxin or *Clostridium spiroforme* toxin. CDT toxin consists of the pore forming binding component CDTb and the enzymatic component CDTa. As it is only produced in about 35 % of *C. difficile* isolates, its pathogenic role is not yet fully understood.

#### 1.2.4.1 CDTb

CDTb (99 kDa) is the binding and translocation component of the CDT toxin produced by *Clostridium difficile*. It shares high homology of more than 80 % to *C. spiroforme* toxin Sb and *C. perfringens* iota toxin Ib (Figure 1.3). Notably, their B components are known to be interchangeable meaning that they are able to translocate the enzymatic components of the respective other toxin into target cells leading to intoxication and cell death (Popoff and Boquet, 1988). Lately the cellular receptor CDTb binds to was identified as the LSR receptor (lipolysis-stimulated lipoprotein receptor) (Papatheodorou *et al.*, 2011).



CDTb	1	MKIQMRNKKVLSFLTITAIIVSQALVYFVYAQTSTSNHNSKKKEIVNEDI LPNGLMGYYFTDEHFKDCLKMAPIKDGNLK	80
Sb	1	MKN----KKIIGLLTCTVLMGOMMTYFVYAKTITONYNDOEVETTNEKTVSSNGLMGYYFADEHFKDLELMAPVKNGLK	76
Ib	1	MNIQI--KNVFSFLTITAMISQTL SYNVYAQTTTQNDTNNQKEEITNENTLSSNGLMGYYFADEHFKDLELMAPIKNGDLK	78
CDTb	81	FEKKKVQKLLDKSDVKSIRWTGRIIPSKDGEYTLSTDRDDVLMQVNTFESTISNTLKVNMMKGGKYKVRIELQDKNLGS	160
Sb	77	FEKNKVEKLLTEKTNIKSIRWTGRIIPSKDGEYTLSTDKDNVLMQINAEGETANTLKVNMIKGGQYSTRIEIQDKDIGY	156
Ib	79	FEKKKVQKLLLEDNSIKSIRWTGRIIPSEEDGEYILSTDRNDVLMQINAKGDI AKTLKVNMMKGGQAYNTRIEIQDKNLGS	158
CDTb	161	IDNLSSPNLYWELDGMMKKI IPEENLFLRDYSNIEKDDPFIPNNFFDPKLMSSD-----WEDDLDLTDNDNIPDSYERN	233
Sb	157	VDDLSPKLYWELNGDKTLIPEKNLFLRDYSKI DENDFPFPKDNFFDLKLSRSARLASGWDDEDLTDNDNIPDAYEKN	236
Ib	159	IDNLSVPKLYWELNGNKTIVPEENLFRDYSKI DENDFPFPNNFFDVRFFS-----AAWEDDLDLTDNDNIPDAYEKN	232
CDTb	234	GYTIKDLIAVKWEDSFAEQGYKKYVSNYLESNTAGDPYTDYEQKASGSDKAIKTEARDPLVAAYPIVGVGMEKLIISTNE	313
Sb	237	GYTIKDSIAVKWEDSFAQGYKKYLSYLESNTAGDPYTDYQKASGSDKAIKAEARDPLVAAYPIVGVGMEKLIISTNE	316
Ib	233	GYTIKDSIAVKWEDSFAEQGYKKYVSNYLESNTAGDPYTDYQKASGSDKAIKLEARDPLVAAYPIVGVGMENLIISTNE	312
CDTb	314	HASIDQKTVSRATTNSKTESNTAGVSVVGVYQNGFTAVVTTNYSHTTNSSTAVQDSNGESWNTGLSINKGESAYINANV	393
Sb	317	HASIDQKTVSRNTTNSKTDANTAGVAINIAYQNGFTSITTTNYSHTTENSTAVQNSNGESWNTSLSINKGESAYINANV	396
Ib	313	HASSDQKTVSRATTNSKTDANTVGVSIAGYQNGFTSNTTTSYSHTTNSSTAVQDSNGESWNTGLSINKGESAYINANV	392
CDTb	394	RYNTGTAPMYKVTPTTNLVLDDGDTLSTIKAEQNIQGNLSPGDTYPPKGLSPLALNTMDQFSSRLIPINYDQLKKLDAG	473
Sb	397	RYNTGTAPMYKVTPTTNLVLDDGDTLTTIKAQDNQIGNLSPNETYPPKGLSPLALNTMDQFSSRLIPINYDQLKKLDAG	476
Ib	393	RYNTGTAPMYKVTPTTNLVLDDGETLATIKAQDNQIGNLSPNETYPPKGLSPLALNTMDQFNARLIPINYDQLKKLDAG	472
CDTb	474	KQIKLETTQVSGNFGIKNSGQIVTEGNSWSDYISQIDISASIIILDTENESYERRVIAKNLQDPEDKTPPELTIGEAIK	553
Sb	477	KQIKLETTQVSGNYGIKNSQGQIITEGNSWSDYISQIDLSASIIILDTGSDVFERRVIAKDNSSNPEDKTPVLTIGEAIK	556
Ib	473	KQIKLETTQVSGNYGFKNSQGQIITEGNSWSNYISQIDSVSASIIILDTGSDVFERRVAAKEQGNPEDKTPPELTIGEAIK	552
CDTb	554	AFGATKKDGLLYFNDIPIDESCVELIFDNTANKIKDSLKTLSDKKIYNVKLGERMILIKTPTYFTNFDDYNNYFSTWS	633
Sb	557	AFGATKNGEIILYFNMPIDESCVELIFDNTANLIKERLNALNDKKIYNVQLGERMKILIKTSTYFNNFDGYNNFPSSWS	636
Ib	553	AFSATKNGELLYFNGIPIDESCVELIFDNTSEIIEKQLKYLDDKKIYNVKLGERMILIKVFSYFTNFDEYNNFPASWS	632
CDTb	634	NVNTTNKDGLOQSANKLNGETKIKIPMSELKPYKRYVFSGYSKDPLTSNSIIVKIKAKEEKTDLVVEEQGYTKFSYEFET	713
Sb	637	NVDSNNQDGLQNAANKLSGETKIVIPMSKLNPKRYVFSGYLKNSSSTSNPIIVNIKAKEOKTYNLVSENYYKFSYEFET	716
Ib	633	NIDTKNDGLOQSVANKLSGETKIIIPMSKLPYKRYVFSGYSKDPSTSNPIIVNIKSKKEOKTYDLVVEEKDYTKFSYEFET	712
CDTb	714	TEKDSSNIEITLIGSGTFLDNLSITELNSTPEILDEPEVKIIPDQEIILDAHKIYFADLNFNPSTENTYINGMYFAPTQT	793
Sb	717	ICRDASNIEITLTSSTGTFIDNLSITELNSTPEILKEPDKVPSDQEIILDAHKIYADLSFNQSTANYYLGLYFPEPTQT	796
Ib	713	TGKDSSNIEITLTSSTGVIIDNLSITELNSTPEILKEPEIKVPSDQEIILDAHNKYADIKLDTNTENTYIDGIYFPEPTQT	792
CDTb	794	NKEALDYIQKYFVEATLQYSGFKDIGTKDKEMRNYLGDNPQPKTNYVNLRSYFTSGGENIMTYKKLRIYATPDDRELLVL	873
Sb	797	NKEVLDYIQKYKVEATLEYSGFKDIGTKDKELRNYTGDSPQPKTNYVNLRSYFTSGGENVMPYKKLRIYATPENRELLVL	876
Ib	793	NKEALDYIQKYFVEATLQYSGFKDIGTKDKEIRNYLGDNPQPKTNYVNLRSYFTSGGENVMTYKKLRIYAVTPDRELLVL	872

**Figure 1.3.** Sequence comparison of *Clostridium difficile* CDTb, *Clostridium spiroforme* Sb and *Clostridium perfringens* Ib. Amino acids which are the same for all three sequences are given in yellow; amino acids which are the same for two sequences are given in purple.

#### 1.2.4.2 CDTa

CDTa (49 kDa) is the enzymatic component of CDT toxin. Similar to C2I of *C. botulinum*, CDTa belongs to the family of actin-ADP-ribosylating toxins, modifying intracellular G-actin into F-actin at position Arg177 by transferring ADP-ribose group of NAD/NADPH. This leads to a blockage of actin polymerization disrupting the cell cytoskeleton and subsequently causing cell rounding and cell death. In low concentration, CDTa induces the formation of microtubule-based protrusions on the cell surface facilitating an increased bacterial adherence and colonization (Schwan *et al.*, 2009). CDTa shares about 84% sequence homology with the enzymatic component of iota toxin of *Clostridium perfringens*. The crystal structure of CDTa was solved in 2009, revealing that the protein possesses two functional domains linked by a loop (Sundriyal *et al.*, 2009). The N-terminal and the C-terminal domain both consist of 8  $\beta$ -strands and 5  $\alpha$ -helices. The N-terminal part is supposed to be responsible for the binding to CDTb, whereas the C-terminal part is thought to be capable of the enzymatic activity (Sundriyal *et al.*, 2009).

### **1.3 AIM OF THIS WORK**

Binary toxins share a common mode of intoxication in which an enzymatic component A is translocated through a channel formed by the component B to affect molecular pathways in the cytosol of target cells. Although lot of work was already done to elucidate the intoxication pathway, the exact mechanism is still not fully solved yet.

Some of the binary toxins gained notoriety, especially Anthrax toxin due its use as a bioterroristic weapon in the context of the attacks of 9/11 in 2001. But also CDT toxin is nowadays in the focus of public attention as the number of nosocomial infections caused by CDT toxin has dramatically increased in the last decade.

The aim of this work was to study the biophysical properties of the pore-forming subunits of these binary toxins in detail as well as binding and translocation characteristics of their enzymatic subunits.





---

---

## BINDING OF N-TERMINAL FRAGMENTS OF ANTHRAX EDEMA FACTOR (EF<sub>N</sub>) AND LETHAL FACTOR (LF<sub>N</sub>) TO THE PROTECTIVE ANTIGEN PORE \*

### 2.1 INTRODUCTION

The plasmid-encoded tripartite Anthrax toxin comprises a receptor-binding moiety termed protective antigen (PA) and two enzymatically active components, edema factor (EF) and lethal factor (LF) (Mock and Fouet, 2001; Abrami *et al.*, 2005; Young and Collier, 2007). Both enzymatic components need the binding component PA for delivery into target cells' cytosol where they exhibit enzymatic activities. LF is a highly specific zinc-dependent metalloprotease (90 kDa) targeting mitogen-activated protein kinase kinases (MAPKKs), e.g. MEK2, thereby initiating still poorly understood mechanisms leading to the death of some types of macrophages and to the inhibition of the release of pro-inflammatory mediators like nitric oxide, tumor necrosis factor- $\alpha$  (TNF- $\alpha$ ) and interleukin-1 $\beta$  (IL-1 $\beta$ ) from macrophages (Hanna *et al.*, 1993; Menard *et al.*, 1996; Pellizzari *et al.*, 1999). Recently, also dendritic cells, B cells and T-cells were found to be inhibited by LF (Agrawal *et al.*, 2003; Paccani *et al.*, 2005; Fang *et al.*, 2006). Edema factor (89 kDa) is a calmodulin- and Ca<sup>2+</sup>-dependent adenylate cyclase, interfering with cell signaling by increasing the cytosolic cAMP level, thereby altering water homeostasis (Mock and Fouet, 2001; Dal Molin *et al.*, 2006; Turk, 2007). In addition, EF is believed to be responsible for the edema found in cutaneous anthrax and was found to be a very effective inhibitor of T-cell activation and proliferation (Dixon *et al.*, 1999; Bradley *et al.*, 2001; Rossi Paccani *et al.*, 2007).

Protective antigen is secreted by *Bacillus anthracis* as water-soluble precursor form PA<sub>83</sub> (83 kDa) that undergoes proteolytic activation by furin-type proteases (Petosa *et al.*, 1997; Young and Collier, 2007). A 20 kDa fragment is cleaved off the N-terminus and the activated PA<sub>63</sub> monomer is able to form heptamers or octamers (Feld *et al.*, 2010), i.e. the prepore, binding to cell-surface

---

\*This work resulted from a collaboration of Michael Leuber, Angelika Kronhardt, Fiorella Tonello, Federica Dal Molin and Roland Benz published in *Biochimica et Biophysica Acta* and is included in this thesis in agreement with all authors.

exposed receptors (Bradley *et al.*, 2001). The prepore is endocytosed and after acidification, it is responsible for translocation of EF and/or LF into the cytosol of target cells (Miller *et al.*, 1999; Nassi *et al.*, 2002). Although the crystal structure of the membrane-bound PA<sub>63</sub>-channel is still not known, both the crystal structure of the prepore and a hypothetical model of the membrane-inserted pore are known to date (Petosa *et al.*, 1997; Nguyen, 2004). In addition, prominent structural and biophysical features of the PA-channel were investigated, e.g. the channel-forming properties of the PA-heptamer (Blaustein *et al.*, 1989; Finkelstein, 1994), blockage of the channels by small molecules (Orlik *et al.*, 2005) and enzymatic compounds EF and LF (Neumeyer *et al.*, 2006a; Neumeyer *et al.*, 2006b), the  $\Phi$ -clamp, including the important loop network for positioning of Phe-427 (Krantz *et al.*, 2005; Krantz *et al.*, 2006; Melnyk and Collier, 2006) and the potential mechanism of translocation of the enzymes (Krantz *et al.*, 2004; Zhang *et al.*, 2004a; Zhang *et al.*, 2004b).

The study of the elusive translocation mechanism of the enzymatic moieties of the binary AB toxins was started from different perspectives. Common approaches are the usage of the N-terminal truncated versions of EF and LF (254 and 268 amino acids, respectively) or the application of the chimeric LF<sub>N</sub>-DTA, a fusion protein of the N-terminal part of LF with diphtheria toxin A chain attached to its C-terminus for detection of successful translocation (Krantz *et al.*, 2004; Zhang *et al.*, 2004b; Zhang *et al.*, 2004c). However, especially the usage of EF<sub>N</sub> and LF<sub>N</sub> has a major drawback since the molecules only have a third of the original size. It was assumed that binding of full-length LF and truncated LF<sub>N</sub> should be comparable (Elliott *et al.*, 2000; Cunningham *et al.*, 2002), although it was already hinted recently that LF<sub>N</sub> shows weaker binding to the PA-pore as compared to LF (Chvyrkova *et al.*, 2007).

Here we present detailed studies of EF<sub>N</sub> and LF<sub>N</sub> binding to the PA<sub>63</sub> pore in artificial bilayer membranes, indicating that the truncated forms of edema and lethal factor show weaker binding affinity to the protective antigen channels as compared to full-length EF and LF. Additionally, we confirmed the increased binding of the enzymatic moieties to PA when a hexahistidine-tag is fused to the N-terminus (Blanke *et al.*, 1996; Zhang *et al.*, 2004b; Neumeyer *et al.*, 2006a; Neumeyer *et al.*, 2006b), supporting the generally accepted mode of N- to C-terminal translocation of the enzymes through endosomal membranes. Furthermore, we present evidence that the binding affinities of EF<sub>N</sub> and LF<sub>N</sub> to the PA<sub>63</sub> heptamers are highly voltage and ionic strength dependent.

---

## 2.2 EXPERIMENTAL PROCEDURES

### 2.2.1 Anthrax Protective Antigen PA<sub>63</sub>

Nicked anthrax protein PA<sub>63</sub> from *Bacillus anthracis* was obtained from List Biological Laboratories Inc., Campbell, CA. One mg of lyophilized protein was dissolved in 1 ml 5 mM HEPES, 50 mM NaCl, pH 7.5 complemented with 1.25% trehalose. Aliquots were stored at -20°C.

### 2.2.2 Cloning, expression and purification of truncated Anthrax Edema Factor (EF<sub>N</sub>) and Lethal Factor (LF<sub>N</sub>)

Genes coding for EF<sub>N</sub> (first 254 amino acids of EF) and for LF<sub>N</sub> (first 268 amino acids of LF) were sub-cloned from the plasmids pMMA187\_EF (Cataldi *et al.*, 1990) and pGEX-2Tk\_LF (Vitale *et al.*, 1998) in the *Bam*HI site of the plasmid pRSET-A (Invitrogen). The protein was expressed in *Escherichia coli* strain BL21 (DE3) (Novagen Inc.) in a native form, fused to a N-terminal hexahistidine-tag and purified with Ni<sup>2+</sup>-charged sepharose beads (Amersham Life Sciences). The proteins were eluted with 250 mM imidazol, 10 mM Tris, pH 7.5, and dialyzed over night with 150 mM NaCl, 10 mM Tris, pH 7.5. The His<sub>6</sub>-tag was removed from His<sub>6</sub>-EF<sub>N</sub> and His<sub>6</sub>-LF<sub>N</sub> by incubation with enteropeptidase as described elsewhere (Neumeayer *et al.*, 2006b).

### 2.2.3 Lipid bilayer experiments

Experiments with painted lipid bilayers were performed as has been described previously (Benz *et al.*, 1978) using diphytanoyl phosphatidylcholine (Avanti Polar Lipids, Alabaster AL) as membrane-forming lipid. The instrumentation consisted of a Teflon chamber with two compartments separated by a thin wall. The membrane hole between the two compartments had a surface area of about 0.4 mm<sup>2</sup>. PA<sub>63</sub> was added from concentrated protein solutions after the membranes had turned black. The temperature was maintained at 20°C during all experiments. The aqueous salt solutions were buffered with 10 mM MES, pH 6. The PA-induced membrane conductance was measured after application of a fixed membrane potential with a pair of silver/silver chloride electrodes with salt bridges inserted into the aqueous solutions on both sides of the membrane. The electrodes were connected in series to a voltage source and a homemade current-to-voltage converter made with a Burr Brown operational amplifier. The amplified signal was monitored on a storage oscilloscope (Tektronix 7633) and recorded on a strip chart recorder.

### 2.2.4 Titration experiments with EF<sub>N</sub> and LF<sub>N</sub>

The binding of EF<sub>N</sub>, His<sub>6</sub>-EF<sub>N</sub>, LF<sub>N</sub> and His<sub>6</sub>-LF<sub>N</sub> to the PA<sub>63</sub> channel was investigated with titration experiments similar to those used previously to study the binding of carbohydrates to the LamB channel of *Escherichia coli* or binding of chloroquine to C2II and PA channels and EF and LF to PA<sub>63</sub> channels in single- or multi-channel experiments (Benz *et al.*, 1987; Neumeyer *et al.*, 2006a; Neumeyer *et al.*, 2006b). The PA channels were reconstituted into lipid bilayer membranes from the *cis*-side, the side of addition of PA. About 30-60 minutes after the start of the reconstitution the rate of channel insertion in the membranes became very small. Then concentrated solutions of EF<sub>N</sub> or LF<sub>N</sub> (or their His<sub>6</sub>-tagged versions) were added to the *cis*-side of the membranes, i.e. the same side where PA<sub>63</sub> was applied, while stirring to allow equilibration. Figure 2.1 shows an example for a titration experiment where His<sub>6</sub>-EF<sub>N</sub> was added in increasing concentrations to the *cis*-side of a membrane containing about 3500 PA<sub>63</sub> channels. The membrane conductance decreased as a function of the concentration of His<sub>6</sub>-EF<sub>N</sub>.

The results of the titration shown in Figure 2.1A and of similar experiments, which all resulted in the block of the PA<sub>63</sub> channels, were analyzed in a similar way as performed previously (Benz *et al.*, 1987). The conductance,  $G(c)$ , of a PA<sub>63</sub> channel in the presence of EF<sub>N</sub> or LF<sub>N</sub> (or their His<sub>6</sub>-tagged derivatives) with the stability constant,  $K$ , and the EF<sub>N</sub>/LF<sub>N</sub> concentration,  $c$ , is given by the maximum conductance (without EF<sub>N</sub> or LF<sub>N</sub>),  $G_{\max}$  times the probability that the EF<sub>N</sub> or LF<sub>N</sub> binding site in the PA<sub>63</sub> channel is free:

$$G(c) = \frac{G_{\max}}{(1 + K \cdot c)} \quad [2.1]$$

Equation 1 may also be written as:

$$\frac{(G_{\max} - G(c))}{G_{\max}} = \frac{K \cdot c}{1 + K \cdot c} \quad [2.2]$$

meaning that the conductance as a function of the EF<sub>N</sub> or LF<sub>N</sub> concentration can be analyzed using Lineweaver-Burk plots.  $K$  is the stability constant for EF<sub>N</sub>, His<sub>6</sub>-EF<sub>N</sub>, LF<sub>N</sub> or His<sub>6</sub>-LF<sub>N</sub> binding to the PA<sub>63</sub> channel. The half saturation constant,  $K_s$ , of its binding is given by the inverse stability constant  $1/K$ . Figure 2.1B shows the fit of the data of Figure 2.1A using a Lineweaver-Burk plot. The good fit of the experimental data by the straight line in Figure 2.1B ( $r = 0.9978$ ) suggests indeed that the interaction between His<sub>6</sub>-EF<sub>N</sub> and the PA<sub>63</sub> channels represents a single-hit process. From the data of Figure 2.1A a stability constant,  $K$ , of  $(9.1 \pm 0.20) \times 10^7 \text{ M}^{-1}$  (half



saturation constant  $K_d = (11 \pm 0.27)$  nM was calculated from a least-squares fit for the binding of His<sub>6</sub>-EF<sub>N</sub> to the PA<sub>63</sub> channel using equation [2.2].

## 2.3 RESULTS

### 2.3.1 Evaluation of the stability constant of the binding of EF<sub>N</sub> or LF<sub>N</sub> to the PA<sub>63</sub> channel

The stability constant for the binding of EF<sub>N</sub> and LF<sub>N</sub> to the PA<sub>63</sub> channel were measured in multi-channel experiments, performed as described previously (Neumeyer *et al.*, 2006a). Concentrated solutions of either EF<sub>N</sub> or LF<sub>N</sub> were applied to the *cis*-side of an artificial lipid bilayer membrane, which contained many reconstituted PA<sub>63</sub> channels and the dose-dependent decrease of conductance was measured as a function of time (see Figure 2.1A). The mean ( $\pm$  SD) of the stability constant for EF<sub>N</sub> or LF<sub>N</sub> binding to the PA<sub>63</sub> channel was  $(6.0 \pm 0.6) \times 10^6 \text{ M}^{-1}$  and  $(5.0 \pm 0.8) \times 10^7 \text{ M}^{-1}$ , respectively, when the aqueous phase contained 150 mM KCl, 10 mM MES, pH 6.0. This means that the affinity for either EF<sub>N</sub> or LF<sub>N</sub> binding to PA<sub>63</sub> channels was more than 10 times smaller as compared to full-length EF and LF (see Table 2.1).

**Table 2.1. Stability constants  $K$  for the block of the PA<sub>63</sub> channel by EF<sub>N</sub>, LF<sub>N</sub>, His<sub>6</sub>-EF<sub>N</sub> and His<sub>6</sub>-LF<sub>N</sub> in lipid bilayer membranes.<sup>a</sup>**

$K [\text{M}^{-1}]$	$K_S [\text{nM}]$	$K [\text{M}^{-1}]$	$K_S [\text{nM}]$
<b>EF<sub>N</sub></b> $(6.0 \pm 0.6) \times 10^6$	166.8	<b>His<sub>6</sub>-EF<sub>N</sub></b> $(2.4 \pm 1.5) \times 10^8$	4.2
<b>LF<sub>N</sub></b> $(5.0 \pm 0.8) \times 10^7$	19.9	<b>His<sub>6</sub>-LF<sub>N</sub></b> $(1.0 \pm 0.6) \times 10^9$	0.97
<b>EF<sup>b</sup></b> $1.45 \times 10^8$	6.9	<b>His<sub>6</sub>-EF<sup>b</sup></b> $62.5 \times 10^8$	0.16
<b>LF<sup>b</sup></b> $3.62 \times 10^8$	2.76	<b>His<sub>6</sub>-LF<sup>b</sup></b> $55.2 \times 10^8$	0.18

The data represent means of at least three individual titration experiments.  $K_S$  is the half saturation constant. <sup>a</sup> Membranes were formed from diphytanoyl phosphatidylcholine/ndecane. The aqueous phase contained 150 mM KCl, 10 mM MES, pH 6.0, and about 1 ng/ml PA<sub>63</sub>; T=20 °C. <sup>b</sup> Taken from (Neumeyer *et al.*, 2006a).

### 2.3.2 His<sub>6</sub>-EF<sub>N</sub> and His<sub>6</sub>-LF<sub>N</sub> have a higher affinity for the PA<sub>63</sub> channel

EF<sub>N</sub> and LF<sub>N</sub> were expressed in *E. coli* with a His<sub>6</sub>-tag at the N-terminal end for easy purification. For most of the experiments the His<sub>6</sub>-tag was removed by treatment with enteropeptidase. His<sub>6</sub>-EF<sub>N</sub> and His<sub>6</sub>-LF<sub>N</sub> exhibited an even higher affinity for binding to the PA<sub>63</sub> channel, as has

previously been described in detail for the full-length EF and LF (Neumeyer *et al.*, 2006a; Neumeyer *et al.*, 2006b), and the truncated form of LF, LF<sub>N</sub> or LF<sub>263</sub> (Blanke *et al.*, 1996; Zhang *et al.*, 2004a; Zhang *et al.*, 2004b). The half saturation constants for His<sub>6</sub>-EF<sub>N</sub> and His<sub>6</sub>-LF<sub>N</sub> binding to the PA<sub>63</sub> channel were on average 4.2 nM ( $K = (2.4 \pm 1.5) \times 10^8 \text{ M}^{-1}$ ) and 0.97 nM ( $K = (1.0 \pm 0.6) \times 10^9 \text{ M}^{-1}$ ), respectively, at an ionic strength of 150 mM KCl and a membrane potential of 20 mV.

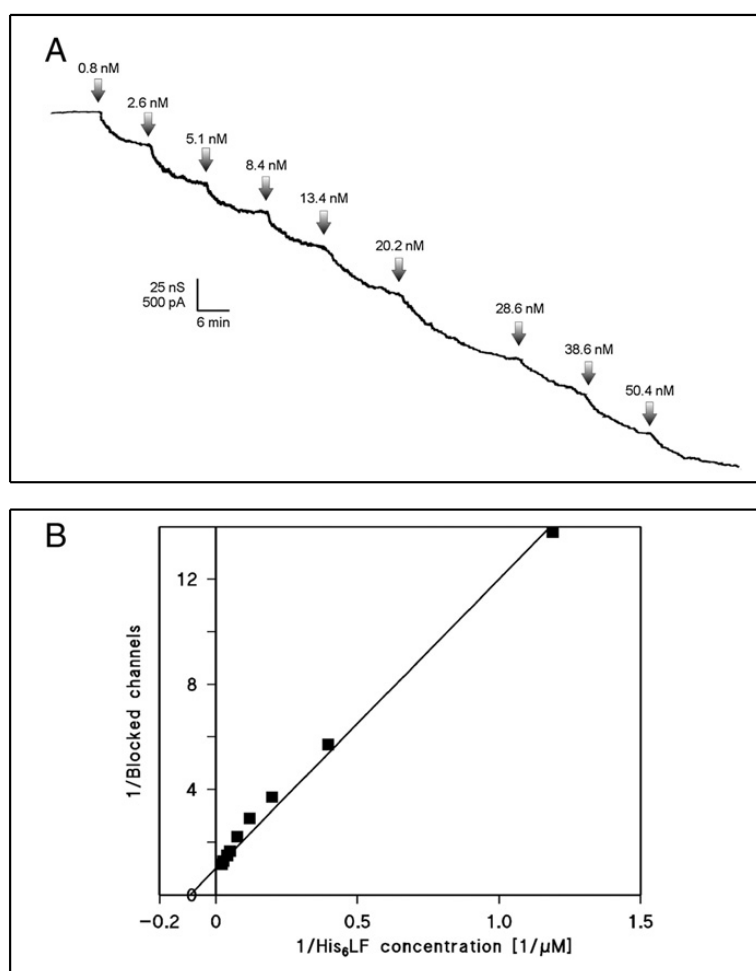


**Figure 2.1. Titration of PA<sub>63</sub>-induced membrane conductance and interpretation.** (A) The recording shows the time course of the current for about 8 min before addition of His<sub>6</sub>-EF<sub>N</sub>. The membrane was formed from diphytanoyl phosphatidylcholine/ n-decane. It contained about 3500 channels. The aqueous phase contained 1 ng/ml PA<sub>63</sub>-protein (added only to the *cis*-side of the membrane), 150 mM KCl, 10 mM MES pH 6. The temperature was 20 °C and the applied voltage was 20mV. His<sub>6</sub>-EF<sub>N</sub> was added at the concentrations shown at the top of the panel. Note that EF<sub>N</sub> blocks only the PA<sub>63</sub>-channels when it is added to the *cis*-side of the membrane (data not shown). The bottom line represents zero level of conductance. (B) Lineweaver–Burke plot of the inhibition of the PA<sub>63</sub>- induced membrane conductance by His<sub>6</sub>-EF<sub>N</sub>. The straight line was obtained from linear regression of the data points of Figure 2.1A ( $r=0.9978$ ) and corresponds to a stability constant  $K$ , for His<sub>6</sub>-EF<sub>N</sub> binding to PA<sub>63</sub> of  $(9.1 \pm 0.20) \times 10^7 \text{ M}^{-1}$  (half saturation constant  $K_S = (11 \pm 0.27) \text{ nM}$ ).

This means that the stability constants for binding for the His<sub>6</sub>-tagged enzymatic components were roughly a factor of 20 higher than those without the N-terminal hexahistidine-tag (see Table 2.1). The influence of the partially positively charged His<sub>6</sub>-tag on EF<sub>N</sub> and LF<sub>N</sub> binding indicates again that the interaction between the N-terminal end of truncated and full-length EF and LF and the PA<sub>63</sub> channels is based on ion-ion interactions similarly as discussed in the case of LF<sub>N</sub> (Zhang *et al.*, 2004b), EF and LF (Neumeyer *et al.*, 2006a; Neumeyer *et al.*, 2006b). It is noteworthy that the effect of the hexahistidine-tags for increased binding of EF<sub>N</sub> and LF<sub>N</sub> to PA channels is more striking as compared to its efficacy on full-length EF or LF.

### 2.3.3 EF<sub>N</sub> and LF<sub>N</sub> block PA<sub>63</sub> channels in a single hit process

The blockage of PA<sub>63</sub> channels by EF<sub>N</sub> and LF<sub>N</sub> was also studied on single-channel level. Therefore, only a few channels were reconstituted into lipid bilayer membranes (Neumeyer *et al.*, 2006a). Figure 2.2 shows an example of such an experiment.

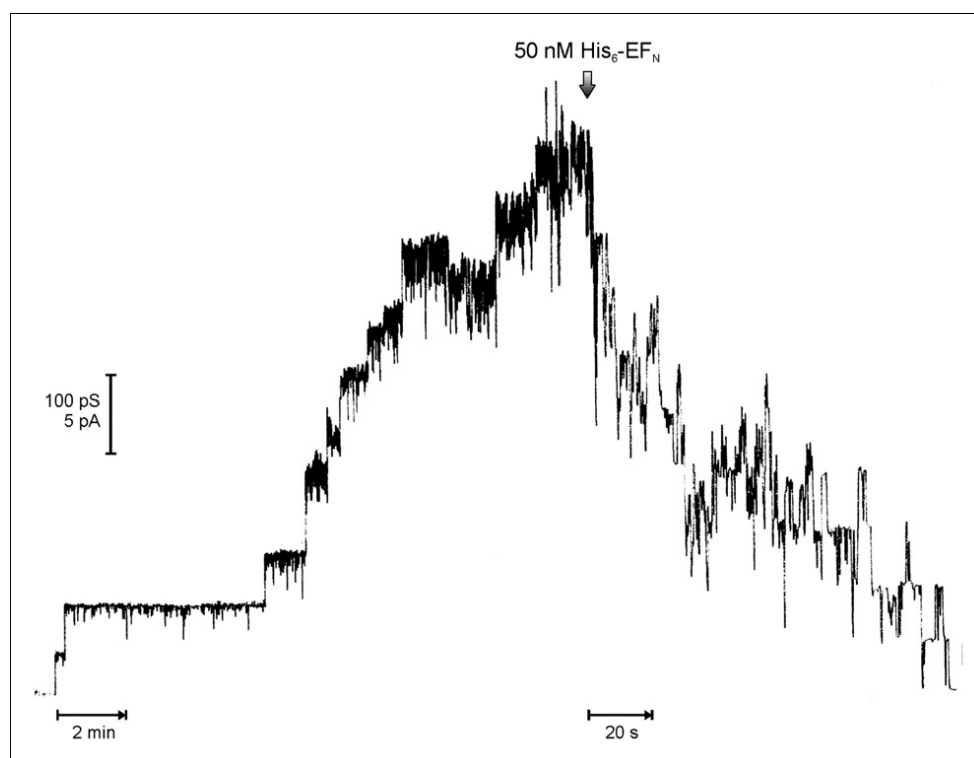


**Figure 2.2. Block of PA<sub>63</sub> channels by His<sub>6</sub>-EF<sub>N</sub> observed on the single channel level.** 50 mV were applied to the *cis*-side of a diphytanoyl phosphatidylcholine/n-decane membrane containing approximately 12 PA<sub>63</sub> channels. His<sub>6</sub>-EF<sub>N</sub> was added in a concentration of 50 nM to the *cis*-side of the membrane (arrow). All PA<sub>63</sub> channels subsequently closed, caused by binding of His<sub>6</sub>-EF<sub>N</sub> to the channels (150 mM KCl, 10 mM MES, pH 6.0). Note the change of the time-scale after the addition of the concentrated His<sub>6</sub>-EF<sub>N</sub> solution.

Only a minor amount of the PA<sub>63</sub> stock solution was added to the *cis*-side of a black lipid bilayer membrane followed by a step-wise increase of conductance by insertion of PA<sub>63</sub> channels. After 15 minutes about 12 PA<sub>63</sub> channels were reconstituted into the membrane. At that time (arrow in Figure 2.2) concentrated His<sub>6</sub>-EF<sub>N</sub> solution was added to the *cis*-side of the membrane (final concentration 50 nM), resulting in a subsequent step-wise decrease of membrane conductance caused by closing of the channels. Addition of His<sub>6</sub>-EF<sub>N</sub> to the *trans*-side did not influence PA<sub>63</sub>-mediated conductance (data not shown). Interestingly, the PA<sub>63</sub> channels exhibited strong flickering and gating, indicating a dynamic process for His<sub>6</sub>-EF<sub>N</sub> binding to the PA<sub>63</sub> channel. The channels closed almost completely after some time demonstrating complete His<sub>6</sub>-EF<sub>N</sub>-mediated channel block of PA<sub>63</sub> channels from the *cis*-side (see Figure 2.2). Complete blockage of the PA<sub>63</sub> channels also occurred with EF<sub>N</sub> and LF<sub>N</sub> where the hexahistidine-tags were removed (data not shown) but higher concentrations were needed for complete block of the channels (see above).

#### 2.3.4 EF<sub>N</sub> and LF<sub>N</sub> binding to PA<sub>63</sub> is ionic-strength dependent

In another set of experimental conditions, the titration experiments were repeated with different potassium chloride concentrations instead of 150 mM KCl. The results showed in principle that the stability constants for EF<sub>N</sub> and LF<sub>N</sub> (and their His<sub>6</sub>-tagged derivatives) binding to the PA<sub>63</sub> channel were highly ionic strength dependent. However, it was not possible to measure the stability constants for binding of EF<sub>N</sub> and LF<sub>N</sub> at an ionic strength of 1 M KCl because of the need of high concentrations of these proteins in the titration experiments due to the high half saturation constants. Even when high concentrations of EF<sub>N</sub> and LF<sub>N</sub> were added to the *cis*-sides of the membranes, no binding was detectable in 1 M KCl (data not shown). Thus it was only possible to measure the stability constants for His<sub>6</sub>-EF<sub>N</sub> and His<sub>6</sub>-LF<sub>N</sub> binding. They increased for decreasing ionic strength from 1 M KCl to 50 mM by a factor of more than 100 (from  $1.7 \times 10^6 \text{ M}^{-1}$  and  $2.3 \times 10^6 \text{ M}^{-1}$  to  $2.0 \times 10^8 \text{ M}^{-1}$  and  $4.2 \times 10^8 \text{ M}^{-1}$  respectively; see Table 2.2). These results suggested that at least part of the binding process between the PA<sub>63</sub> channel and both EF<sub>N</sub> and LF<sub>N</sub> is controlled by ion-ion interaction similar as in the case of full length EF and LF (Neumeyer *et al.*, 2006a; Neumeyer *et al.*, 2006b).

**Table 2.2. Ionic strength dependency of the stability constants,  $K$ , for the block of the PA<sub>63</sub> channel by His<sub>6</sub>-EF<sub>N</sub> and His<sub>6</sub>-LF<sub>N</sub> in lipid bilayer membranes<sup>a</sup>.**

Ionic strength [mM]	$K$ [M <sup>-1</sup> ]	$K_S$ [nM]	$K$ [M <sup>-1</sup> ]	$K_S$ [nM]
	<b>His<sub>6</sub>-EF<sub>N</sub></b>		<b>His<sub>6</sub>-EF<sup>b</sup></b>	
50	$2.0 \times 10^8$	4.9	$7.9 \times 10^8$	1.27
150	$2.4 \times 10^8$	4.2	$62.5 \times 10^8$	0.16
1000	$1.7 \times 10^6$	547	$3.4 \times 10^8$	2.93
	<b>His<sub>6</sub>-LF<sub>N</sub></b>		<b>His<sub>6</sub>-LF<sup>b</sup></b>	
50	$4.2 \times 10^8$	2.4	$31.6 \times 10^8$	0.32
150	$1.0 \times 10^9$	0.97	$55.2 \times 10^8$	0.18
1000	$2.3 \times 10^6$	432	$5.4 \times 10^8$	1.86

The data represent means of at least two individual titration experiments.  $K_S$  is the half saturation constant. <sup>a</sup>The membranes were formed from diphytanoyl phosphatidylcholine/*n*-decane. The aqueous phase contained the indicated KCl concentrations, including 10 mM MES, pH 6.0, and about 1 ng/ml PA<sub>63</sub>; T=20°C. <sup>b</sup>Taken from (Neumeyer *et al.*, 2006a).

### 2.3.5 Voltage increases binding affinity of EF<sub>N</sub> and LF<sub>N</sub> to the PA<sub>63</sub> channel

PA<sub>63</sub> channels show asymmetric voltage dependence. When a negative voltage is applied for a longer time to the *trans*-side of the membrane the current shows decreasing behavior probably because of slow PA<sub>63</sub> channel closure whereas positive voltages up to 150 mV do not induce channel gating (Blaustein *et al.*, 1990; Zhang *et al.*, 2004b; Orlik *et al.*, 2005; Neumeyer *et al.*, 2006b). Binding of full length LF to the PA<sub>63</sub> channels resulted in asymmetric current voltage curves showing a diode-like behavior whereas such a behavior was not observed when full size EF was added to the *cis*-side of the membrane (Halverson *et al.*, 2005; Neumeyer *et al.*, 2006a; Neumeyer *et al.*, 2006b). Addition of EF<sub>N</sub> to the *cis*-side resulted in a decrease of the membrane current similar to that of the titration experiments (see above). This means that EF<sub>N</sub>-binding to the PA<sub>63</sub> channel was more or less symmetrical for positive and negative potentials at the *cis*-side. Channel block was also observed when the side of addition of PA<sub>63</sub> and EF<sub>N</sub>, the *cis*-side, was negative, which means that channel block was not reversible under these conditions. This is demonstrated in Figure 2.3, which shows voltage pulses of  $\pm 20$  to  $\pm 70$  mV applied to the *cis*-side of a membrane containing about 500 PA<sub>63</sub> channels and 100 nM His<sub>6</sub>-EF<sub>N</sub> (Figure 2.3A) and pulses from  $\pm 50$  to  $\pm 70$  mV with 80 nM LF<sub>N</sub> (Figure 2.3B). The initial current response to the

applied voltages was symmetric with respect to the sign of the applied voltage. After the initial current response to the voltage step the current decreased in an exponential fashion. Following a voltage step of negative sign at the *cis*-side it decreased because of slow closure of the PA<sub>63</sub> channels, which had nothing to do with EF<sub>N</sub>/LF<sub>N</sub> binding but reflects voltage-induced gating of the channel (Blaustein *et al.*, 1990; Zhang *et al.*, 2004b; Orlik *et al.*, 2005; Neumeyer *et al.*, 2006a).

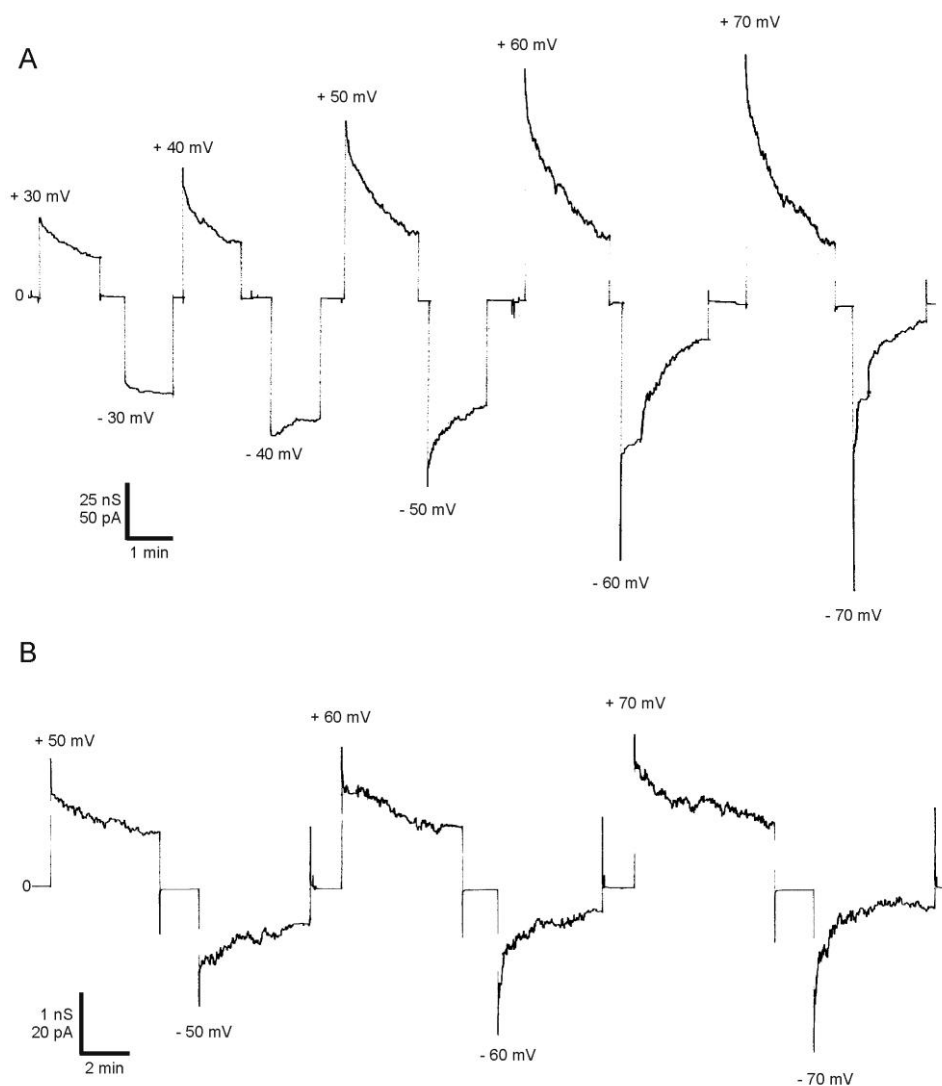


**Figure 2.3. Current response of PA channels in the presence of His<sub>6</sub>-EF<sub>N</sub> and LF<sub>N</sub>.** Voltage pulses between  $\pm 30$  mV and  $\pm 70$  mV (**A**) and  $\pm 50$  mV and  $\pm 70$  mV (**B**) were applied to the *cis*-side of a diphytanoyl phosphatidylcholine/*n*-decane membrane in the presence of 1 ng/ml PA<sub>63</sub> protein (added only to the *cis*-side of the membrane). The aqueous phase contained 150 mM KCl, 10 mM MES, pH 6, and 100 nM His<sub>6</sub>-EF<sub>N</sub> (**A**) or 80 nM LF<sub>N</sub> (**B**), respectively, both added to the *cis*-side. The temperature was 20°C.

Positive potentials at the *cis*-side resulted in an increased binding of His<sub>6</sub>-EF<sub>N</sub> to the PA<sub>63</sub> channels similar as has been observed for full size EF (Neumeyer *et al.*, 2006a). Starting with

about 20 to 30 mV the stability constant for His<sub>6</sub>-EF<sub>N</sub> binding to the channel increased considerably as the data of Figure 2.3A (upper traces) clearly indicate. This result indicated that channels, which were not blocked before by His<sub>6</sub>-EF<sub>N</sub> at 10 mV closed as a result of the higher voltage. The increase of the stability constant for binding could be calculated from the data of Figure 2.3 and similar experiments by dividing the initial current (which was a linear function of voltage) by the stationary current after the exponential relaxation and multiplying the ratio with the stability constant derived at 10 mV.

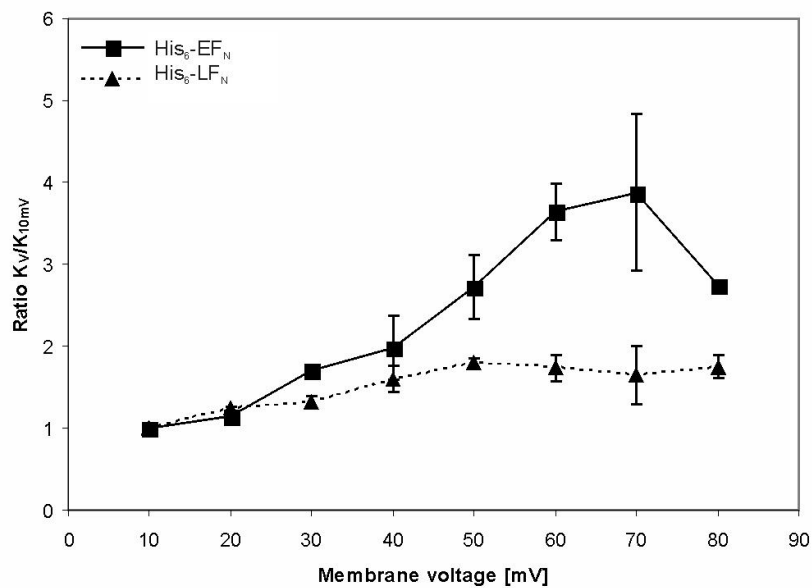


**Figure 2.4. Voltage-dependence of His<sub>6</sub>-EF<sub>N</sub> and His<sub>6</sub>-LF<sub>N</sub> binding to the PA<sub>63</sub> channel.** The stability constants of His<sub>6</sub>-EF<sub>N</sub> (squares) and His<sub>6</sub>-LF<sub>N</sub> (triangles) binding are given as a function the applied membrane potential taken from experiments similar to that shown in Figure 2.3. Means of at least three experiments are shown.

Figure 2.4 summarizes the effect of the positive membrane potential on the stability constant  $K$  for EF<sub>N</sub> and LF<sub>N</sub> binding as a function of the voltage. With EF<sub>N</sub>, starting with 20 mV,  $K$  started to increase and reached with about 60 to 70 mV a maximum. At that voltage  $K$  was roughly 4 times greater than at 10 mV (see Figure 2.4 squares). For higher voltages the stability constant decreased probably because of secondary effects of the high voltage on the PA<sub>63</sub> channel or on EF<sub>N</sub> binding. A significant increase of the stability constant for the PA<sub>63</sub>-binding of LF<sub>N</sub> at higher applied voltages could not be detected (see Figure 2.4, triangles). Experiments with LF<sub>N</sub> showed a different behavior because positive voltages caused a much smaller effect on LF<sub>N</sub> binding (see Figure 2.4), which means that the increase of the stability constant for LF<sub>N</sub> binding was not as



significant (see Figure 2.4, triangles). It is noteworthy that  $\text{LF}_N$ -binding to the  $\text{PA}_{63}$  channel was not asymmetric with respect to the sign of the applied voltage (Figure 2.4). This means that  $\text{LF}_N$ -binding does not induce a diode-like current-voltage relationship as full-size LF does. This result represents another difference to that obtained with full-size LF (Halverson *et al.*, 2005; Neumeyer *et al.*, 2006b).

## 2.4 DISCUSSION

In this study we investigated the interaction of the truncated versions of Anthrax edema (EF<sub>N</sub>) and lethal factor (LF<sub>N</sub>) to PA<sub>63</sub> channels in multi- and single-channel experiments in a quantitative manner. We could show that EF<sub>N</sub> and LF<sub>N</sub> are able to block PA channels in a single hit process when applied to the *cis*-side of membranes with only few channels or with many channels. Addition of EF<sub>N</sub> or LF<sub>N</sub> to the *trans*-side of a membrane with inserted PA channels showed no binding indicating the oriented insertion of the asymmetric PA pore in artificial and endosomal membranes *in vitro* and *in vivo* (Nassi *et al.*, 2002; Orlik *et al.*, 2005; Neumeyer *et al.*, 2006a). Titration experiments with a large number of channels allowed the calculation of half saturation constants in the nanomolar range for EF<sub>N</sub> and LF<sub>N</sub> binding or the binding of their His<sub>6</sub>-tagged derivatives. This means that the truncated enzymatic components are still able to bind to protective antigen channels. Examples for these experiments are shown in Figures 2.1A and 2.2. When compared to the full-length proteins, we present clear evidence that the 30 kDa N-terminal fragments show much weaker binding, i.e. the half saturation constants increased by a factor of about 10 to 20 as compared to the binding of full-size LF and EF (see Table 2.1).

The crystal structure of the protective antigen heptamer is not solved in its membrane-inserted conformation. However, the structure of the water-soluble prepore is known and a hypothetical model of the PA channel exists (Petosa *et al.*, 1997; Nguyen, 2004). The structure is derived from the *Staphylococcus aureus*  $\alpha$ -hemolysin, revealing a mushroom-shaped heptamer with a 14-stranded  $\beta$ -barrel inserted in the membrane and a large vestibule domain on the *cis*-side (Song *et al.*, 1996). This means that the initial binding of the enzymatic moieties will occur in the outer rim area of the channel, a fact confirmed by numerous studies (Cunningham *et al.*, 2002; Lacy and Collier, 2002; Krantz *et al.*, 2005; Lacy *et al.*, 2005). It was assumed that the binding of full-length and truncated versions of EF and LF shows roughly the same affinity, because the amino acids which are known to be responsible for binding of EF and LF to the PA<sub>63</sub> channel are localized within the N-terminal part of the protein, i.e. within the domains of EF<sub>N</sub> and LF<sub>N</sub> (Elliott *et al.*, 2000; Cunningham *et al.*, 2002; Lacy and Collier, 2002). However, based on the results presented here, we propose that additional interactions must exist either between the C-terminal part of the enzymatic components EF and LF (amino acids 255 and 269 onwards, respectively) and the vestibule domain of PA, or between C- and N-terminal domains of EF and LF that strengthen the conformation of the N-terminal binding motif, e.g. ion-ion interactions between Lys169 and Asp531, because binding of only the N-terminal 30 kDa of EF and LF is reduced by a significant degree as shown in Table 2.1, left column. Figure 2.1A presents good evidence that the blockage of the PA<sub>63</sub> channels is a single hit process, as indicated by the excellent fit of the experimental data by Lineweaver-Burk plots (Figure 2.1B). The single steps correspond to the size of

previously reconstituted PA pores into the membrane. This property of the truncated forms of EF and LF is comparable to the full-length enzymes as published previously (Elliott *et al.*, 2000; Halverson *et al.*, 2005; Neumeyer *et al.*, 2006a; Neumeyer *et al.*, 2006b).

Another prominent feature of the full-length enzymatic moieties of Anthrax toxin is the previously described increase of binding to the PA<sub>63</sub> channel caused by additional positively charged groups attached to the N-terminus (Blanke *et al.*, 1996; Zhang *et al.*, 2004b; Neumeyer *et al.*, 2006a; Neumeyer *et al.*, 2006b). Here, we confirmed the increased binding of EF<sub>N</sub> and LF<sub>N</sub> to PA channels *in vitro* when the proteins contained N-terminal hexahistidine-tags. His<sub>6</sub>-EF<sub>N</sub> and His<sub>6</sub>-LF<sub>N</sub> showed an at least 20-fold increase of binding as compared to their counterparts (see Table 2.1, right column). It has been previously described that the binding of EF and LF to the heptameric PA<sub>63</sub> channel is highly ionic strength-dependent because at least part of the binding between the enzymatic moieties and the PA<sub>63</sub> channel is caused by an interaction between oppositely charged groups localized on both molecules (Neumeyer *et al.*, 2006a; Neumeyer *et al.*, 2006b). In this study, we confirmed that ion-ion interactions between EF<sub>N</sub> and LF<sub>N</sub> and PA<sub>63</sub> channels are involved in binding. Decrease of the electrolyte concentration from 1 M to 50 mM potassium chloride increased the stability constant by a factor of more than 100 (see Table 2.2).

It has previously been shown that full-length LF binds to the PA<sub>63</sub> channel in a highly asymmetric manner with respect to the sign of the applied membrane potential, which leads to an asymmetric diode-like current-voltage curve (Halverson *et al.*, 2005; Neumeyer *et al.*, 2006a). However, this effect was considerably less pronounced with truncated LF<sub>N</sub>, which means that current-voltage curves were almost symmetrical for positive and negative potentials at the *cis*-side (data not shown). This result indicates that LF<sub>N</sub> binding to the PA<sub>63</sub> channel is different to that of full-size LF, indicating that part of the diode-like behavior of full-size LF may be localized within the region of LF that is missing in LF<sub>N</sub>. It is noteworthy that EF<sub>N</sub> or LF<sub>N</sub> binding has nothing to do with PA<sub>63</sub> channel inactivation that can be observed at low ionic strength and negative potentials applied to the *cis*-side (Blaustein *et al.*, 1990; Orlik *et al.*, 2005). This voltage-dependent channel-gating is a unique property of the heptameric PA<sub>63</sub> channel.

Positive potentials at the *cis* side resulted in an increased affinity of EF<sub>N</sub> binding to the PA<sub>63</sub> channel. Starting with 20 to 30 mV the stability constant for EF<sub>N</sub> binding to the channel increased up to about 4-fold for voltages of 60-70 mV (see Figure 2.4). For higher voltages the stability constant decreased slightly. A similar effect was also described for voltage-dependent binding of full-length EF, but the increase of the stability constant was higher (Neumeyer *et al.*, 2006b); this represents another indication that the PA<sub>63</sub>-binding properties of the truncated enzymatic components differ to their full-length counterparts, which may have also some

implications *in vivo* for the binding of EF to the Anthrax pore bound to target cells (i.e. macrophages) because of their membrane potential of about -60 to -80 mV (Ward *et al.*, 2006). This means that EF-binding to target cells should be enhanced when the target cell is polarized. Similarly, an effect of membrane voltage on EF-binding can also be expected in endosomes because of the action of the H<sup>+</sup>-ATPase and several ion channels that result in positive potentials inside the endosomes (Grabe and Oster, 2001). However, the magnitude of endosomal potentials is not known, which means that it is not clear if the potentials are able to decrease the half saturation constant of EF-binding to the PA<sub>63</sub> channels. On the other hand it seems to be important for efficient cell intoxication that the PA<sub>63</sub> channels on its surface are all decorated with EF before clathrin-dependent endocytosis occurs.

The considerations about the results presented in this study suggest that ion-ion interactions contribute substantially to the binding of EF<sub>N</sub> and LF<sub>N</sub> to PA. These interactions occur in addition to a variety of amino acids in LF, which are known by alanine-scanning mutagenesis to be responsible for LF binding to PA<sub>63</sub> (Cunningham *et al.*, 2002; Lacy and Collier, 2002). These amino acids are Asp182, Asp187, Leu188, Tyr223, His229, Leu235, and Tyr236 whose mutation resulted in significant binding defects of LF to PA<sub>63</sub>, effects that could be confirmed by mutation of the corresponding amino acids of EF. This surface-exposed cluster of amino acids, presumably involved in binding to PA, is formed by the intersection of  $\alpha$ -helices 1 $\alpha$ 6 and 1 $\alpha$ 10 and Tyr223, projecting outwards from helix 1 $\alpha$ 9 (Lacy and Collier, 2002). Here we present clear evidence that at least some additional forces must be involved in EF and LF binding to the PA<sub>63</sub> channel. However, our results also indicate that EF and LF-binding to the PA<sub>63</sub> channel are highly related processes. From this point of view, both enzymes have the same probability to penetrate inside the cells as it was also found *in vivo* (Paccani *et al.*, 2005).





---

---

## INTERACTION OF CHLOROQUINE-LIKE 4-AMINOQUINOLINES WITH ANTHRAX TOXIN PROTECTIVE ANTIGEN \*

### 3.1 INTRODUCTION

The Anthrax toxin is one of the main virulence factors of *Bacillus anthracis*. It represents a plasmid-encoded tripartite toxin composed of a receptor-binding moiety termed protective antigen (PA) and two different enzymatically active components, lethal factor (LF) and edema factor (EF) (Friedlander, 1986; Mock and Fouet, 2001; Collier and Young, 2003). The binding component PA transports both (EF and LF) into the cytosol of target cells where they exert their enzymatic activity. The 90 kDa highly specific zinc-dependent metalloprotease lethal factor targets mitogen-activated protein kinase kinases (MAPKKs), e.g. MEK2. Interference with this important pathway leads to subsequent death by apoptosis for some types of macrophages. Furthermore, the release of pro-inflammatory mediators like nitric oxide, tumour necrosis factor-alpha (TNF- $\alpha$ ) and interleukin-1 $\beta$  (IL-1  $\beta$ ) from macrophages is inhibited (Hanna *et al.*, 1993; Menard *et al.*, 1996; Pellizzari *et al.*, 1999). The second factor, termed edema factor (89 kDa), is a calmodulin- and Ca<sup>2+</sup>- dependent adenylate cyclase. By an increase of the cytosolic cAMP level, EF interferes with cell signalling. Altered processes including water homeostasis cause the cells to die finally (Dixon *et al.*, 1999; Mock and Fouet, 2001; Lacy and Collier, 2002).

*B. anthracis* secretes monomeric protective antigen (83 kDa) as a water-soluble precursor form (PA<sub>83</sub>). PA oligomerizes into heptamers or octamers (Feld *et al.*, 2010) after proteolytic cleavage of a 20 kDa N-terminal fragment (PA<sub>20</sub>) by a furin-like proteases, which leaves an activated PA<sub>63</sub> monomer (Petosa *et al.*, 1997; Young and Collier, 2007). Afterwards, up to three molecules of EF and/or LF can bind with high affinity to this prepore (Escuyer and Collier, 1991; Elliott *et al.*, 2000; Cunningham *et al.*, 2002). Binding to a cell-surface exposed receptor (Bradley *et al.*, 2001) is followed by endocytosis of the complex. The acidification of the endosome results in

---

\* This work resulted from a collaboration of Angelika Kronhardt, Christoph Beitzinger, Kerstin Duscha, György Hajos and Roland Benz and is included in this thesis in agreement with all authors.

translocation of the enzymatic components into the target cells' cytosol (Miller *et al.*, 1999; Nassi *et al.*, 2002). C2 toxin from *Clostridium botulinum* and iota toxin from *Clostridium perfringens* share this translocation mechanism (Barth *et al.*, 2002a).

Although the crystal structure of the prepore and a hypothetical model deliver a useful idea of the membrane-spanning functional pore, it would be helpful to know the crystal structure of the membrane-associated PA<sub>63</sub> channel (Petosa *et al.*, 1997; Nguyen, 2004). Due to the high toxicity of Anthrax toxin, channel-forming properties, as well as prominent structural and biophysical features of the PA<sub>63</sub> channel were investigated (Blaustein *et al.*, 1989; Finkelstein, 1994). The  $\Phi$ -clamp, including the loop network for stabilization of Phe427, was characterized as an important structure in recent studies (Krantz *et al.*, 2005; Krantz *et al.*, 2006; Melnyk and Collier, 2006). It has been proven to steer a potential translocation mechanism (Krantz *et al.*, 2004; Zhang *et al.*, 2004a; Zhang *et al.*, 2004b; Zhang *et al.*, 2004c). *In vitro* as well as *in vivo* PA and C2II channels can be blocked by chloroquine and related compounds (Orlik *et al.*, 2005). The binding site was identified inside the lumen of the C2II channel (Neumeyer *et al.*, 2008).

Here we studied the binding properties of chloroquine-based blocker-substrates to the protective antigen channel in artificial membranes leading to a dose-dependent decrease of membrane conductance in titration experiments. On- and off-rate constants of *in vitro*-binding to the PA channels were determined by the current noise analysis indicating a strong relationship between compound structure and binding kinetic to the PA channels.



## 3.2 MATERIAL AND METHODS

### 3.2.1 Materials

Recombinant, nicked PA<sub>63</sub> from *B. anthracis* was obtained from List Biological Laboratories Inc., Campbell, CA. One mg of lyophilized protein was dissolved in 1 ml 5 mM HEPES, 50 mM NaCl, pH 7.5 complemented with 1.25% trehalose. Aliquots were stored at -20°C.

### 3.2.2 Lipid bilayer experiments

Black lipid bilayer experiments were performed as described previously (Benz *et al.*, 1978) using a 1% solution of diphytanoyl phosphatidylcholine (Avanti Polar Lipids, Alabaster AL) in n-decane as membrane forming lipid. The instrumentation consisted of a Teflon chamber with two aqueous compartments separated by a thin wall. The small circular whole between the two compartments had a surface area of about 0.4 mm<sup>2</sup>. The aqueous salt solutions were buffered with 10mM MES, pH 6. All salts were obtained from Merck (Darmstadt, Germany). PA<sub>63</sub> was added from concentrated stock solutions after the membrane had turned black, to the aqueous phase to one side (the *cis*-side) of the membrane. The PA-induced membrane conductance was measured after application of a fixed membrane potential with a pair of silver/silver chloride electrodes with salt bridges inserted into the aqueous phase on both sides of the membrane. The electrodes were connected in series to a voltage source and a homemade current-to-voltage converter made with a Burr Brown operational amplifier. The amplified signal was monitored on a storage oscilloscope (Tektronix 7633) and recorded on a strip chart recorder (Rikandenki, Freiburg, Germany). The temperature was kept at 20°C throughout.

### 3.2.3 Titration experiments

The binding of the blocker-substrates to PA<sub>63</sub> channels was studied by titration experiments similar to those used previously to investigate binding of carbohydrates to the LamB channel of *E. coli* or binding of chloroquine or EF and LF, respectively, to C2II and PA<sub>63</sub> channels in single- or multi-channel experiments (Benz *et al.*, 1987; Bachmeyer *et al.*, 2003; Orlik *et al.*, 2005; Neumeyer *et al.*, 2006a; Neumeyer *et al.*, 2006b). PA<sub>63</sub> channels were reconstituted into lipid bilayer membranes from the *cis*-side of the artificial membrane and about 30-60 minutes after addition the rate of channel insertion decreased rapidly. Subsequently, concentrated solution of one blocker-compound was added to the same side of the membrane while stirring to allow equilibration. Figure 3.1 shows an example of a titration experiment of substance HA1383. The membrane conductance decreased as a function of concentration of the added substance. The

data of the channel blockage were analysed similar as performed previously (Benz *et al.*, 1978). The conductance,  $G(c)$ , of a PA channel in the presence of HA 1383 or a related compound with the stability constant,  $K$ , and the ligand concentration,  $c$ , is given by the maximum conductance (without ligand),  $G_{\max}$ , times the probability that the binding site is free.

$$G(c) = \frac{G_{\max}}{(1 + K \cdot c)} \quad [3.1]$$

This equation may also be written as follows,

$$\frac{(G_{\max} - G(c))}{G_{\max}} = \frac{K \cdot c}{1 + K \cdot c} \quad [3.2]$$

which means that the conductance as a function of the ligand concentration can be analysed using Lineweaver-Burk plots.  $K$  is the stability constant for the ligand binding to the PA channel. The half saturation constant,  $K_s$ , of its binding is given by the inverse stability constant  $K_s = K^{-1}$ .

### 3.2.4 Current-noise analysis

The membrane current was measured by a pair of silver/silver chloride electrodes switched in series with a battery operated voltage source and a current amplifier (Keithley 427 with a four pole filter or a home-made operational amplifier with a three pole filter). Feedback resistors between 0.01 and 10 G $\Omega$  were used. The membrane current increased as a result of insertion of reconstituted PA channels. The amplified signal was simultaneously monitored by a strip chart recorder and fed through a low pass filter (4 Pole Butterworth Low-Pass Filter) into an AD-converting card of an IBM-compatible PC. The digitized data were analysed with a homemade fast Fourier transformation program, which yielded identical results as compared to a commercial digital signal analyser (Ono Sokki CF210, Addison, IL). The spectra were composed of 400 points and averaged either 128 or 256 times. To analyse the data commercial graphic programs were used. For the derivation of the rate constants of ligand binding they were fitted to equations described in previously performed studies (Benz *et al.*, 1987; Andersen *et al.*, 1995; Orlik *et al.*, 2002b;2002a).

### 3.3 RESULTS

#### 3.3.1 Binding of blocker-substrates to the PA<sub>63</sub> channel

The PA<sub>63</sub> channel is fully oriented in artificial membranes when it is added to only one side of the membrane (Blaustein *et al.*, 1989). In previous studies we demonstrated that reconstituted PA channels as well as C2II channels can be blocked in lipid bilayer membranes by the addition of 4-aminoquinolines (Orlik *et al.*, 2005) and identified the binding site for chloroquine to C2II channels (Neumeyer *et al.*, 2008). The binding affinity strongly depends on negatively charged amino acids near the vestibule of PA channels.

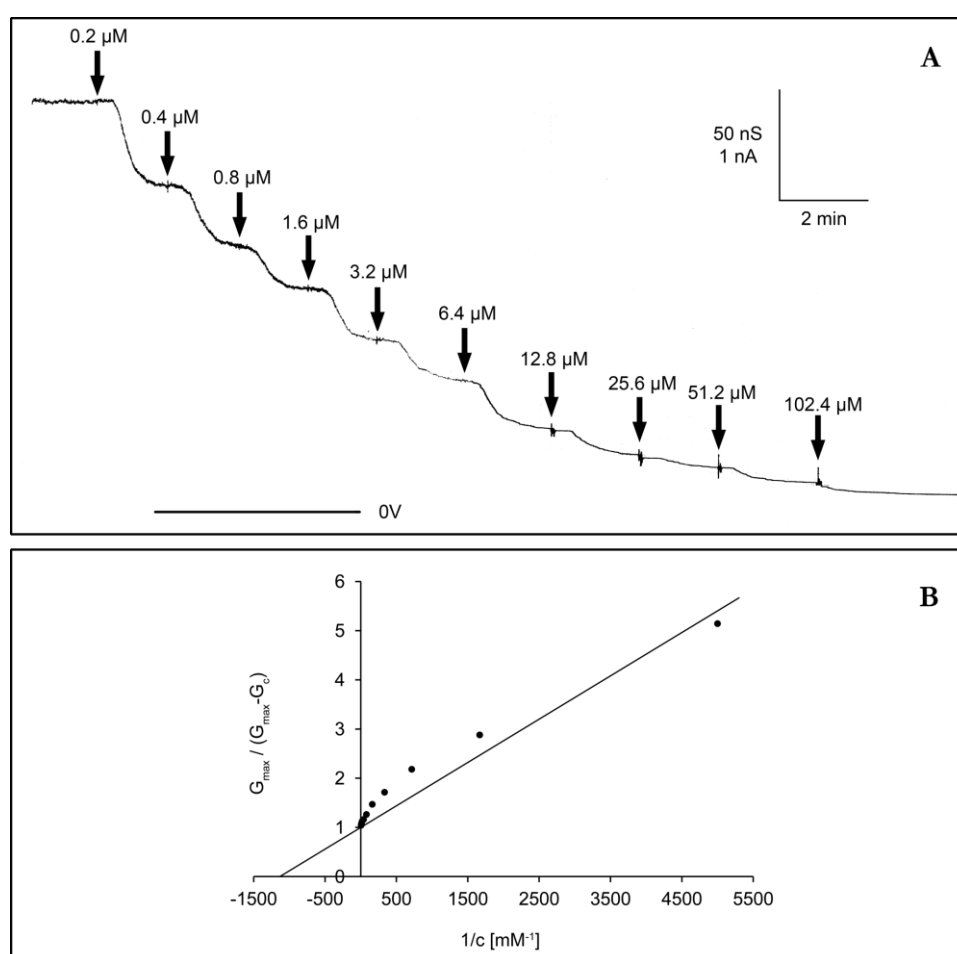


**Figure 3.1. Titration of PA<sub>63</sub> channels with HA 1383 and interpretation.** (A) Titration experiment of PA<sub>63</sub> induced membrane conductance with HA 1383. The membrane was formed from diphytanoyl phosphatidylcholine/n-decane. The aqueous phase contained 1 ng/ml PA<sub>63</sub> protein (added to the *cis*-side of the membrane), 150 mM KCl, 10 mM MES, pH 6.0. The temperature was constantly 20°C and the applied voltage was 20 mV. The membrane contained about 2250 PA<sub>63</sub> channels. HA 1383 was added to *cis*-side in the concentrations indicated. The bottom line represents zero level of conductance. (B) Lineweaver-Burke plot of the inhibition of PA<sub>63</sub> induced membrane conductance by chloroquine and related blocker-substrates. The straight lines correspond to the data points taken from titration experiments (Figure 3.1A).

The stability constants  $K$  for substrate binding to the PA channels were calculated by multi-channel titration experiments. Activated PA<sub>63</sub> was added to the *cis*-side (the side of the applied potential) of an artificial bilayer membrane while stirring. This leads to an increase of conductivity caused by channel insertion in the membrane which was monitored by a strip chart recorder. After about one to three hours when the conductance was virtually stationary the titration with blocker-substrates was started. Small amounts of concentrated solution of one compound were added to the aqueous phase on the *cis*-side of the membrane while stirring to allow equilibration. Subsequently, the PA channels were blocked and a dose-dependent decrease of conductance was measured as a function of time.

**Table 3.1. Stability constants  $K$  and half saturation constants  $K_s$  for chloroquine and related blocker-substrates to PA channels added to the *cis*-side of lipid bilayer membranes.**

Substrate	$K$ [ $M^{-1}$ ]	$K_s$ [mM]
HA 42	1456	0.69
HA 47	503	1.99
HA 112	18455	0.057
HA 486	37840	0.027
HA 708	11308	0.089
HA 728	11755	0.085
HA 766	29368	0.035
HA 1196	3750	0.37
HA 1212	7028	0.17
HA 1221	5967	0.17
HA 1371	3156	0.32
HA 1383	749020	0.0014
HA 1495	274457	0.0042
HA 1504	82911	0.012
HA 1568	477501	0.0027
HA 1882	7900	0.13
HA 1885	108620	0.0014
Chloroquine	861620	0.0014
Primaquine	51086	0.02

The data represent means of several individual titration experiments.  $K_s$  values from chloroquine are given for comparison and are taken from (Orlik *et al.*, 2005). Membranes were formed from diphytanoyl phosphatidylcholine/*n*-decane. The aqueous phase contained 150 mM KCl, 10 mM MES, pH 6.0, and about 1 ng/ml PA<sub>63</sub>; T=20 °C.

The titration curve shown in Figure 3.1A was analysed by Lineweaver-Burk plot (Figure 3.1B), which yielded a binding constant  $K$  of  $749 \times 10^3 \text{ M}^{-1}$  (half saturation constant  $K_s$  of  $1.34 \mu\text{M}$ ) for the binding of HA 1383 to the PA channel. This was considerably the lowest measured half saturation concentration, which is comparable to that of chloroquine ( $K_s = 1.43 \mu\text{M}$ ). The half saturation constants of the other blocker-substrates were higher than for chloroquine. While HA 1568, which possesses high homologies to HA 1383 and reached nearly the same half saturation concentration ( $K_s = 2.65 \mu\text{M}$ ), HA 1196 and HA 1371 revealed considerably higher half saturation constants ( $K_s = 368 \mu\text{M}$  and  $K_s = 320 \mu\text{M}$  respectively). In total we tested 17 substrates (Table 3.1 and Figure 3.2). The determined half saturation constants range from  $K_s = 1.34 \mu\text{M}$  for HA 1383 to  $K_s = 368 \mu\text{M}$  for HA 1196.

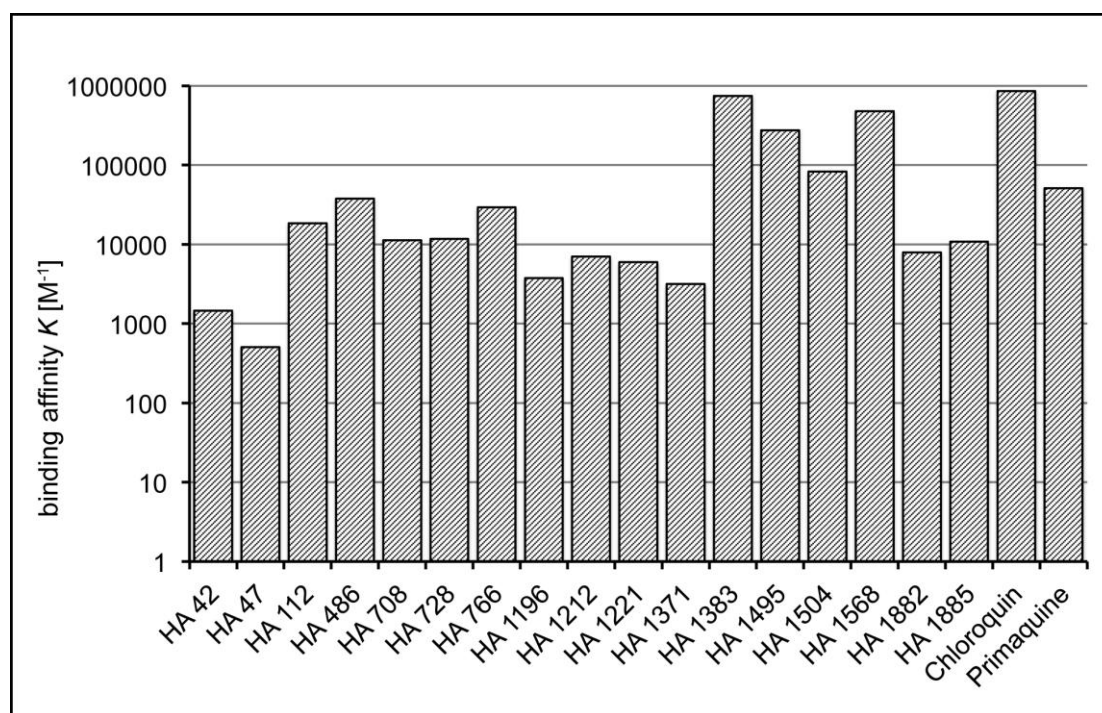


**Figure 3.2.**  $K$  values calculated from titration experiments to the PA channel. Data for chloroquine and primaquine are given for comparison (Orlik *et al.*, 2005).

### 3.3.2 Substrate-induced current-noise analysis of the $\text{PA}_{63}$ channel

The frequency-dependence of the spectral density values were measured using Fast-Fourier transformation of the current noise parallel to the titration experiments. The measurement of the current noise requires absolutely stationary conditions (Nekolla *et al.*, 1994; Andersen *et al.*, 1995). Therefore, the time between membrane formation and the start of the measurement was

extended compared to standard titration experiments. Afterwards, recording of a reference spectrum with only PA present in the aqueous phase, exhibits  $1/f$  noise in the frequency range between 1 and 50 Hz (Nekolla *et al.*, 1994; Wohnsland and Benz, 1997). Figure 3.3 depicts an example of a current noise measurement from PA<sub>63</sub> channels before adding any substrate (trace 0). At small frequencies up to  $\sim 100$  Hz the spectral density was dependent on  $1/f$ , which is typical for several open bacterial porin channels (Nekolla *et al.*, 1994; Jordy *et al.*, 1996; Wohnsland and Benz, 1997; Bezrukov and Winterhalter, 2000).

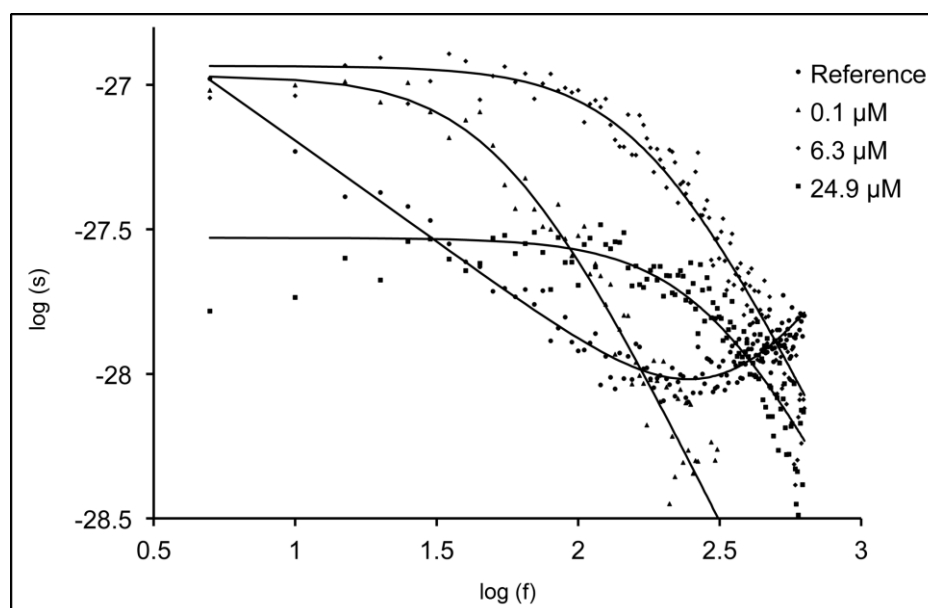


**Figure 3.3. Power density spectra of HA 1383 with PA<sub>63</sub> channels.** Power density spectra of HA 1383 induced current noise of about 450 PA<sub>63</sub> channels (added to the *cis*-side). Trace 0 shows the control (PA without substrate). Trace 1-3: The aqueous phase contained 0.1, 6.3 and 24.9  $\mu\text{M}$  HA 1383. The power density spectrum of trace 0 was subtracted.

The intrinsic noise of the preamplifier that produces a frequency-dependent current noise through the membrane capacity  $C_m$  led to an increase of the spectral density at frequencies above  $\sim 200$  Hz. In further experiments the concentration of the prevailing substrate was increased in defined steps. The power density spectra of the current noise in Figure 3.3 corresponded to that of Lorentzian type and could be fitted to a single Lorentzian after the subtraction of the reference spectrum. The power density spectrum,  $S(f)$ , is given by a Lorentzian function:

$$S(f) = \frac{S_0}{1 + (f/f_c)^2} \quad [3.3]$$

Such a type of noise is expected for a random switch with different on- and off-probabilities (Verveen and DeFelice, 1974; Conti and Wanke, 1975; Lindemann and DeFelice, 1981). The corner frequencies,  $f_c$ , of the Lorentzians are dependent on the on- and off-rate constants,  $k_{on}$  and  $k_{off}$ . This means that the corner frequencies  $f_c$  should increase with increasing substrate concentration.

**Table 3.2. Parameters of substrate-induced current noise in PA<sub>63</sub>.**

Substrate	$K$ [M <sup>-1</sup> ]	$K_s$ [μM]	$K_{on}$ [10 <sup>3</sup> M <sup>-1</sup> s <sup>-1</sup> ]	$K_{off}$ [s <sup>-1</sup> ]
HA 1383	443493	2.4	245025	516

$k_{on}$  and  $k_{off}$  were derived from a fit of the corner frequencies as a function of the ligand concentration.  $K$  is the stability constant for ligand binding derived from the ratio  $k_{on}/k_{off}$ . The data represent means of multiple individual experiments with the same substrate. Membranes were formed from diphytanoyl phosphatidylcholine/n-decane. The aqueous phase contained 150 mM KCl, 10 mM MES, pH 6.0, and about 1 ng/ml PA<sub>63</sub> on the *cis*-side; T=20 °C.

Assuming small perturbations in the number of closed channels due to microscopic variations in the number of bound ligand molecules, the reaction rate of the second order reaction is given by equation [3.4]:

$$\frac{1}{\tau} = 2\pi \times fc = k_1 \times c + k_{-1} \quad [3.4]$$

As  $k_{on}$  and  $k_{off}$  stand for the on- and off-rate of binding-events, they are also called  $k_{on}$  and  $k_{off}$ , respectively. Figure 3.4 depicts the linear fit over the corner frequencies derived over the time course of a complete current-noise-analysis measurement of HA1383 and PA. The according  $k_{on}$ -value is calculated to  $120 \times 10^6 \text{ M}^{-1}\text{s}^{-1}$ , which is in the range of diffusion limited processes. The off-rate for HA 1383 is very slow ( $k_{off} = 352 \text{ s}^{-1}$ ), reasoning a stable plug being formed in the PA channel. The corresponding constants  $K$  and  $K_s$  are in good agreement with the binding parameters derived from titration experiments.

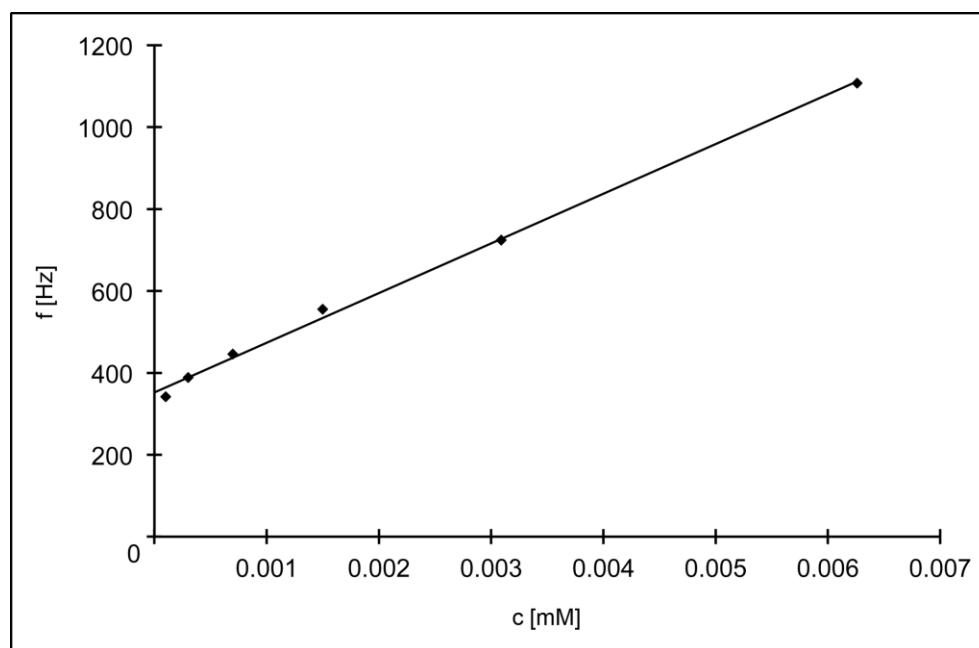


Figure 3.4. Tau-diagram of current noise analysis for the interaction of HA1383 and PA.



## 3.4 DISCUSSION

### 3.4.1 Half saturation constants emphasize the possibility to block PA<sub>63</sub>

Comparison of the half saturation constants derived from titration experiments (Table 3.1 and Figure 3.2) lead to the conclusion that changes in functional groups of the designed blocker-substrates result in large differences of binding affinity. One could easily determine substances with lower and more or less equal affinities to PA<sub>63</sub> pores compared with chloroquine, which is well known as a strong binding reagent towards that channel (Neumeyer *et al.*, 2008). Thereby, substrates with similar affinity are of special interest regarding a good possibility to rival binding of LF and EF, in order to inhibit intoxication. The high  $K$  values of HA 1383 and HA 1568 are in an interesting range to presumably block the uptake of enzymatic domains. These results have to be proven right by cell-based assays.

### 3.4.2 Titration and noise data allow deeper insight in the chemical-group-dependent binding constants

Regarding the results of the noise analysis (Table 3.2) one has to recognise that  $k_{on}$  is merely in the range of a diffusion controlled process, while the  $k_{off}$  values determine the time the substrate stays bound to the pore and therefore the stability of the blockage. This has been found for LF and EF in former measurements, too (Neumeyer *et al.*, 2006a; Neumeyer *et al.*, 2006b). Concerning merely equal  $k_{on}$ -values the stability constant  $K$ , being calculated by a quotient of  $k_{on}$  over  $k_{off}$ , is mainly depending on  $k_{off}$ .

Presumably, the plug, formed by HA 1383, surrounds the  $\Phi$ -clamp and is very stable under the acidic conditions in the endosome. Additionally, the aromatic core combined with positive charges should lead to assimilation in this compartment. These results imply the assumption that the blockage of PA channels for the transport of the native effectors could be achieved *in vivo* as well.

A closer look to the results reveals that positive charges in the substrates have the strongest influence on the binding affinity. The role of positive charges in binding or transport through PA channels has been analysed in many different publications (Blanke *et al.*, 1996; Beitzinger *et al.*, 2011; Kronhardt *et al.*, 2011a). There have been speculations about a profound binding which is related to two negative charged rings of amino acids surrounding the constriction site of the  $\Phi$ -clamp. On the one hand, this would represent a motive, which could introduce the unfolding and therefore trafficking via PA. On the other hand, substrates, which bind tightly in that region

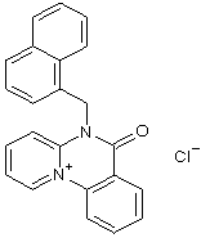
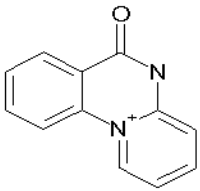
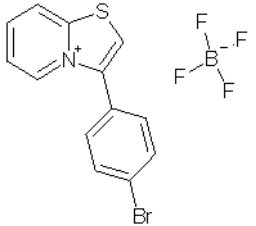
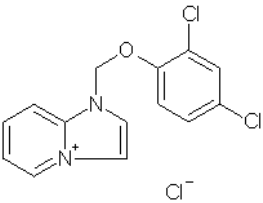
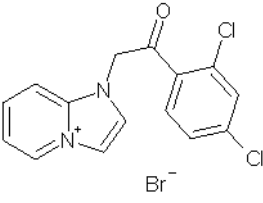
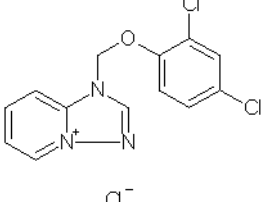
of the pore, would form a block that hinders the entrance of effectors even if they are bound to the channel before.

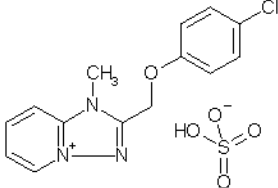
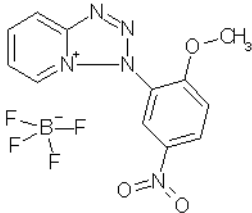
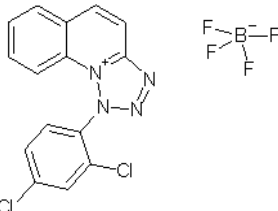
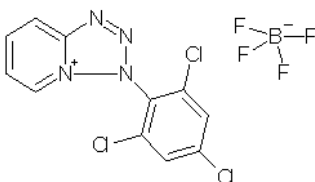
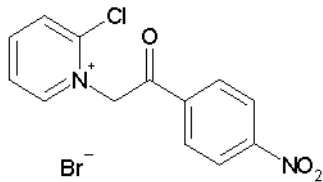
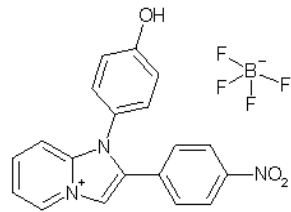
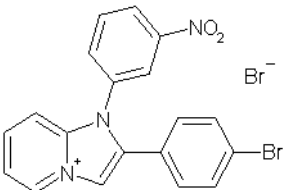
The ionic interaction of the blocker-substrates with the channel is contradictory to the effect of accumulation in the endosomes. Only substrates that have a change in overall charge from neutral in the cytosol or cell exterior to positive under acidic conditions in the endosome possess this desired feature. Therefore, the tested substrates are designed to have the charge dispersed over a large aromatic system, which should render them possible to cross membranes. In the endosome, the charges stabilize by acidic pH and the functional groups of the molecules. Additionally, there could be hydrophobic interactions between the aromatic ring system of the substrate and those of the  $\Phi$ -clamp. In former studies the enhanced affinity of cyclodextrins, which inherit aromatic residues was found, but could not be explained (Blanke *et al.*, 1996; Nestorovich *et al.*, 2010; Nestorovich *et al.*, 2011). In the duality of the aromatic group described above, we now present a hypothesis that has to be proven right by cell-based assays.

The most interesting results could be achieved by comparing the binding of two very homologue substrates: HA 1383 and HA 1568. They just differ in two functional groups. While HA 1383 has an OH- and a NO<sub>2</sub>-group, HA 1568 possesses chloride and bromide residues in the correlating positions (Table 3.3). All four administrate electron-pulling forces to the structure, thereby stabilizing the positive charge over the aromatic system. Nevertheless, a significant difference in  $K_i$  values of HA 1383 (1.34  $\mu$ M) and HA 1568 (2.65  $\mu$ M) was observed, implementing the important feature of those residues. Especially for the pharmacological characteristics and further design of blocker-substrates the possibility to alter certain qualities and at the same time residing in the desired range of affinity is crucial.

The results presented in this work were acquired in an *in vitro* system. Nevertheless, they strongly suggest a possible use of blocker-substrates tested for further experiments. These should include a cytotoxicity assay for the substances to get more information about critical concentrations in living organisms. Afterwards, cell-based assays should be used to determine whether the assumption of a stable block for the transport of the toxic-moieties of Anthrax is formed. The experiments with cell cultures could further proof if assimilation in the endosomal compartments is taking place, which would allow the use of lower overall concentrations of the substrates. In the end, *in vivo* studies could lead to the development of a new sort of drugs, which prevent infected persons to suffer from the symptoms of Anthrax intoxication. This would buy time to invent agents to deal with the infection and therefore could be a “live safer” after bio-terroristic assaults with multi-resistant strains.

Table 3.3. Structures of different blocker-substrates.

Substrate	Structure	Formula	Mass [g/mol]
HA 42		$C_{23}H_{17}ClN_2O$	372.86
HA 47		$C_{12}H_9ClN_2O$	232.67
HA 112		$C_{13}H_9BBrF_4NS$	378.00
HA 486		$C_{14}H_{11}Cl_3N_2O$	329.62
HA 708		$C_{15}H_{11}BrCl_2N_2O$	386.08
HA 728		$C_{13}H_{10}Cl_3N_3O$	330.60

Substrate	Structure	Formula	Mass [g/mol]
HA 766		$C_{14}H_{14}ClN_3O_5S$	371.80
HA 1196		$C_{12}H_{10}BF_4N_5O_3$	359.05
HA 1212		$C_{15}H_9BCl_2F_4N_4$	402.98
HA 1221		$C_{11}H_6BCl_3F_4N_4$	387.36
HA 1371		$C_{13}H_{10}BrClN_2O_3$	357.59
HA 1383		$C_{19}H_{14}BF_4N_3O_3$	419.15
HA 1495		$C_{19}H_{13}Br_2N_3O_2$	475.14

Substance	Structure	Formula	Mass [g/mol]
HA 1504		$C_{22}H_{18}Br_2N_2O_3$	518.21
HA 1568		$C_{19}H_{13}BBrClF_4N_2$	471.49
HA 1882		$C_{19}H_{15}BF_4N_4O_2S$	450.23
HA 1885		$C_{19}H_{15}BF_4N_4O_3S$	466.23
Chloroquine		$C_{18}H_{26}ClN_3$	319.87
Primaquine		$C_{15}H_{21}N_3O$	259.35



---

---

## CROSS-REACTIVITY OF ANTHRAX AND C2 TOXIN: PROTECTIVE ANTIGEN PROMOTES THE UPTAKE OF BOTULINUM C2I TOXIN INTO HUMAN ENDOTHELIAL CELLS\*

### 4.1 INTRODUCTION

Binary toxins of the AB<sub>7</sub> type are highly potent and specialized bacterial protein toxins and are organized in two different polypeptide chains that are separately secreted in the external media of Gram-positive bacteria (Barth *et al.*, 2004). Component A is responsible for the intracellular enzymatic activity of the toxin, whereas heptamers or octamers (Kintzer *et al.*, 2009), of the component B are necessary for receptor-binding and translocation of component A into target cells. Given the close homology of structure of the binding components of these two-component toxins it is of importance to decipher whether each component can functionally substitute for each other to intoxicate cells, that we termed cross-reactivity.

One of the most prominent toxins of this type of toxin is Anthrax toxin from *Bacillus anthracis* (Collier and Young, 2003). This toxin possesses a binding and translocation component, protective antigen (PA) and two enzymatic subunits, edema factor (EF) and lethal factor (LF). Edema factor (EF) is a 89 kDa Ca<sup>2+</sup>- and calmodulin-dependent adenylate cyclase which catalyzes the production of intracellular cAMP and causes severe edema. Lethal factor (LF) is a 90 kDa Zn<sup>2+</sup>-binding metalloprotease that cleaves mitogen-activated protein kinase kinases (MAPK-kinases) and thereby interferes with the MAPK cascade, a major signaling pathway, triggered by surface receptors, controlling cell proliferation and survival (Turk, 2007; Young and Collier, 2007). The binding component PA is essential for delivery of both enzymes into the target cells (Mock and Fouet, 2001; Ascenzi *et al.*, 2002; Young and Collier, 2007). It is secreted as an 83 kDa water-soluble precursor form (PA<sub>83</sub>) and needs to undergo proteolytic activation by cell-bound

---

\* This work resulted from a collaboration of Angelika Kronhardt, Monica Rolando, Christoph Beitzinger, Caroline Stefani, Michael Leuber, Gilles Flatau, Michel R. Popoff, Roland Benz and Emmanuel Lemichez published in *PLoS ONE* and is included in this thesis in agreement with all authors.

furin. After the activation of PA<sub>83</sub>, the remaining 63 kDa PA<sub>63</sub> forms an oligomeric channel responsible for the binding and translocation of EF and/or LF into the cytosol of target cells (Petosa *et al.*, 1997; Miller *et al.*, 1999; Abrami *et al.*, 2004; Abrami *et al.*, 2005).

*Clostridium botulinum*, well known for the production of potent neurotoxins, produces various protein toxins, such as the AB<sub>7</sub> type C2 toxin (Boquet and Lemichez, 2003; Aktories and Barth, 2004; Aktories *et al.*, 2004). The binding component of C2 toxin, C2II (60 kDa after proteolytic cleavage with trypsin), forms heptamers that insert into biological and artificial membranes at an acidic pH and promotes the translocation of the 45 kDa enzymatic component C2I into the cytosol of the target cells upon receptor-mediated endocytosis of the complex (Barth *et al.*, 2000; Blocker *et al.*, 2000). C2I acts as an ADP-ribosyltransferase on monomeric G-actin, causing disruption of the actin cytoskeleton (Considine and Simpson, 1991; Blocker *et al.*, 2003b).

The enzymatic components of Anthrax and C2 toxin differ significantly in their enzymatic activity and do not show any homology in their primary structures. However, the binding components PA and C2II share a considerable sequence homology of about 35% in two of three domains, indicating that they are closely related in structure and hence also in function (Petosa *et al.*, 1997; Neumeyer *et al.*, 2006a; Schleberger *et al.*, 2006; Young and Collier, 2007). In recent years, many important structural features, particularly concerning PA, have been unveiled, such as the  $\Phi$ -clamp and the loop network responsible for allocation of the seven PA monomers (Krantz *et al.*, 2005; Melnyk and Collier, 2006). Interesting details concerning the possible mode of translocation are known, all favoring an acid-induced disassembly of the enzymatic components to a molten globular state, followed by threading of the N-terminal part of the polypeptide chain through the pore (Krantz *et al.*, 2004; Krantz *et al.*, 2005; Krantz *et al.*, 2006; Melnyk and Collier, 2006). However, the exact mode of transporting the enzymatic components into the cytosol of target cell is still not fully solved. The first crucial step of the translocation mechanism is the binding of the enzymatic components to the receptor-bound heptamers on the cell surfaces (Barth 2004a). Previous results of our and other groups evidenced that truncated forms of the enzymatic components as well as full size EF and LF block the pores formed by PA<sub>63</sub>, and that an N-terminal His<sub>6</sub>-tag strengthens their affinity (Zhang *et al.*, 2004b; Halverson *et al.*, 2005; Neumeyer *et al.*, 2006a). Binding of the N-terminal ends of EF and LF to PA<sub>63</sub> is followed by endocytosis, acidification of the endosomes and finally release of the enzymatic components into the cytosol of target cells, where they exert their fatal enzymatic activities (Abrami *et al.*, 2004; Abrami *et al.*, 2005; Wei *et al.*, 2006). Interestingly, LF's amino-terminal part, LF<sub>N</sub> (LF<sub>1-254</sub>), is sufficient to confer the ability to associate with PA<sub>63</sub> heptamers. It can even be used to drive the translocation of unrelated polypeptides into target cells via PA<sub>63</sub> or C2II (Leppla *et al.*, 1999; Rolando *et al.*, 2009).



To further elucidate the mode of binary toxins' translocation into target cells and the possible cross-reactivity of the different enzymatic components via the homologous binding component of the other toxin, we performed *in vitro* and *in vivo* (i.e. cell-based assay) experiments interchanging the different A-B components of Anthrax and C2 toxin. Most importantly our data show the high capacity of PA<sub>63</sub> to bind C2I *in vitro* in the black lipid bilayer assay. Complementary to these findings we evidence the functionality of PA/C2I chimera toxin in cell intoxication. Further, C2II appeared more specifically involved in C2I binding and translocation. Together our data unveiled the remarkable plasticity of PA for supporting cell intoxication by a C2I distantly related AB toxin component.

## 4.2 EXPERIMENTAL PROCEDURES

### 4.2.1 Materials

PA, LF and EF genes were PCR-amplified from genomic DNA of *Bacillus anthracis* strain Sterne (a kind gift of Patrice Boquet, Nice, France) and cloned into the pQE30 (Qiagen), pET28a and pET22b (Novagen) expression plasmids, respectively. The N-terminal His<sub>6</sub>-tag was removed from His<sub>6</sub>-EF by incubation with thrombin and from His<sub>6</sub>-LF with enteropeptidase, respectively. Nicked Anthrax PA<sub>63</sub> from *B. anthracis* was obtained from List Biological Laboratories Inc., Campbell, CA. One mg of lyophilized protein was dissolved in 1 ml 5 mM HEPES, 50 mM NaCl, pH 7.5 complemented with 1.25% trehalose. Aliquots were stored at -20°C. Channel formation by PA<sub>63</sub> was stable for months under these conditions. C2I and C2II genes were PCR-amplified from genomic DNA of *Clostridium botulinum* D strain 1873 and cloned into pET22 (Novagen) and pQE30 (Qiagen) expression plasmids. All genes were cloned with *Bam*HI-*Sac*I restriction sites. Recombinant toxins containing His<sub>6</sub>-tags were expressed in *E. coli* BL21 (DE3) and purified on a Chelating Sepharose Fast Flow column previously chelated with nickel (Amersham Biosciences) as recommended by the manufacturer and described previously (Leppla *et al.*, 1999; Rolando *et al.*, 2009). Fractions containing toxin were pooled and dialyzed over night against 250 mM NaCl and 25 mM Tris-HCl, pH 8. Recombinant C2II and C2I proteins used for bilayer measurements were cloned in pGEX-2T vector in *Escherichia coli* BL21 cells and expressed as glutathione *S*-transferase (GST) fusion proteins with the glutathione *S*-transferase-fusion Gene Fusion System from Amersham Pharmacia Biotech (Blocker 2000, 2003b). The proteins were purified as described previously (Blocker *et al.*, 2003a) and incubated with thrombin (3.25 NIH units/ml bead suspension) for cleavage of the GST-tag (Blocker *et al.*, 2003b). C2II was activated with 0.2 µg of trypsin per microgram of protein for 30 min at 37°C (Blocker *et al.*, 2003a).

### 4.2.2 Western Blots

The polyclonal antibodies against the N-terminal part of MEK2 (N20) were purchased from Santa Cruz Biotechnology; monoclonal antibodies against β-actin were obtained from Sigma-Aldrich (clone AC-74). Primary antibodies were visualized using goat anti-mouse or anti-rabbit horseradish peroxidase-conjugated secondary antibodies (DakoCytomation), followed by chemiluminescence detection ECL (GE Healthcare).

### 4.2.3 Cell culture

Human umbilical vein endothelial cells (HUVECs, a human primary cell line obtained from PromoCell) were grown in serum-free medium (SFM) supplemented with 20% FBS (Invitrogen), 20 ng/ml basic BFGF (Invitrogen), 10 ng/ml EGF (Invitrogen) and 1 µg/ml heparin (Sigma-Aldrich) as described previously (Doye *et al.*, 2006).

### 4.2.4 Adenylate cyclase activity

Intracellular concentration of cyclic AMP (cAMP) was determined using the Cyclic AMP Assay (R&D Systems).

### 4.2.5 ADP-ribosylation

Control cells or intoxicated HUVECs ( $10^5$  cells/conditions) were homogenized in 0.25 ml cold BSI buffer (3 mM imidazole pH 7.4, 250 mM sucrose) supplemented extemporaneously with 1 mM phenylmethylsulfonyl fluoride. Cells were lysed by passing through a 1 ml syringe equipped with a 25G x 5/8"-needle (U-100 Insulin, Terumo) 40 times. Nuclei were removed by centrifugation for 10 minutes at 4°C. Protein concentrations of the post-nuclear supernatants were determined using Dc protein assay (Bio-Rad). ADP-ribosylation was performed for 90 minutes at 37°C on 5 µg of intoxicated cell lysates, supplemented with 0.5 µCi [ $^{32}$ P]-NAD (800 Ci/mmol) and 1 µg of C2I. Proteins were resolved on 12% SDS-PAGE and *in vitro* ADP-ribosylated actin was revealed using a phosphorimaging system.

### 4.2.6 Lipid bilayer experiments

Black lipid bilayer measurements were performed as described previously (Benz *et al.*, 1987). The instrumentation consisted of a Teflon chamber with two aqueous compartments connected by a small circular hole. The hole had a surface area of about 0.4 mm<sup>2</sup>. Membranes were formed by painting a 1% solution of diphytanoyl phosphatidylcholine (Avanti Polar Lipids, Alabaster, AL) in n-decane onto the hole. The aqueous salt solutions (Merck, Darmstadt, Germany) were buffered with 10 mM MES to pH 5.5 to pH 6. Control experiments revealed that the pH was stable during the time course of the experiments. The binding components of the binary toxins were reconstituted into the lipid bilayer membranes by adding concentrated solutions to the aqueous phase to one side (the *cis*-side) of a black membrane. The temperature was kept at 20°C throughout. Membrane conductance was measured after application of a fixed membrane potential with a pair of silver/silver chloride electrodes inserted into the aqueous solutions on

both sides of the membrane. Membrane current was measured using a homemade current-to-voltage converter made with a Burr Brown operational amplifier. The amplified signal was monitored on a storage oscilloscope and recorded on a strip chart recorder.

#### 4.2.7 Binding experiments

The binding of EF and LF to the C2II channel and the binding of C2I to the PA<sub>63</sub> and to the C2II channel was investigated performing titration experiments similar to those used previously to study the binding of 4-aminoquinolones to the PA<sub>63</sub> and C2II channels and LF to the PA<sub>63</sub> channel in single- or multi-channel experiments (Bachmeyer *et al.*, 2003; Orlik *et al.*, 2005; Neumeyer *et al.*, 2006b). The PA<sub>63</sub> and C2II channels were reconstituted into lipid bilayers. About 60 minutes after the addition of either activated PA<sub>63</sub> or C2II to the *cis*-side of the membrane, the rate of channel insertion in the membranes was very small. Then concentrated solutions of EF, LF or C2I were added to the *cis*-side of the membranes while stirring to allow equilibration. The results of the titration experiments, i.e. the blockage of the channels, were analyzed using Langmuir adsorption isotherms (see eqn. [4.1]) (Benz *et al.*, 1987; Neumeyer *et al.*, 2006a).

$$G(c) = G_{\max} \frac{1}{(K \cdot c + 1)} \quad [4.1]$$

$G(c)$  is the conductance of the channels at a given concentration  $c$  of the enzymatic components and  $G_{\max}$  is their conductance before the start of the titration experiment (at  $c = 0$ ).  $K$  is the stability constant for binding of the enzymatic components of the binary toxins to the PA<sub>63</sub> or C2II channels. The half saturation constant  $K_s$  of binding is given by the inverse stability constant  $1/K$ . The percentage of blocked channels is given by:

$$\% \text{ closed channels} = \frac{100 \cdot K \cdot c}{K \cdot c + 1} \quad [4.2]$$

#### 4.2.8 Statistics

Unpaired, two-sided Student's t-test was used to analyze biological data with \*  $p < 0.05$ . The statistical software used was Prism 5.0b. The fit of the data from the titration experiments with lipid bilayers was performed using Fig.P. For most of the fits of the titration data with equation [4.2] we obtained  $r^2 > 0.99$ .

## 4.3 RESULTS

### 4.3.1 Interaction of PA<sub>63</sub> with C2I *in vitro*

The stability constant  $K$  for the binding of C2I to the PA<sub>63</sub> channel was measured in multi-channel experiments, performed as described previously (Neumeyer *et al.*, 2006b). About 60 minutes after addition of the protein, the rate of conductance increase had slowed down considerably. At that time, small amounts of a concentrated enzyme solution were added to the *cis*-side of the membrane and the PA<sub>63</sub>-induced membrane conductance decreased in a dose-dependent manner. Figure 4.1A shows an example for a titration experiment with an applied voltage of 20 mV in 150 mM KCl in which increasing concentrations of C2I (arrows) were added to the *cis*-side of a membrane containing about 5500 PA<sub>63</sub> channels. The membrane conductance decreased as a function of the C2I concentration within a few minutes after addition of C2I (see Figure 4.1A). The data of Figure 4.1A and of similar experiments were analyzed using equation [4.2] as described previously (Benz *et al.*, 1986; Neumeyer *et al.*, 2006b). The plots of the percentage of closed channels as a function of the enzyme concentrations were used to calculate the stability constants  $K$  for binding as it is shown in Figure 4.1B for the data of Figure 4.1A. The fit curve (solid line in Figure 4.1A) corresponds to a stability constant  $K$  of  $(3.98 \pm 0.063) \times 10^6 \text{ M}^{-1}$  for C2I binding to PA<sub>63</sub> (half saturation constant  $K_s = 251 \text{ nM}$ ). The stability constant  $K$  of the binding of C2I to the PA<sub>63</sub> channels was averaged out of at least five individual experiments resulting in  $K (5.1 \pm 1.5) \times 10^6 \text{ M}^{-1}$  (half-saturation constant  $K_s = 196 \text{ nM}$ ) (see Table 4.1). Measurements with artificial bilayer membranes of the wild-type AB<sub>7</sub> components C2II and C2I revealed a stability constant  $K$  of  $(3.7 \pm 0.4) \times 10^7 \text{ M}^{-1}$  with a half saturation constant  $K_s$  of 27.2 nM.

### 4.3.2 Binding of C2II with EF and LF *in vitro*

As demonstrated in recent studies, EF and LF of Anthrax toxin are able to block the PA<sub>63</sub> pore in artificial bilayer membranes at nanomolar concentrations (Neumeyer *et al.*, 2006a) and C2II channels can be blocked by their enzymatic counterpart C2I (Blocker *et al.*, 2003b). The possible binding of EF and LF to the C2II channels was studied using titration experiments as described above for PA<sub>63</sub> and C2I shown in Figure 4.1. These measurements allowed the calculation of the stability constants  $K$  of EF and LF binding to the C2II channels, resulting in  $(7.7 \pm 4.8) \times 10^7 \text{ M}^{-1}$  and  $(2.0 \pm 0.3) \times 10^7 \text{ M}^{-1}$ , respectively (see Table 4.1). The data indicated that EF and LF have a high affinity for the C2II channels *in vitro*, as the half saturation constants  $K_s$  for EF and LF binding to the C2II channels were 13.0 nM and 49.9 nM, respectively.

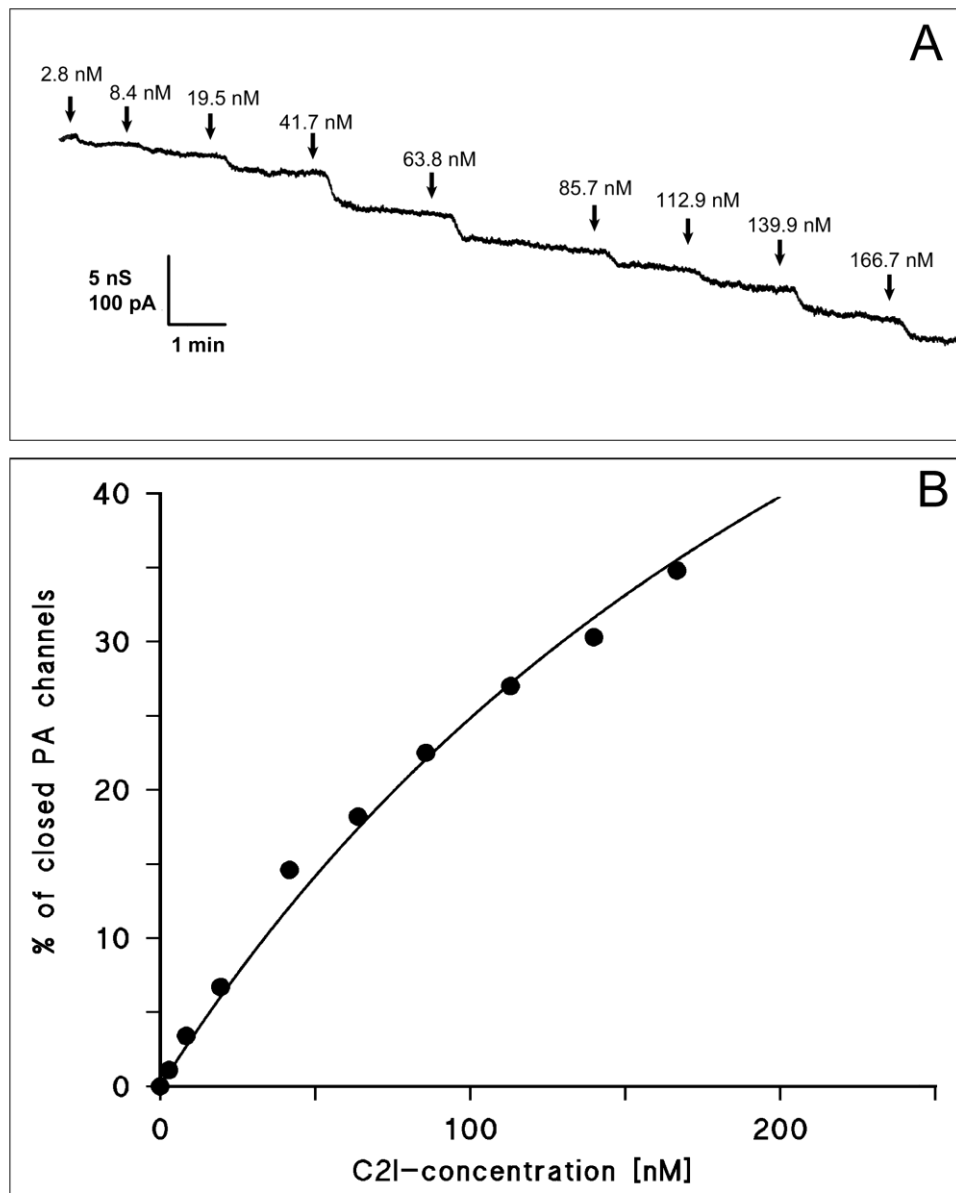


**Figure 4.1. Interaction of C2I with PA<sub>63</sub> channels.** (A) Titration of PA<sub>63</sub>-induced membrane conductance with C2I. The membrane was formed from diphytanoyl phosphatidylcholine/n-decane, containing about 5500 channels. C2I was added at the concentrations shown at the top of the panel. Finally, about 40% of the PA<sub>63</sub> channels were blocked. The aqueous phase contained 1 ng/ml activated PA<sub>63</sub> protein (added only to the *cis*-side), 150 mM KCl, 10 mM MES pH 6. The temperature was 20°C and the applied voltage was 20 mV. Note that C2I only blocks PA<sub>63</sub> channels when they are added to the *cis*-side of the membrane (data not shown). (B) Lineweaver-Burke plot of the inhibition of the PA<sub>63</sub>-induced membrane conductance by C2I. The fit was obtained by linear regression of the data points taken from Figure 1A ( $r^2=0.996654$ ) and corresponds to a stability constant  $K$  for C2I binding to PA<sub>63</sub> of  $(3.98 \pm 0.063) \times 10^6 \text{ M}^{-1}$  for C2I binding to PA<sub>63</sub> (half saturation constant  $K_S = 251 \text{ nM}$ ).

#### 4.3.3 PA<sub>63</sub> translocates C2I in cells

C2I acts as an ADP-ribosyltransferase targeting cellular G-actin. Therefore, successful delivery of this enzymatic component into target cells can be detected by disruption of the cytoskeleton

followed by rounding up of target cells and detachment of target cells from the extracellular matrix, defined as intoxicated cells (Blocker *et al.*, 2003b) or by direct measurement of the modified G-actin as described in *Materials and Methods*. C2I, added to different concentrations of its native binding component C2II, led to increasing numbers of round cells after 24 hours of intoxication (data not shown).

**Table 4.1. Stability constants  $K$  for the binding of C2I, EF or LF to PA<sub>63</sub> or C2II channels reconstituted in lipid bilayer membranes.**

<b>Toxin combination</b>	$K$ [M <sup>-1</sup> ]	$K_s$ [nM]
<b>PA with</b>		
C2I	$(0.51 \pm 0.15) \times 10^7$	196
EF*	$14.5 \times 10^7$	6.9
LF*	$36.2 \times 10^7$	2.8
<b>C2II with</b>		
EF	$(7.7 \pm 4.8) \times 10^7$	13
LF	$(2.0 \pm 0.3) \times 10^7$	49.9
C2I	$(3.7 \pm 0.4) \times 10^7$	27.2

The membranes were formed from diphytanoyl phosphatidylcholine/n-decane. The aqueous phase contained 150 mM KCl, buffered to pH 5.5 to 6 using 10 mM MES-KOH; T = 20°C. Measurements were performed at a membrane potential of 20 mV. The data represent the means of at least three individual titration experiments.  $K_s$  is the half saturation constant, i.e.  $1/K$ . Some of the wild-type toxin combinations (given in bold) were taken from reference (Neumeyer *et al.*, 2006a).

Figure 4.2A shows the direct measurement of cellular ADP-ribosylated actin (ADPr-actin) in HUVECs after treatment with different PA-C2I and C2II-C2I combinations. The cells were intoxicated with different concentrations of binding components and effectors as indicated. Levels of ADP-ribosylated actin (ADPr-actin) were determined by *in vitro* ADP-ribosylation of cell lysates with C2I and radiolabeled [<sup>32</sup>P]-NAD. Under these conditions ADP-ribosylated actin produced by the intoxication process is no longer labeled by *in vitro* ADP-ribosylation. The results clearly demonstrated that the radioactivity combined with labeled ADPr-actin decreased for the combinations PA-C2I and C2II-C2I suggesting that both channels were able to transport C2I into HUVECs. Controls did not reveal any change of the labeling of actin, which means that neither PA nor C2I alone, respectively, modified intracellular actin.

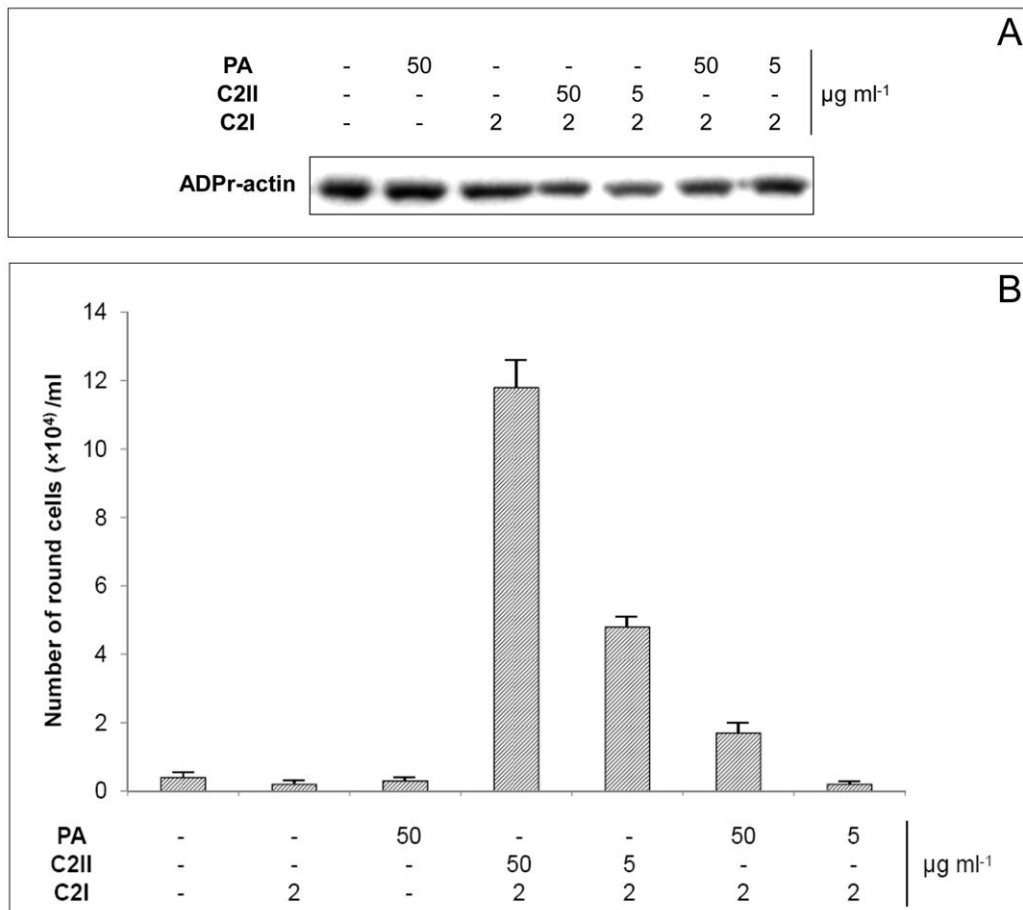


**Figure 4.2. HUVECs ( $5 \times 10^5$  cells/100 mm well) were intoxicated with the indicated concentration of polypeptides during 48 (A) or 24 hours (B). (A)** Cells were intoxicated as indicated and levels of cellular ADP-ribosylated actin (ADPr-actin) were determined by *in vitro* ADP-ribosylation of cell lysates with C2I and radiolabeled [ $^{32}\text{P}$ ]-NAD. Under these conditions ADP-ribosylated actin formed during the intoxication process is no longer labeled by *in vitro* ADP-ribosylation. Immunoblotting anti-beta-actin was performed in parallel on cell lysates to show actin protein levels engaged in the ADP-ribosylation experiments. ADP-ribosylation signals were normalized to actin immunoblot signals and expressed as fold, as compared to PA-treated cells. **(B)** Efficiency of cell intoxication. Cells were intoxicated and the number of round cells was directly assessed by counting floating cells. The columns show mean values of 5 independent counting for the individual conditions  $\pm$  SEM (ns: not significant; \*  $p < 0.05$  versus control).

Similar results were obtained when the number of intoxicated HUVECs was determined by counting round cells as a result of C2I activity on actin. Figure 4.2B shows the efficiency of cell intoxication under different experimental conditions. HUVECs were incubated with different combinations of PA-C2I and C2II-C2I as indicated, and the number of intoxicated cells was directly assessed. The results shown in Figure 4.2B revealed that the number of intoxicated cells was highest for the native combination C2II-C2I. However, when HUVECs were incubated with C2I and different quantities of PA, rounding of cells was detected even at lower probability (Figure 4.2B). This demonstrated that C2I was transported by PA channels into HUVECs. The results of Figure 4.2B indicated a dose-dependent process as some combinations failed to induce any significant effect compared to the controls.



#### 4.3.4 Interaction of C2II with LF and EF *in vivo* (cell-based assay)

The enzymatic activity of the lethal factor (LF) of Anthrax toxin can be measured by monitoring the cleavage of MAPKK, e.g. with MEK2 amino-terminal antibodies (anti-MEK2) (Turk, 2007). HUVEC monolayers were intoxicated overnight with different combinations of PA-LF or C2II-LF and the activity of LF was analyzed on cell lysate by anti-MEK2 immunoblotting.

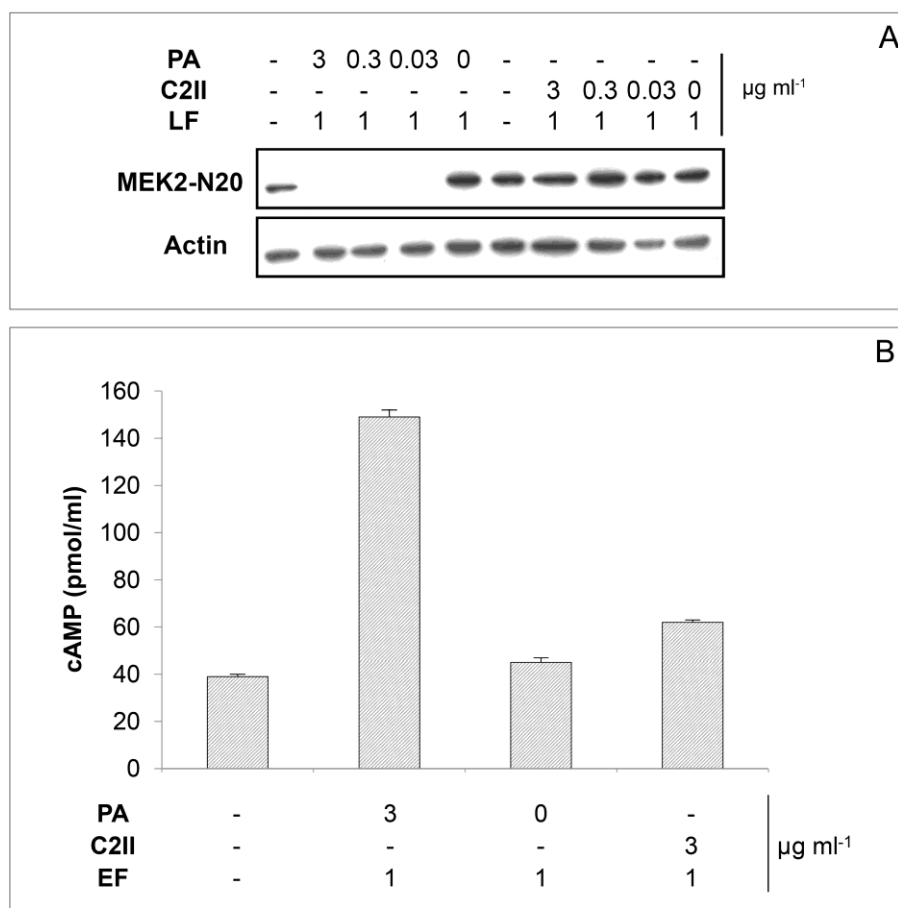


**Figure 4.3. Intoxication experiments performed on HUVEC monolayers.** Cells were treated overnight with either 1  $\mu\text{g}/\text{ml}$  of LF or EF in the presence or absence of different amounts of PA or C2II, as indicated. **(A)** Immuno-blot anti-MEK2 showing the effect of MEK2 proteolysis by LF. 30  $\mu\text{g}$  of total protein lysate were resolved on 12% SDS-PAGE. Anti-beta-actin immuno-blot shows protein loading. MEK2 signals were normalized to actin and expressed as fold, as compared to untreated control condition. **(B)** Graph shows measure of cyclic AMP (cAMP) cellular concentrations, expressed as pmol/ml. Mean values of two independent experiments  $\pm$  SEM (ns: not significant and \*  $p < 0.05$ ).

Control experiments were performed in the absence of binding components. Whereas the wild-type lethal toxin (PA-LF) did not give any MEK2 signal after blotting, the combination of LF with different quantities of C2II revealed a defined signal of intact MEK2 (Figure 4.3A). Considering our findings that C2II mediated an efficient translocation of C2I into cells under

these conditions (Figure 4.2A and 4.2B) we can present evidence that C2II has a dramatically lower capacity to promote translocation of LF into target cells.

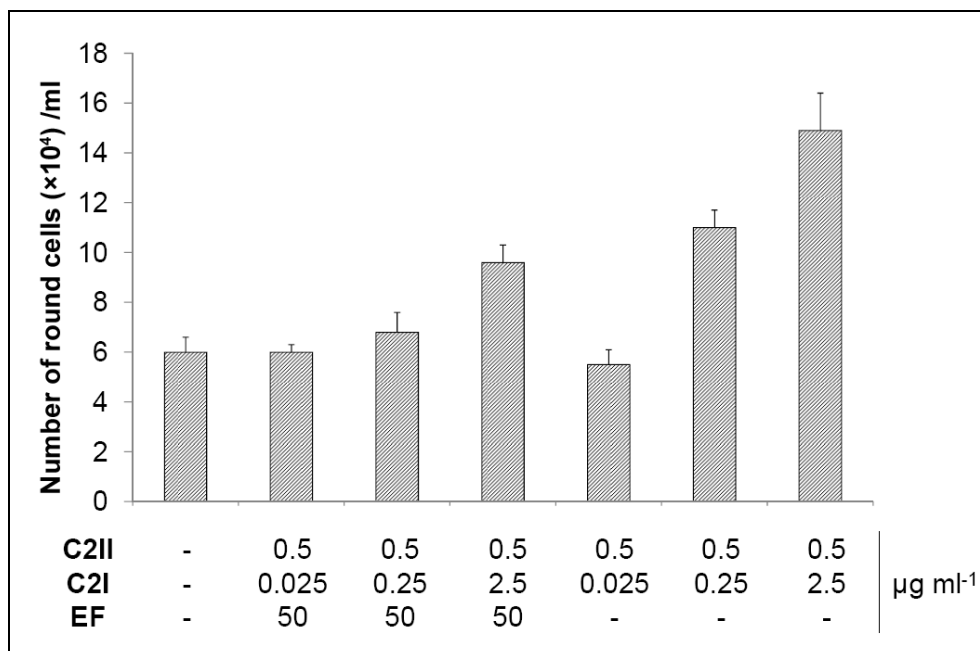


**Figure 4.4. EF-mediated inhibition of C2II-promoted C2I uptake into HUVEC cells.** Cells were intoxicated with different concentrations of the binding component C2II and the effectors EF and C2I, as indicated, and the number of intoxicated cells was directly assessed by counting round cells. One representative experiment showing mean values of 5 independent counting for each condition.

Anthrax edema factor (EF) is known to increase cAMP in target cells when applied with its native binding partner PA<sub>63</sub> (Dal Molin *et al.*, 2006). We next tested whether C2II is able to promote translocation of EF by measure of the intracellular concentration of cAMP after overnight incubation of HUVEC monolayers. The combination of PA with EF led to a 3-fold increase of intracellular cAMP level, while the application of C2II-EF did not increase significantly cAMP cellular levels (Figure 4.3B). We next verified that addition of EF was able to compete with C2I binding to C2II. The results are summarized in Figure 4.4. At a concentration of 50 µg/ml EF could partially block C2II-mediated transport of C2I into HUVECs. These data further suggest that EF binds to the C2II channel *in vivo* (cell-based assay). Together, these findings show that C2II does not efficiently promote cell intoxication by EF and LF.

#### 4.4 DISCUSSION

In previous studies we already demonstrated that the enzymatic components EF and LF of Anthrax toxin bind to their B component protective antigen (PA<sub>63</sub>) and C2I of C2 toxin binds to its B component C2II *in vitro* (Bachmeyer *et al.*, 2003; Blocker *et al.*, 2003b; Neumeyer *et al.*, 2006a). PA shares significant sequence homology (35%) with C2II, indicating that the two proteins have similar modes of action. PA<sub>63</sub> has been crystallized in its monomeric and heptameric prepore form (Petosa *et al.*, 1997) and a model of the C2II prepore structure has been constructed based on the corresponding assembly of the protective antigen prepore (Schleberger *et al.*, 2006). The similarity of both structures supports the view of a common mode of action, including the assumption that the enzymes bind in the vestibule of the heptamer of the corresponding binding component.

The results presented here suggest an interesting cross-over reactivity of Anthrax and C2 toxins, despite a completely different primary and 3D-structure of the enzymatic compounds EF, LF and C2I (Han *et al.*, 1999; Pannifer *et al.*, 2001; Shen *et al.*, 2005). The stability constants  $K$  for binding in the cross-over experiments *in vitro* were generally smaller than those for the native combinations, except the combination of C2II-EF. However, EF, LF and C2I show a high stability constant  $K$  for binding to PA<sub>63</sub> and C2II heptamers in the cross-over experiments as the half saturation constants  $K_5$  are between 10 and about 100 nM (see Table 4.1). These results refer to a common mechanisms and binding motifs within the enzymes' primary structures, in particular within the first three hundred amino acids of EF, LF and C2I. Truncated forms of EF and LF, called EF<sub>N</sub> and LF<sub>N</sub> bind with high affinity to the PA<sub>63</sub> channels and (support the transport of other polypeptides into target cells (Blanke *et al.*, 1996; Elliott *et al.*, 2000; Mogridge *et al.*, 2002; Zhang *et al.*, 2004b; Rolando *et al.*, 2009; Feld *et al.*, 2010), although the binding affinity of EF<sub>N</sub> and LF<sub>N</sub> for the PA<sub>63</sub> channel is substantially reduced as compared to wild-type EF and LF (Leuber *et al.*, 2008). Similarly, the N-terminal part of C2I is sufficient for transport of truncated forms of C2I and chimera proteins between the N-terminal end of C2I and other proteins into target cells (Barth *et al.*, 2002a; Barth *et al.*, 2002b). This means that the N-terminal ends of all enzymatic compounds interact with the PA<sub>63</sub> and the C2II heptamers. Some of the amino acids responsible for these interactions are well known within the primary sequence of PA<sub>63</sub> and its water-soluble heptamer, e.g. amino acids E398, D425 and F427 (also known as the  $\Phi$ -clamp) (Cunningham *et al.*, 2002; Krantz *et al.*, 2005; Lacy *et al.*, 2005), but relatively unknown for C2II, although there exist some indications that the corresponding amino acids E399, D426 and F428 may play a similar role for C2I binding (Neumeyer *et al.*, 2008). However, further amino acids responsible for this interaction still need to be identified.

The amino acids responsible for binding within the N-terminal end of the enzymatic components are relatively unknown, although there is clear evidence that positively charged amino acids are involved as they form salt bridges between the enzymatic components and the heptamers. The positively charged N-termini of the enzymes is presumably decisive as quaternary ammonium ions and 4-aminoquinolones show a blockage of PA<sub>63</sub> and C2II channels in lipid bilayer experiments (Blaustein *et al.*, 1990; Finkelstein, 1994; Bachmeyer *et al.*, 2003; Orlik *et al.*, 2005). The selectivity of the two channels for cations, which is at least partially due to the charged amino acids in the  $\beta$ -barrel, may also play a significant role. Both channels are known to prefer cations over anions in zero-current membrane-potentials, the  $P_{\text{cation}}$  over  $P_{\text{anion}}$ , as described by the Goldman-Hodgkin-Katz equation (Benz *et al.*, 1979a), are 20 for PA<sub>63</sub> channels and 10 for C2II channels, respectively (Blaustein *et al.*, 1989; Schmid *et al.*, 1994). Therefore cations have a strong effect on the single channel conductance as compared to anions (Blaustein *et al.*, 1989; Schmid *et al.*, 1994). It may be possible that the differently charged channel interiors of PA and C2II have a decisive influence on binding and transport of the enzymatic components (see below). Altogether there exist strong indications that binding to the different channels follows different mechanisms.

Another conceivable possibility is that the structure of the channel itself is important for translocation. The extended channel-forming  $\beta$ -sheets of the PA<sub>63</sub> monomers contain three glutamic acids and three aspartic acids (E302, E308, E343 and D276, D315, D335), so the extended  $\beta$ -barrel could contain up to 42 negatively charged groups, which probably cannot be counterbalanced by the at least partially positively charged histidines H304 and H310 (Nassi *et al.*, 2002; Nguyen, 2004; Santelli *et al.*, 2004). However, the C2II channel contains 7 glutamic acids (E307) and 14 histidines (H296 and H332), indicating that it has a much smaller overall charge (Blocker *et al.*, 2003a). The interaction of the charged groups of the channel interior and the bound enzymatic components could be different for channels leading to divergent uptake efficiency. Considering the fact that the charges in the vestibule domain are quite balanced in both PA<sub>63</sub> and C2II, i.e. both have 14 acidic amino acids facing the interior of the vestibule domain, the effect of the charges in the water filled  $\beta$ -barrels should be striking. As mentioned beforehand, the C2II channel is missing most of them.

The most interesting result of this study was that the combination of PA with C2I showed HUVEC toxicity. This appeared specific of PA considering the rather poor capacity of C2I to bind to and trigger cell intoxication by LF. This clearly reveals that PA has the remarkable ability to bind and to translocate an enzymatic component of another AB<sub>n</sub> type toxin into cells. The level of cell intoxication with C2I via PA, however, was approximately 5-fold lower than with the wild-type combination C2II-C2I. We can only speculate about the reasons of this higher flexibility of PA as compared to C2II. One possibility is that a different driving force is required

to translocate LF and EF through the C2II channel because EF and LF are released at the state of the late endosome (Abrami *et al.*, 2004), whereas C2I leaves the early endosome following acidification and, in addition, depends on the help of the cytosolic chaperon Hsp90 (Barth *et al.*, 2000; Haug *et al.*, 2003). A similar requirement is not known for the translocation of LF, EF or LF's N-terminal domain (LF<sub>N</sub>) through the PA<sub>63</sub> channel, where a pH-gradient across the membrane creates a sufficient driving force for translocation of the proteins (Krantz *et al.*, 2006). With the evidence presented here, i.e. that some components of the highly specialized binary toxins can be interchanged without loss of toxicity, further work with mutated binding components, enzymatic moieties and chimeras seems to be necessary to understand the different translocation capacities of PA<sub>63</sub> and C2II channels.



---

---

## ANTHRAX TOXIN PROTECTIVE ANTIGEN PROMOTES UPTAKE OF N- TERMINAL HIS<sub>6</sub>-TAG LABELED POLYPEPTIDES INTO CELLS IN A VOLTAGE-DEPENDENT WAY \*

### 5.1 INTRODUCTION

Gram-positive bacteria such as *Bacillus anthracis* and *Clostridium botulinum* possess special AB toxins as one of their most potent virulence factors. These toxins are composed of two components which are supposed to be nontoxic by themselves when added to the external media of target cells (Barth *et al.*, 2004). One or more A components of the toxins feature intracellular enzymatic activity and are responsible for the toxicity. The B component binds to cellular receptors or directly to the membrane and transports the enzymatic component into the cell. Anthrax toxin from *B. anthracis* belongs to the AB<sub>7</sub> type of toxins classified by a pore forming B component, protective antigen (PA) and two enzymes, edema factor (EF) and lethal factor (LF). PA has an 83 kDa water soluble precursor, which has to be activated by cleavage of a 20 kDa N-terminal part to form the functional PA<sub>63</sub> heptamers (Petosa *et al.*, 1997; Miller *et al.*, 1999; Abrami *et al.*, 2004; Abrami *et al.*, 2005). The proteolytic activation is performed *in vivo* by cell bound furin and renders possible pore formation and transport of the two enzymatic components EF and LF (Mock and Fouet, 2001; Ascenzi *et al.*, 2002; Turk, 2007; Young and Collier, 2007). EF is an 89 kDa Ca<sup>2+</sup>- and calmodulin-dependent adenylate cyclase which causes severe edema by uncontrolled increasing the intracellular cAMP. LF is a Zn<sup>2+</sup>-binding metalloprotease that cleaves mitogen-activated protein kinase kinases (MAPK-kinases) and thereby interferes with the MAPK cascade, a major signaling pathway. It is triggered by surface receptors, controlling cell proliferation and survival and causes cell death by interfering with intracellular signaling leading to apoptosis.

\* This work resulted from a collaboration of Christoph Beitzinger, Monica Rolando, Angelika Kronhardt, Caroline Stefani, Gilles Flatau, Michel R. Popoff, Emmanuel Lemichez and Roland Benz submitted to *PLoS ONE* and is included in this thesis in agreement with all authors.

*C. botulinum*, well known for the production of potent neurotoxins, also produces other protein toxins such as the binary C2 toxin and the single-component C3 exoenzyme (Boquet and Lemichez, 2003; Aktories and Barth, 2004; Aktories *et al.*, 2004). The homologue pore forming B component to PA is C2II. After proteolytic cleavage with trypsin (60 kDa) it forms heptamers that insert into biological and artificial membranes at an acidic pH and promotes the translocation of the 45 kDa enzymatic component C2I. Similar to Anthrax toxin the receptor-mediated endocytotic pathway of the cell is used (Barth *et al.*, 2000; Blocker *et al.*, 2000). C2I acts as an NAD-dependent ADP-ribosyltransferase on Arg177 of monomeric G-actin, causing disruption of the actin cytoskeleton of eukaryotic cells (Considine and Simpson, 1991; Blocker *et al.*, 2003b).

The toxins of the AB type represent simple but sophisticated molecular syringes for protein delivery into target cells. This means that they could be important systems for development of new strategies for efficient injection of polypeptides into target cells. Possible Trojan Horses could be binary toxins of the AB<sub>7</sub> type such as Anthrax and C2 toxin because they represent highly potent bacterial toxins composed of two polypeptide chains that are secreted in the external media of Gram-positive bacteria (Barth *et al.*, 2004). The binding of the N-terminal ends of the enzymatic components to the heptameric channel formed by the binding components is followed by receptor-mediated endocytosis, acidification of the endosomes and final release of the enzymatic components into the cytosol of target cells, where they exert their enzymatic activities (Abrami *et al.*, 2004; Abrami *et al.*, 2005; Wei *et al.*, 2006). Interestingly, the amino-terminal part of LF is sufficient to confer the ability to associate with PA<sub>63</sub> heptamers on LF. It can be used to drive the translocation of unrelated polypeptides fused to LF<sub>1-254</sub> into target cells in a PA<sub>63</sub>-dependent manner (Leppla *et al.*, 1999). Although the enzymatic components of Anthrax and C2 toxin differ considerably in their enzymatic activity and in their primary structures as well, the binding components PA and C2II share a significant overall sequence homology of about 35%, which means that they are closely related in structure and probably also in function (Petosa *et al.*, 1997; Neumeyer *et al.*, 2006a; Schleberger *et al.*, 2006; Young and Collier, 2007). Important for the binding of channel blockers and enzymes to be delivered into the target cells are besides the so called  $\Phi$ -clamp - F427 in PA and F428 in C2II - two rings of seven negatively charged amino acids - E399 and D428 in PA and E398 and D427 in C2II (Krantz *et al.*, 2005; Melnyk and Collier, 2006). These negatively charged amino acids seem to interact with the positively charged N-terminal ends of the enzymatic components (Krantz *et al.*, 2004; Neumeyer *et al.*, 2008).

In this study we have investigated the influence of additional charges on the N-terminal end on binding of the enzymatic factors to the channels formed by PA<sub>63</sub> and C2II. First results in the field were found with polycationic peptides fused to LF<sub>N</sub> and EF<sub>N</sub> (Blanke *et al.*, 1996; Neumeyer *et al.*, 2006a). The results suggested that the binding of LF and EF to C2II is possible and that



C2I binds to PA<sub>63</sub> in the black lipid bilayer assay as well. The most significant result that was observed was a preferential binding of His<sub>6</sub>-C2I to PA<sub>63</sub>. Interestingly, PA<sub>63</sub> is able to transport His<sub>6</sub>-C2I into target cells with high efficiency, exhibiting host cell toxicity, whereas C2II does not transport His<sub>6</sub>-EF or His<sub>6</sub>-LF. This prompted us to investigate whether a His<sub>6</sub>-tag might also lead to an increase in binding affinity for heterologous polypeptides to PA<sub>63</sub>. In fact, we could demonstrate that the epidermal cell differentiation inhibitor EDIN of *Staphylococcus aureus* fused to a His<sub>6</sub>-tag enters cells via PA. Both EDIN and His<sub>6</sub>-EDIN bind *in vitro* to PA<sub>63</sub>. In addition, the binding constant of His<sub>6</sub>-EDIN and not that of EDIN to PA<sub>63</sub> channels was found to be highly voltage-dependent.

## 5.2 EXPERIMENTAL PROCEDURES

### 5.2.1 Materials

Protective antigen encoding gene was cloned with *Bam*HI-*Sac*I restriction sites into pET22 (Novagen) as previously described (Rolando 2009). The translocation-defective PA mutant F427A (Sellman *et al.*, 2001; Krantz *et al.*, 2005) was constructed by site-directed mutagenesis using the QuickChange™ kit (Stratagene) according to the manufacturer's instructions. The PA-gene cloned in the plasmid pET19 (Novagen) (Cataldi *et al.*, 1990; Tonello *et al.*, 2004), was used as a template. The construct was confirmed by DNA sequencing. The protein was expressed with an N-terminal His<sub>6</sub>-tag in BL21 (DE3) (Novagen) and purified by HiTrap chelating (Pharmacia) charged with Ni<sup>2+</sup> ions. C2I and C2II genes were PCR-amplified from genomic DNA of *Clostridium botulinum* D strain 1873 and cloned into pET22 (Novagen) and pQE30 (Qiagen) expression plasmids with *Bam*HI-*Sac*I restriction sites. The plasmid coding for the chimera protein MBP-gpJ (maltose-binding-protein attached to amino acids 684-1132 of Lambda phage tail protein J) was a kind gift of Alain Charbit, Paris, France. Expression and purification of MBP-gpJ was performed as described previously (Wang *et al.*, 2000). gpJ was obtained by treatment of MBP-gpJ bound to starch column beads (amylose-Sepharose, New England Biolabs) with factor X<sub>a</sub> (Invitrogen). His<sub>6</sub>-gpJ (684-1132) was obtained as described previously (Berkane 2006). The DNA encoding EDIN (NCBI M63917) was cloned into pET28a vector using *Bam*HI-*Eco*RI restriction site as described previously (Boyer *et al.*, 2006). Recombinant toxins containing His<sub>6</sub>-tags were expressed in *E. coli* BL21 (DE3) and purified on a Chelating Sepharose Fast Flow column previously chelated with nickel (Amersham Biosciences) as recommended by the manufacturer. Fractions containing toxin were pooled and dialyzed over night against 250 mM NaCl and 25 mM Tris-HCl, pH 8. The N-terminal His<sub>6</sub>-tag was removed by incubation with thrombin. Nicked Anthrax PA<sub>63</sub> from *B. anthracis* was obtained from List Biological Laboratories Inc., Campbell, CA. One mg of lyophilized protein was dissolved in 1 ml 5 mM HEPES, 50 mM NaCl, pH 7.5 complemented with 1.25% trehalose. Aliquots were stored at -20°C. Channel formation by PA<sub>63</sub> was stable for months under these conditions.

### 5.2.2 Cell culture and biochemical products

HUVECs (human umbilical vein endothelial cells, a human primary cell line obtained from PromoCell) were grown in serum-free medium (SFM) supplemented with 20% FBS (Invitrogen), 20 ng/ml basic βFGF (Invitrogen), 10 ng/ml EGF (Invitrogen) and 1 μg/ml heparin (Sigma-Aldrich) as described previously (Doye *et al.*, 2006). Monoclonal antibodies used were: anti-RhoA (BD Biosciences, [clone 26C4]); anti-β-actin (SIGMA, [clone AC9-74]); anti-His-tag (Qiagen,

[Penta-His]). Primary antibodies were visualized using goat anti-mouse horseradish peroxidase-conjugated secondary antibodies (DakoCytomation), followed by chemiluminescence detection ECL (GE Healthcare). Levels of active Rho were determined by GST-rhotekin RBD pull-down that was modified as described previously (Doye *et al.*, 2006).

### 5.2.3 Lipid bilayer experiments

Black lipid bilayer measurements were performed as described previously (Benz *et al.*, 1978). The instrumentation consisted of a Teflon chamber with two aqueous compartments connected by a small circular hole. The hole had a surface area of about  $0.4 \text{ mm}^2$ . Membranes were formed by painting a 1% solution of diphytanoyl phosphatidylcholine (Avanti Polar Lipids, Alabaster, AL) in *n*-decane onto the hole. The aqueous salt solutions (Merck, Darmstadt, Germany) were buffered with 10 mM MES to pH 5.5 to pH 6. Control experiments revealed that the pH was stable during the time course of the experiments. The binding components of the binary toxins were reconstituted into the lipid bilayer membranes by adding concentrated solutions to the aqueous phase on one side (the *cis*-side) of a black membrane. The temperature was kept at  $20^\circ\text{C}$  throughout. Membrane conductance was measured after application of a fixed membrane potential with a pair of silver/silver chloride electrodes inserted into the aqueous solutions on both sides of the membrane. Membrane current was measured using a homemade current-to-voltage converter combined with a Burr Brown operational amplifier. The amplified signal was monitored on a storage oscilloscope and recorded on a strip chart recorder.

### 5.2.4 Binding experiments

The binding of the His-tagged proteins to the C2II channel and the binding component  $\text{PA}_{63}$  was investigated with titration experiments similar to those performed previously to study the binding of 4-aminoquinolones to the C2II and  $\text{PA}_{63}$  channels and EF and LF to the  $\text{PA}_{63}$  channel in single- or multi-channel experiments (Bachmeyer *et al.*, 2003; Orlik *et al.*, 2005; Neumeyer *et al.*, 2006b). The C2II and  $\text{PA}_{63}$  channels were reconstituted into lipid bilayers. About 60 minutes after the addition of either activated C2II or  $\text{PA}_{63}$  to the *cis*-side of the membrane, the rate of channel insertion in the membranes was very small. Then concentrated solutions of His-tagged proteins were added to the *cis*-side of the membranes while stirring to allow equilibration. The results of the titration experiments, i.e. the blockage of the channels, were analyzed using Langmuir adsorption isotherms (Benz and Hancock, 1987; Neumeyer *et al.*, 2006a). The conductance as a function of the concentration of the enzymatic components was analyzed using Lineweaver-Burke plots.  $K$  is the stability constant for binding of the enzymatic components of the binary

toxins to the PA<sub>63</sub> or C2II channels. The half saturation constant  $K_s$  is given by the inverse stability constant  $1/K$ .

$$\frac{(G_{\max} - G(c))}{G_{\max}} = \frac{K \cdot c}{(K \cdot c + 1)} \quad [5.1]$$

## 5.3 RESULTS

### 5.3.1 Interaction of PA<sub>63</sub> pores with His<sub>6</sub>-C2I in artificial black lipid bilayer membranes

We compared the binding affinity of different proteins with and without a His<sub>6</sub>-tag to the PA<sub>63</sub> and C2II channels. Taking into account that positive charges seem to have a huge influence in binding to the PA<sub>63</sub> pore but only less to the C2II pore (Orlik *et al.*, 2005; Leuber *et al.*, 2008), we chose the enzymatic component C2I as the first substrate. In a previous study we could show that it binds to PA<sub>63</sub> pores and could even be translocated into cells albeit with very low efficiency (Rolando *et al.*, 2010). We now addressed the question, if binding and translocation are enhanced by addition of a His<sub>6</sub>-tag to C2I.

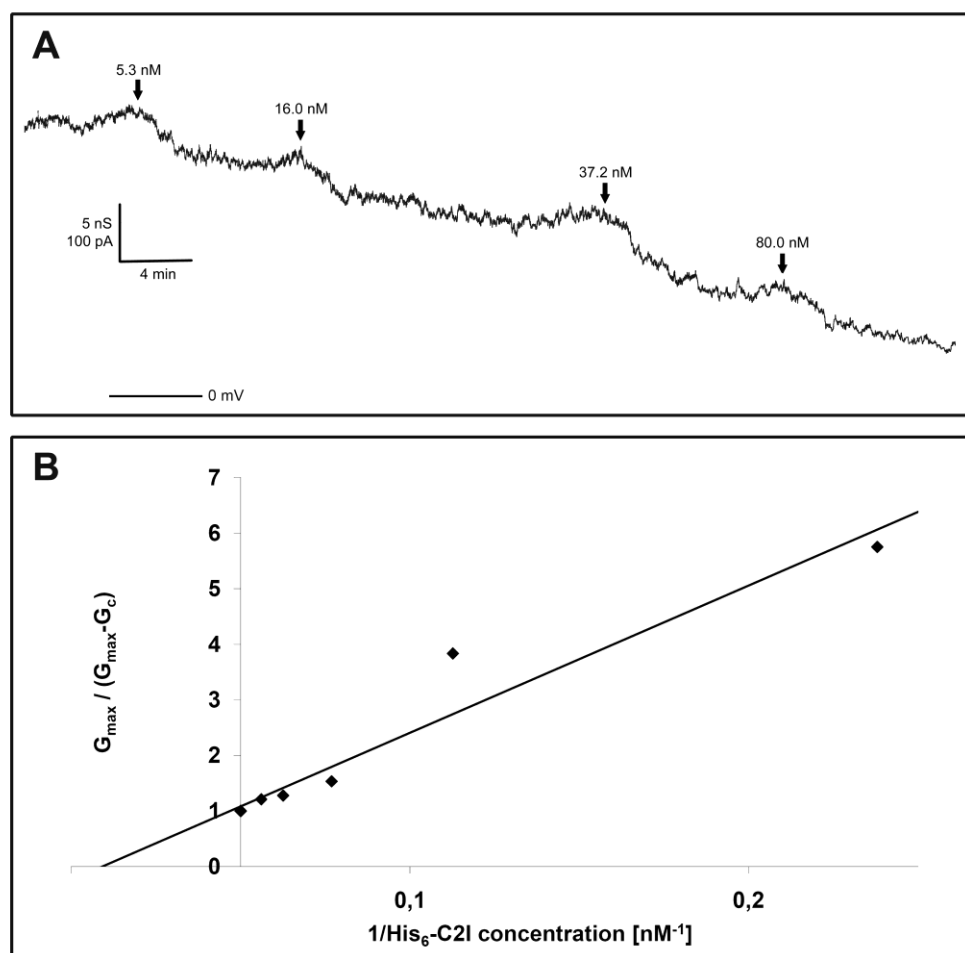


**Figure 5.1. Titration of PA<sub>63</sub> with His<sub>6</sub>-C2I and interpretation. (A)** The membrane was painted from diphytanoyl phosphatidylcholine/n-decane containing about 300 PA<sub>63</sub> channels. His<sub>6</sub>-C2I was added at the concentrations shown at the top of the panel. Finally, about 83% of the PA<sub>63</sub> channels were blocked. The aqueous phase contained 1 ng/ml activated PA<sub>63</sub> (added only to the *cis*-side), 150 mM KCl, 10 mM MES pH 6. The temperature was 20°C and the applied voltage was 20 mV. **(B)** Lineweaver-Burke plot of the inhibition of the PA<sub>63</sub>-induced membrane conductance by His<sub>6</sub>-C2I. The fit was obtained by linear regression of the data points taken from Figure 5.1A and corresponds to a stability constant  $K$  for His<sub>6</sub>-C2I binding to PA<sub>63</sub> of  $(3.85 \pm 0.52) \times 10^7 \text{ M}^{-1}$  (half saturation constant  $K_s = 180 \text{ nM}$ ).

The stability constants  $K$  and  $K_s$  for the binding of His<sub>6</sub>-C2I to the PA<sub>63</sub> channel were measured in multichannel experiments, performed as described previously (Neumeyer *et al.*, 2006b). A receptor is required for the binding and oligomerization of PA<sub>63</sub> on the surface of mammalian cells (Young and Collier, 2007). However, this is not necessary for reconstitution of PA<sub>63</sub> channels in artificial lipid bilayers, where channel formation is obtained under mildly acidic conditions (Finkelstein, 1994). 60 minutes after the addition of the protein to the *cis*-side of the lipid bilayer, the rate of conductance increase had slowed down considerably at an applied membrane potential of 20 mV. At that time, small amounts of a concentrated protein solution were added to the *cis*-side of the membrane and the PA<sub>63</sub>-induced membrane conductance decreased in a stepwise manner.

**Table 5.1. Stability constants  $K_s$  for the binding of C2I, gpJ or EDIN to either PA<sub>63</sub> or C2II channels in lipid bilayer membranes.**

Toxin combination		$K_s$ [nM]		$K_s$ [nM]
<b>PA<sub>63</sub></b> with	EF*	6.9	His <sub>6</sub> -EF*	0.2
	LF*	2.8	His <sub>6</sub> -LF*	0.2
	C2I	150	His <sub>6</sub> -C2I	16
	gpJ	no binding	His <sub>6</sub> -gpJ	5
	EDIN	2,700	His <sub>6</sub> -EDIN	700
<b>C2II</b> with	EF**	13	His <sub>6</sub> -EF	19
	LF**	50	His <sub>6</sub> -LF	29
	C2I	27	His <sub>6</sub> -C2I	29
	gpJ	no binding	His <sub>6</sub> -gpJ	no binding
	EDIN	23,000	His <sub>6</sub> -EDIN	900

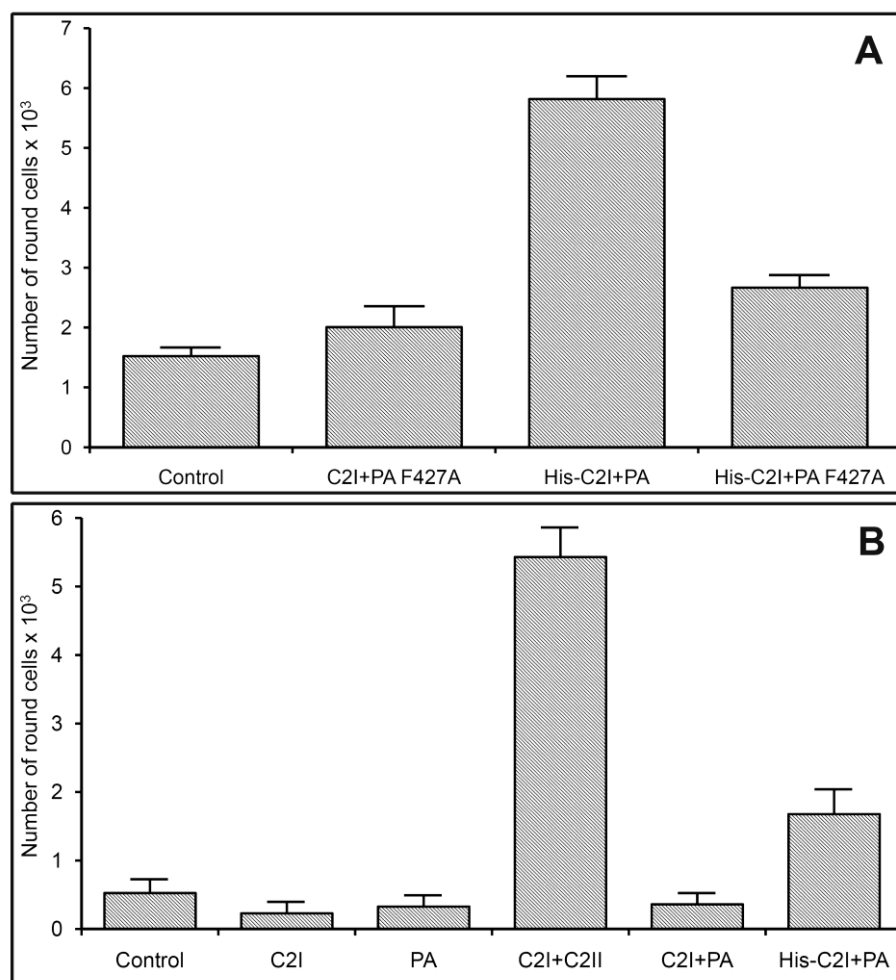
The membranes were painted from diphytanoyl phosphatidylcholine/n-decane. The aqueous phase contained 150 mM KCl, buffered to pH 5.5 to 6 using 10 mM MES-KOH; T = 20°C. Measurements were performed at a membrane potential of 20 mV. The data represent the means of at least three individual titration experiments.  $K_s$  is the half saturation constant, i.e.  $1/K$ . Stability constants given in bold were adjusted to the voltage dependent behavior of binding. (\* taken from (Neumeyer *et al.*, 2006a) \*\* taken from (Rolando *et al.*, 2010).

Figure 5.1A shows an experiment of this type in which increasing concentrations of His<sub>6</sub>-C2I (arrows) were added to the *cis*-side of a membrane containing about 300 PA<sub>63</sub> channels. The membrane conductance decreased as a function of the His<sub>6</sub>-C2I concentration. The data of Figure 5.1A and of similar experiments were analyzed using equation [5.1] assuming Langmuir isotherms for binding (Benz *et al.*, 1986; Benz and Hancock, 1987; Neumeyer *et al.*, 2006b). Lineweaver-Burke plots were used to calculate the stability constant  $K$  for binding as shown in Figure 5.1B for the data of Figure 5.1A. The resulting curve corresponds to a stability constant  $K$  of  $(3.85 \pm 0.52) \times 10^7 \text{ M}^{-1}$  for His<sub>6</sub>-C2I binding to PA<sub>63</sub> pores.

At least three individual experiments were used to calculate the stability constant  $K$  of His<sub>6</sub>-C2I binding to the PA<sub>63</sub> channel. The average of the stability constant  $K$  of C2I binding was  $(6.8 \pm 4.2) \times 10^6 \text{ M}^{-1}$  (half-saturation constant  $K_s = 150 \text{ nM}$ ) whereas the stability constant  $K$  for His<sub>6</sub>-C2I to PA<sub>63</sub> channels averaged to  $(6.2 \pm 4.2) \times 10^7 \text{ M}^{-1}$  ( $K_s = 16 \text{ nM}$ ) in 150 mM KCl. This means that the stability constant  $K$  for binding of His<sub>6</sub>-C2I was roughly ten times higher than for C2I without His<sub>6</sub>-tag (Table 5.1). Titration experiments with artificial bilayer membranes of the wildtype AB components C2II and C2I of C2 toxin revealed a binding constant  $K$  of  $(3.7 \pm 0.4) \times 10^7 \text{ M}^{-1}$ , with a half saturation constant  $K_s$  of 27 nM. Interestingly, a His<sub>6</sub>-tag attached to the N-terminal end had no obvious effect on binding of C2I to C2II pores (Table 5.1).

### 5.3.2 Addition of His<sub>6</sub>-tag to C2I potentiates its transfer via PA<sub>63</sub>

In further experiments we tested if addition of His<sub>6</sub>-tag to C2I triggers its entry into cells via PA<sub>63</sub> channels *in vivo*. C2I acts as an ADP-ribosyltransferase, targeting cellular G-actin (Aktories *et al.*, 1986b). Therefore, successful delivery of this enzymatic component into target cells can be detected by disruption of the cytoskeleton followed by rounding up and detachment of target cells from the extracellular matrix, defined as intoxicated cells (Blocker *et al.*, 2003a). HUVECs were intoxicated with C2I and His<sub>6</sub>-C2I driven by PA, as indicated, and the number of intoxicated cells was directly assessed by counting (Figure 5.2A). These results were compared to that of native toxin combination C2I and C2II. We observed a cytotoxic effect with the combination of His<sub>6</sub>-C2I and PA. No effect could be detected for C2I and PA under the same conditions. The specificity of this internalization was verified by using a mutant of PA<sub>63</sub>, PA F427A. This mutant is competent for receptor binding and internalization, but defective in the pH-dependent functions: pore formation and ability to translocate bound ligand (Sun *et al.*, 2008). Intoxication of cells with His<sub>6</sub>-C2I and PA F427A did not induce any cellular effect (Figure 5.2B). Thus, the increase of affinity between PA and C2I, upon addition of His<sub>6</sub>-tag to C2I allows His<sub>6</sub>-C2I to efficiently intoxicate cells via PA<sub>63</sub> channels.



**Figure 5.2. Intoxication of HUVEC monolayers.** HUVECs ( $5 \times 10^5$  cells/100 mm well) were intoxicated during 24 hours and the number of intoxicated cells (round cells) was assessed by counting floating cells. **(A)** PA and C2II at 5  $\mu\text{g}/\text{ml}$  and C2I and His<sub>6</sub>-C2I at 2  $\mu\text{g}/\text{ml}$ . One representative experiment showing mean values of 5 independent counting for each condition.  $\pm$  SD \* $p < 0.05$  versus control condition. **(B)** PA and PA F427A at 50  $\mu\text{g}/\text{ml}$  and C2I and His<sub>6</sub>-C2I at 2  $\mu\text{g}/\text{ml}$ . mean values are of  $n=3$  experiments  $\pm$  SD, \* $p < 0.05$  versus control condition.

### 5.3.3 His<sub>6</sub>-tag does not facilitate binding of EF and LF to C2II channels

To examine whether the N-terminal His<sub>6</sub>-tag of EF and LF have a similar effect on binding kinetics to the C2II channel, as previously shown for His<sub>6</sub>-EF and His<sub>6</sub>-LF and PA<sub>63</sub> (Neumeyer *et al.*, 2006a), we omitted the cleavage of the His<sub>6</sub>-tag after the affinity purification and studied binding to C2II channels. Interestingly, His<sub>6</sub>-EF and His<sub>6</sub>-LF did not exhibit any significant changes of their affinity to C2II channels as compared to EF and LF. The binding constants  $K$  of the interactions between His<sub>6</sub>-EF and His<sub>6</sub>-LF and the C2II channels were  $(5.2 \pm 1.6) \times 10^7 \text{ M}^{-1}$  and  $(3.4 \pm 1.9) \times 10^7 \text{ M}^{-1}$ , respectively. The half saturation constants  $K_s$  were calculated to be 19 nM for His<sub>6</sub>-EF and about 29 nM for His<sub>6</sub>-LF (Table 5.1).



### 5.3.4 Binding of His<sub>6</sub>-gpJ and gpJ proteins to PA<sub>63</sub> and C2II channels

The His<sub>6</sub>-tag had a remarkable influence on binding of enzymatic components to the PA<sub>63</sub> channel but not to the C2II channel. To check if this interaction was specific for the presence of the His<sub>6</sub>-tag we performed titration experiment with a His-tagged protein that is not related to the effectors EF, LF or C2I. gpJ is a 447 amino acids C-terminal fragment of protein J (amino acids 684-1131), which is responsible for binding of bacteriophage Lambda to Lamb on the surface of *E. coli* K-12 (Berkane *et al.*, 2006). His<sub>6</sub>-gpJ exhibited high affinity binding (block) to the PA<sub>63</sub> channel. The half saturation constant  $K_S$  for binding of His<sub>6</sub>-gpJ to PA<sub>63</sub> was calculated to be  $(5.0 \pm 1.5)$  nM in 150 mM KCl, 10 mM MES, pH 6.0 (mean of three measurements) (Table 5.1). Similar experiments with gpJ obtained by cleavage of MBP-gpJ with factor X<sub>a</sub> (i.e. without His<sub>6</sub>-tag) did not exploit any binding of gpJ to the PA<sub>63</sub> channel. This implies half saturation constants  $K_S$  of gpJ-binding to PA<sub>63</sub> were much higher than 10  $\mu$ M. We could not detect any binding of His<sub>6</sub>-gpJ nor of gpJ to the C2II channel (Table 5.1). These results indicate the substantial role of the His<sub>6</sub>-tag at the N-terminal end of polypeptides for their binding to the PA<sub>63</sub> but not to the C2II channel.

### 5.3.5 Binding of EDIN and His<sub>6</sub>-EDIN to PA<sub>63</sub> and C2II channels

To further test if transport through PA<sub>63</sub> pores is enabled for unrelated proteins we investigated binding of the epidermal cell differentiation inhibitor EDIN of *Staphylococcus aureus* as well as His<sub>6</sub>-EDIN. EDIN is a *Staphylococcus aureus* exoenzyme with ADP-ribosylating activity on RhoA. EDIN targets RhoA in cells for inactivation producing actin cable disruption in target cells (Boyer *et al.*, 2006). Interestingly, PA<sub>63</sub> pores bound both EDIN and His<sub>6</sub>-EDIN with stability constants that were considerably lower than those reported before for the crossing over of the AB<sub>7</sub> types of toxin (Rolando *et al.*, 2010). The stability constant  $K$  for EDIN binding to PA<sub>63</sub> channels was on average  $(4.0 \pm 1.1) \times 10^5$  M<sup>-1</sup> ( $K_S = 2.7$   $\mu$ M) in 150 mM KCl, whereas this constant increased to  $(1.4 \pm 0.15) \times 10^6$  M<sup>-1</sup> ( $K_S = 0.7$   $\mu$ M) for His<sub>6</sub>-EDIN. The results of these experiments are summarized in Table 5.1 and demonstrate that EDIN without His<sub>6</sub>-tag bound at low transmembrane voltage (5 mV) with a roughly three-fold lower affinity to the PA<sub>63</sub> channels than His<sub>6</sub>-EDIN. When higher voltages were applied we noticed a remarkable effect of voltage on His<sub>6</sub>-EDIN binding (see below). The affinity of EDIN to the C2II channels ( $K_S = 23$   $\mu$ M) was by a factor of about eight lower as compared to binding to the PA<sub>63</sub> channels. Surprisingly, we observed a considerable effect when the His<sub>6</sub>-tag was attached to the N-terminal end of EDIN. The half saturation constant dropped in this case to 0.9  $\mu$ M for its binding to C2II pores (Table 5.1).

### 5.3.6 His<sub>6</sub>-tag promotes EDIN internalization via PA<sub>63</sub> pores

We tested the affinity of the exoenzyme EDIN, a C3 like protein, which is unrelated to the AB<sub>7</sub> toxin family, to PA<sub>63</sub> channels. We next verified the role of His<sub>6</sub>-tag in the uptake of EDIN into cells. After purification the His<sub>6</sub>-tag was cleaved as described in the material and methods section. We verified the cleavage by immunoblotting the purified proteins using an antibody against the His<sub>6</sub>-tag (Figure 5.3A). The efficiency of RhoA targeting by EDIN was assessed by GST-Rhotekin pull down of active RhoA (GTP-bound RhoA). No effect on cells was measured with His<sub>6</sub>-EDIN (1 and 10 µg/ml) alone. A decrease of RhoA activity of 36% could be achieved at a higher dose of 100 µg/ml His<sub>6</sub>-EDIN (Figure 5.3B).

We then intoxicated cells with His<sub>6</sub>-EDIN in the presence of PA. Strikingly, this revealed that the addition of PA with EDIN (10 µg/ml) increased the capacity of EDIN to intoxicate cells. This led us to test the role of His<sub>6</sub>-tag on this effect. Cells were intoxicated with PA together with EDIN or His<sub>6</sub>-EDIN. This clearly established that addition of His<sub>6</sub>-tag to EDIN in presence of PA produced a 78% decrease of RhoA activation specifically (Figure 5.3C). In conclusion, addition of His<sub>6</sub>-tag to EDIN triggers its internalization via PA.

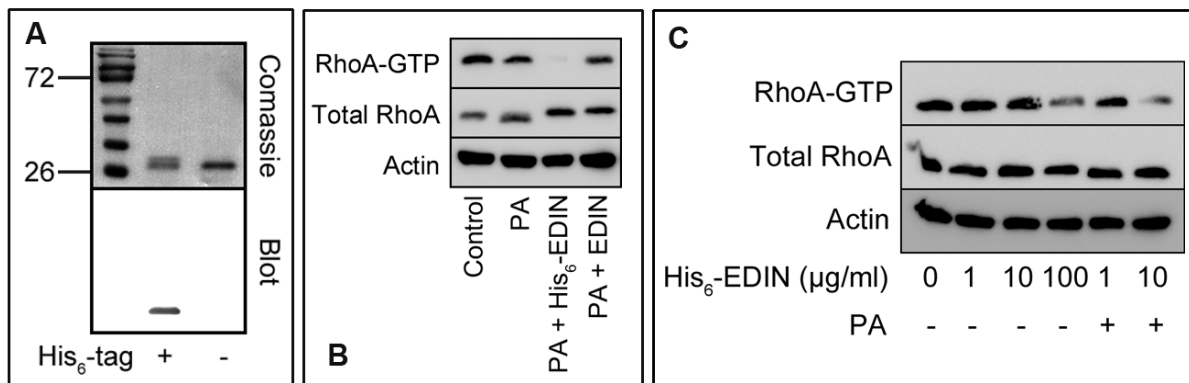


**Figure 5.3.** (A) Upper panel: SDS-PAGE of recombinant His-tagged EDIN before and after thrombin treatment. (Lane Mw) 10-120 kDa pre-stained protein marker (Fermentas). Lower panel: immuno-blot anti-His-tag on His-tagged EDIN before and after cleavage by thrombin. (B, C) Immuno-blots showing cellular levels of active RhoA (RhoA-GTP) in HUVECs determined by GST-Rhotekin RBD pull-down (labeled RhoA-GTP). Cellular content of RhoA (Total RhoA) was assessed by anti-RhoA on 2% of total protein extracts. Immuno-blot anti-actin antibody exhibits equal protein loading. (B) Cells were intoxicated with different quantities of EDIN, His<sub>6</sub>-EDIN, as indicated, and 3µg/ml of PA. (C) Cells were intoxicated with 10µg/ml of EDIN, His<sub>6</sub>-EDIN and 3µg/ml of PA, as indicated.

### 5.3.7 The voltage-dependency of PA<sub>63</sub> channels is changed when His<sub>6</sub>-EDIN is bound to the pore

PA<sub>63</sub> channels exhibit a well described voltage dependency (Neumeyer *et al.*, 2006a). If only added to the *cis*-side, PA<sub>63</sub>-induced conductivity decreases when applied voltage is higher than +50 mV or lower than -20 mV at the *cis*-side. It is also known that His<sub>6</sub>-EF bound to the channel changes the voltage dependency (Neumeyer *et al.*, 2006a).

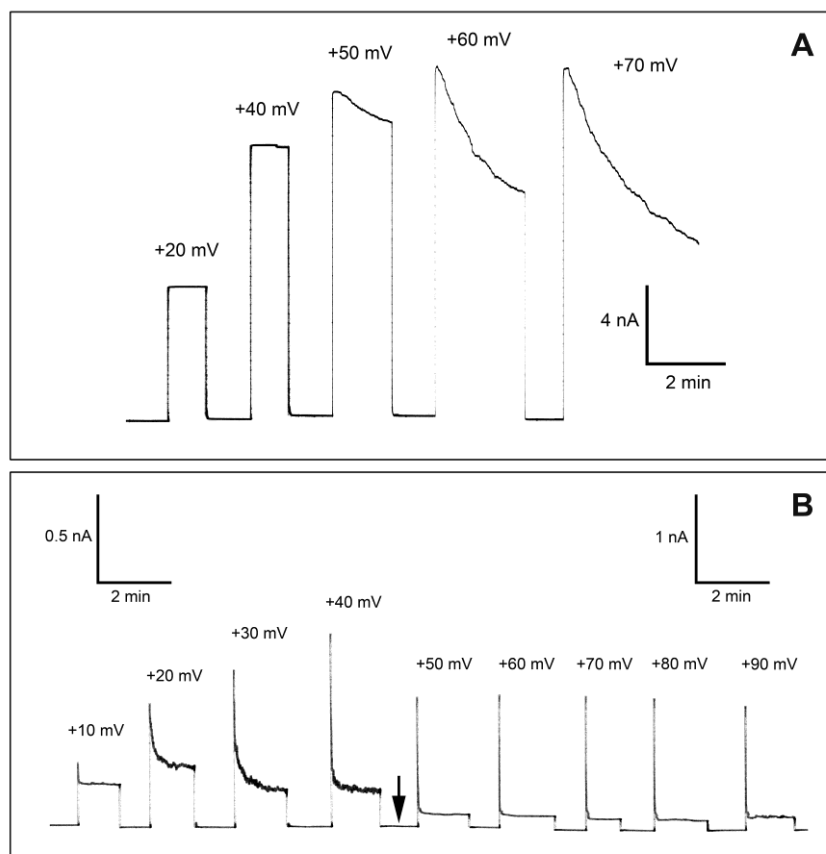


**Figure 5.4. Voltage-dependency of PA channels after titration with EDIN (A) or His<sub>6</sub>-EDIN (B).** (A) Current response of PA<sub>63</sub>-channels in presence of EDIN. Voltage pulses between +20 and +70 mV were applied to a diphytanoyl phosphatidylcholine/*n*-decane membrane in the presence of PA<sub>63</sub>-pores and EDIN (both added only to the *cis*-side). The aqueous phase contained 150 mM KCl, 10 mM MES, pH 6. The temperature was 20 °C. (B) Current response of PA channels in the presence of His<sub>6</sub>-EDIN. Voltage pulses between +10 and +90 mV were applied to a diphytanoyl phosphatidylcholine/*n*-decane membrane in the presence of PA<sub>63</sub> pores and His<sub>6</sub>-EDIN (both added only to the *cis*-side). The aqueous phase contained 150mM KCl, 10 mM MES, pH 6. The temperature was 20 °C. Note the change of the scale (arrow).

When different potentials were applied to membranes after the titration of PA<sub>63</sub> pores with EDIN, there was only little change in voltage dependency of the channel (Figure 5.4A). On the other hand, His<sub>6</sub>-EDIN bound to PA<sub>63</sub> channels induced dramatic responses even at low positive

voltages (Figure 5.4B). Starting at +10 mV, the conductivity decreased exponentially immediately after the onset of the voltage with a voltage-dependent exponential relaxation time. Its time constant decreased with higher positive potentials at the *cis*-side (negative at the *trans*-side). This result indicated that channels, which were not blocked before by His<sub>6</sub>-EDIN at low voltage bound this compound and closed as a result of the higher voltage. This result suggested an increase of the stability constant of binding up to very high voltages an effect that has already been observed with full length EF (Blaustein *et al.*, 1989).

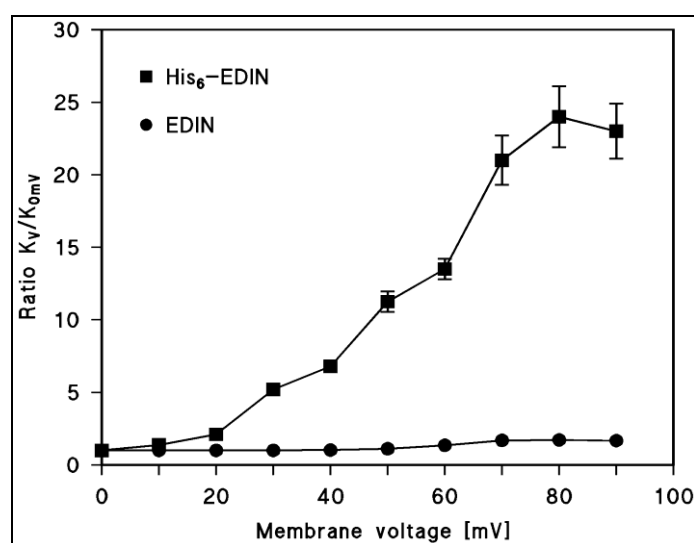


**Figure 5.5. Voltage effect of EDIN and His<sub>6</sub>-EDIN bound to PA<sub>63</sub>.** The stability constants of EDIN and His<sub>6</sub>-EDIN binding to the PA<sub>63</sub>-channel are given as a function of the applied membrane potential taken from experiments similar to that shown in Figure 5.4A and 5.4B. Means of three experiments are shown.

The increase of the stability constant for binding could be calculated from the data of Figures 5.4A and 5.4B and similar experiments by dividing the initial current (which was a linear function of voltage) by the stationary current after the exponential relaxation and multiplying the ratio with the stability constant derived at 5 mV. Figure 5.5 summarizes the effect of the positive membrane potential on the stability constant  $K$  for EDIN and His<sub>6</sub>-EDIN binding as a function of the voltage. Starting already with -10 mV at the *trans*-side the stability constant  $K$  for His<sub>6</sub>-EDIN binding started to increase and reached with about 60 to 70 mV a maximum. At that voltage  $K$  was roughly 25 times greater than at 5 mV. For higher voltages the stability constant saturated probably because of secondary effects of the high voltage on the PA<sub>63</sub> channel or on His<sub>6</sub>-EDIN binding. Figure 5.5 shows also the effect of the positive membrane potential at the *cis*-side on the stability constant  $K$  for EDIN binding to PA<sub>63</sub> pores as a function of the voltage. Interestingly, EDIN binding was only little affected by voltage as Figure 5.5 clearly indicated.

## 5.4 DISCUSSION

### 5.4.1 His<sub>6</sub>-tag addition to several bacterial factors increased the protein binding affinity to PA<sub>63</sub> but not to C2II channels

Recent studies demonstrated that negatively charged amino acids in the vestibule of the PA<sub>63</sub> channel play a crucial role in binding of effector molecules (Orlik *et al.*, 2005; Leuber *et al.*, 2008). Thus, it is possible that a His<sub>6</sub>-tag, which adds positive charges under mildly acidic conditions to the N-terminal end of His<sub>6</sub>-EF and His<sub>6</sub>-LF affects binding and transport. This has indeed been shown for the native combinations of EF-PA<sub>63</sub> or LF-PA<sub>63</sub> and the potential ion-ion interaction discussed with EF<sub>N</sub> (Zhang *et al.*, 2004a; Zhang *et al.*, 2004b; Neumeyer *et al.*, 2006a; Neumeyer *et al.*, 2006b). Recently, we could show that C2I binds to PA<sub>63</sub> and may even be transported into target cells albeit at high PA<sub>63</sub> concentration and with very low efficiency compared with the native combination of C2I with C2II (Kronhardt *et al.*, 2011b). Here we studied the cross reactivity of Anthrax and C2 toxin in more detail and found a strong relation between binding affinity and the presence of a His<sub>6</sub>-tag at the N-terminal end of the enzymatic components. The addition of positive charges at the N-terminal end of C2I (due to the partially charged histidines) enhanced binding to and translocation into target cells via PA<sub>63</sub> pores and agreed very well with the findings previously reported for His<sub>6</sub>-tags attached to EF and to LF (Neumeyer *et al.*, 2006a; Neumeyer *et al.*, 2006b). Binding to PA<sub>63</sub> channels was found to be strongly enhanced for the three enzymatic components EF, LF and C2I when they contained a His<sub>6</sub>-tag at the N-terminal end.

Interestingly, we did not observe major effects if these His-tagged proteins were combined with C2II channels. The results of binding experiments with His<sub>6</sub>-EF and His<sub>6</sub>-LF to C2II channels suggested that the increased positive charge at the N-terminal end, due to the partially charged histidines, did not increase the binding of these enzymatic components to the C2II-channels. In agreement with these observations the C2II channel was not able to transport His<sub>6</sub>-EF and His<sub>6</sub>-LF into cells. These results definitely imply that binding of the enzymatic components to PA<sub>63</sub> channels occurs in a different way than binding to C2II channels.

To gain deeper insight in the influence of N-terminal His<sub>6</sub>-tags on binding of proteins to PA<sub>63</sub> channels we choose a protein that was not related to any of the enzymatic components used in this study. gpJ-protein is a truncated form (amino acids 684-1132) of the tail protein J of the Lambda phage, which is responsible for the binding of the phage tail to LamB-porin on the cell surface of enteric gram-negative bacteria (Berkane *et al.*, 2006). As expected, we did not observe any binding of gpJ to PA<sub>63</sub> or C2II channels ( $K_d \gg 10 \mu\text{M}$ ). However, the whole story changed completely when a His<sub>6</sub>-tag was attached to the N-terminal end of gpJ. This protein had a half-

saturation constant for binding to the PA<sub>63</sub> channels of 5 nM, which suggested that the affinity of His<sub>6</sub>-gpJ to PA<sub>63</sub> channels was almost the same as that of LF and EF (Neumeyer *et al.*, 2006a; Neumeyer *et al.*, 2006b). This means that the affinity increase is mainly determined by the positive charges of the His<sub>6</sub>-tag. It is interesting to note that His<sub>6</sub>-gpJ did accordingly not interact with C2II channels; revealing again for a somewhat different process for binding of His<sub>6</sub>-tagged proteins to PA<sub>63</sub> channels than to C2II channels.

#### 5.4.2 Influence of the His<sub>6</sub>-tag on uptake of EF, LF and C2I into cells

The binding step is necessary, but not sufficient for the delivery of enzymatic subunits into target cells. Thus, in order to complement the results of binding studies we went on to investigate the translocation by analyzing the enzymatic activity in a cellular system. We verified that a His<sub>6</sub>-tag attached to the N-terminal end of C2I increased its transport by PA<sub>63</sub> channels, which correlates with the difference of 10-fold measured between the binding constants of C2I and His<sub>6</sub>-C2I. No difference in transport was observed by using EF or LF with or without a His<sub>6</sub>-tag in combination with PA<sub>63</sub> channels. This discrepancy may be due to the already existing high affinity of LF/EF N-terminal domains to PA<sub>63</sub> heptamers (Neumeyer *et al.*, 2006a; Neumeyer *et al.*, 2008). Although the binding of EF<sub>N</sub> and LF<sub>N</sub> (truncated forms of EF and LF) to the PA<sub>63</sub> channel is substantially weaker as compared to wild-type enzymatic components (Leuber *et al.*, 2008), those proteins interact with high affinity with the PA<sub>63</sub> channels and are accordingly transported into the cell (Elliott *et al.*, 2000; Mogridge *et al.*, 2002; Zhang *et al.*, 2004a). Similarly, short stretches of positively charged amino acids attached to the N-terminal end of foreign proteins can lead to a PA<sub>63</sub>-dependent delivery as it has been demonstrated for the amino terminus of the enzymatic A chain of diphtheria toxin (DTA; residues 1-193) or for EDIN (Blanke *et al.*, 1996; Rolando *et al.*, 2009).

#### 5.4.3 Bound (His<sub>6</sub>-)EDIN causes a difference in voltage-dependency of PA<sub>63</sub> pores

Experiments with the epidermal cell differentiation inhibitor EDIN of *S. aureus* were performed to gain deeper insight in the binding and translocation processes through PA<sub>63</sub> channels and its His<sub>6</sub>-tag dependence. Surprisingly, black lipid bilayer experiments displayed that not only His<sub>6</sub>-EDIN but also EDIN itself bound to PA<sub>63</sub> channels. The affinity of EDIN and His<sub>6</sub>-EDIN to the PA<sub>63</sub> channels was in the same range at low trans-membrane potentials because His<sub>6</sub>-EDIN exhibited only a three times higher affinity for binding to the PA<sub>63</sub> channels than EDIN. Under normal conditions the PA<sub>63</sub> channels only close for higher negative voltages applied to the *cis*-side (Neumeyer *et al.*, 2006a). For positive potential the channels are open and do not show a voltage-

dependent closure until 100-150 mV (Neumeyer *et al.*, 2006a). However, His<sub>6</sub>-EDIN binding to the PA<sub>63</sub> channels showed an extremely high voltage-dependence when the voltage was positive at the *cis*-side of the membrane indicating that the potential pulled His<sub>6</sub>-EDIN into the channels. As a result the stability constant for binding of His<sub>6</sub>-EDIN to the PA<sub>63</sub> channels increased at voltages of +70 mV at the *cis*-side (corresponding to -70 mV at the *trans*-side) by a factor of roughly 25 as compared to zero voltage. Bound EDIN displayed an only minor voltage-dependence. This means that the His<sub>6</sub>-tag is responsible for the binding of all these foreign proteins to the PA<sub>63</sub> channels. Binding is presumably essential for translocation because it is the first step of the whole process (see below).

#### 5.4.4 The PA<sub>63</sub> channel transports His<sub>6</sub>-C2I and His<sub>6</sub>-EDIN into HUVECs

EDIN uptake into target cells can easily be detected because it decreases RhoA activity. Import of EDIN via PA<sub>63</sub> channels could not be observed. Import was however, possible when EDIN contained a His<sub>6</sub>-tag. This finding demonstrated that His<sub>6</sub>-tag itself provides the ability for proteins to be transported into cells through PA<sub>63</sub> pores. This effect was presumably promoted by the voltage-dependence of His<sub>6</sub>-EDIN binding to the PA<sub>63</sub> channels. Biological membranes are polarized to about -60 mV to -70 mV (inside negative). This may explain the much higher effect of His<sub>6</sub>-EDIN compared to EDIN on cells described above. In any case it clearly indicates the potentiating effect of a His<sub>6</sub>-tag and applied voltage on binding and translocation of protein molecules to PA<sub>63</sub> channels. Summarizing the results, there definitely exists a difference in the binding and translocation mechanism between the two very homologous binding components PA<sub>63</sub> and C2II of Anthrax and C2 toxin. Obviously, this distinction is induced by unequal binding surroundings inside the head region of the two protein channels.

The amino acids responsible for binding within the N-terminal end of the enzymatic components are relatively unknown, although there is clear evidence that positively charged amino acids are involved in binding, forming salt bridges between the enzymatic components and the heptamers. The positively charged N-termini of the enzymes presumably play a crucial role, because quaternary ammonium ions and 4-aminoquinolones show PA<sub>63</sub> and C2II channel block in lipid bilayer experiments (Blaustein *et al.*, 1990; Finkelstein, 1994; Bachmeyer *et al.*, 2003; Orlik *et al.*, 2005). Both channels show a high selectivity for cations, i.e. cations have a strong influence on the single channel conductance as compared to anions (Blaustein *et al.*, 1989; Schmid *et al.*, 1994). This means that negative charged amino acids play a crucial role in the binding and constriction region of the PA<sub>63</sub> channels, where they form two rings of seven putative negatively charged amino acids in the vestibule of this pore (E398 and D426). Similarly, the channel lumen contains

additional three rings of seven possibly negatively charged groups (E302, E308 and D315). Some of these charges cannot be found in the C2II channel lumen, resulting in minor effects of His<sub>6</sub>-tag on binding and transport. However, transport into cells seems to be possible with C2II pores and when N-terminal parts of C2I are coupled to foreign proteins (Barth *et al.*, 2002a; Barth *et al.*, 2002b; Barth *et al.*, 2004). The most interesting result of this study was that we could use the Anthrax PA<sub>63</sub> channels to deliver into cells a polypeptide completely unrelated to the AB type toxins. In fact, we here provide evidence that the His<sub>6</sub>-tag addition on EDIN allows its entry in target cells, in a PA-dependent manner. Thus it seems possible to design a very simple transportation system using His<sub>6</sub>-tag on proteins unrelated to the AB<sub>7</sub> family and PA<sub>63</sub> channels. Further tests of His<sub>6</sub>-tagged proteins and PA *in vitro* and *in vivo* have to proof if this potential mechanism could be used for biological purposes.







---

---

## BINDING PARTNERS OF PROTECTIVE ANTIGEN FROM *BACILLUS ANTHRACIS* SHARE CERTAIN COMMON MOTIVES\*

### 6.1 INTRODUCTION

Anthrax toxin represents one of the main virulence factors of *Bacillus anthracis*. The plasmid-encoded tripartite toxin comprises a receptor-binding moiety termed protective antigen (PA) and two intracellular active enzymes, edema factor (EF) and lethal factor (LF) (Friedlander, 1986; Mock and Fouet, 2001; Collier and Young, 2003). EF is a calcium and calmodulin-dependent adenylate-cyclase (89 kDa) that causes a dramatic increase of intracellular cAMP level, upsetting water homeostasis and destroying the balance of intracellular signaling pathways (Dixon *et al.*, 1999; Mock and Fouet, 2001; Lacy and Collier, 2002). LF is a highly specific zinc metalloprotease (90kDa) that removes specifically the N-terminal tail of mitogen-activated protein kinase kinases (MAPKKs) (Collier and Young, 2003; Turk, 2007; Rolando *et al.*, 2010). This cleavage leads to subsequent cell death by apoptosis.

Protective antigen (PA) is a cysteine-free 83 kDa protein that binds to two possible receptors, a ubiquitously expressed integral membrane receptor (ATR) and also to the LDL receptor-related protein LRP6, which can both be involved in Anthrax toxin internalization ((Scobie and Young, 2005; Wei *et al.*, 2006). PA<sub>83</sub> present in the serum or bound to receptors is processed by furin to a 63 kDa protein PA<sub>63</sub> (Ezzell and Abshire, 1992; Petosa *et al.*, 1997). PA<sub>63</sub> spontaneously oligomerizes in the serum and/or on the cell surface into a heptamer or octamer (Petosa *et al.*, 1997; Feld *et al.*, 2010) and binds EF and/or LF with very high affinity (Escuyer and Collier, 1991; Elliott *et al.*, 2000; Cunningham *et al.*, 2002). The assembled toxic complexes are then endocytosed and directed to endosomes. There, low pH results in the translocation of EF and LF across the endosomal membrane. Combined with acidification is channel formation by PA<sub>63</sub>, which could represent the mechanism for the translocation scheme of the toxins (Finkelstein, 1994; Miller *et al.*, 1999; Zhang *et al.*, 2004b; Abrami *et al.*, 2005).

---

\* This work resulted from a collaboration of Christoph Beitzinger, Angelika Kronhardt and Roland Benz published in *Toxins and Ion transfers* and is included in this thesis in agreement with all authors.

## 6.2 EXPERIMENTAL PROCEDURES

### 6.2.1 Materials

Recombinant, nicked anthrax protein PA<sub>63</sub> from *B. anthracis* was obtained from List Biological Laboratories Inc., Campbell, CA. One mg of lyophilized protein was dissolved in 1 ml 5 mM HEPES, 50 mM NaCl, pH 7.5 complemented with 1.25% trehalose. Aliquots were stored at -20°C.

### 6.2.2 Black lipid bilayer measurements

Black lipid bilayer membranes were formed as described previously (Benz *et al.*, 1978). The instrumentation consisted of a Teflon chamber with two aqueous compartments connected by a small circular hole. The hole had a surface area of about 0.4 mm<sup>2</sup>. Membranes were formed by painting onto the hole a 1% solution of diphytanoyl phosphatidylcholine (Avanti Polar Lipids, Alabaster, AL) in n-decane. The aqueous salt solutions (Merck, Darmstadt, Germany) were buffered with 10 mM MES-KOH, pH 6. Control experiments revealed that the pH was stable during the time course of the experiments. PA<sub>63</sub> was reconstituted into the lipid bilayer membranes by adding concentrated stock solutions to the aqueous phase to the *cis*-side of a membrane in the black state. Membrane reconstitution reached its maximum between 60 to 120 minutes after addition of PA to the *cis*-side.

Membrane conductance was measured after application of a fixed membrane potential from a battery-operated voltage source with a pair of silver/silver chloride electrodes with salt bridges inserted into the aqueous solutions on both sides of the membrane. The membrane current was measured with a homemade current-to-voltage converter using a Burr Brown operational amplifier with feedback resistors between 0.1 and 10 GΩ. The potentials applied to the membranes throughout the study always refer to those applied to the *cis*-side, the side of addition of PA. Similarly, positive currents were caused by positive potentials at the *cis*-side and negative ones by negative potentials at the same side. The temperature was kept at 20°C throughout.

Titration experiments were performed with membranes containing only a few or many PA<sub>63</sub> channels, respectively. The amplified signal was recorded with a strip chart recorder to measure the absolute magnitude of the membrane current and to calculate the stability constant *K* for substrate binding to PA. The conductance data of the titration experiments were analyzed using a formalism derived earlier for the carbohydrate-induced block of the maltoporin and CymA channels (Benz *et al.*, 1987; Orlik *et al.*, 2002a; Orlik *et al.*, 2003) and the block of the PA<sub>63</sub> channels with LF and EF (Neumeyer *et al.*, 2006a; Neumeyer *et al.*, 2006b). The conductance,

$G(c)$ , at a given concentration  $c$  of substrates relative to the initial conductance,  $G_{\max}$  (in the absence of substrates), was analyzed using the following equation:

$$\frac{G_{\max} - G(c)}{G_{\max}} = \frac{K \cdot c}{K \cdot c + 1} \quad [6.1]$$

$K$  is the stability constant for the binding of substrates to the  $PA_{63}$  channel. The half saturation constant,  $K_s$ , of its binding is given by the inverse stability constant  $1/K$ .

## 6.3 RESULTS

There are different substrates which are characterized to bind to protective antigen. These are proteins, related or not related to the AB<sub>7</sub> type toxins, and small molecule inhibitors.

### 6.3.1 Native effector proteins of protective antigen

#### 6.3.1.1 Full length EF and LF

Anthrax toxin consists of the binding and translocation component protective antigen (PA) and the two enzymatic components edema factor (EF) and lethal factor (LF). They both bind to the same motif located in domain 1 of the PA<sub>63</sub> prepore (Lacy and Collier, 2002; Pimental *et al.*, 2004). As two monomers of the heptameric prepore are required to bind one enzymatic component (Cunningham *et al.*, 2002) the heptameric form of the PA channel is able to bind up to three molecules at the same time (Mogridge *et al.*, 2002), whereas the PA octamer provides up to four binding sites (Feld *et al.*, 2010). Both EF and LF attach with their N-terminal end to PA. Arora and Leppla could show that the N-terminal domain is sufficient to bind to PA and also to translocate fusion proteins (Arora and Leppla, 1993). Recently, Feld and colleagues demonstrated that LF initially binds with its N-terminal domain to an amphipatic cleft on the surface of the PA<sub>63</sub> prepore, the so called  $\alpha$ -cleft (Feld *et al.*, 2010).

In lipid bilayer membranes titration experiments revealed that binding only occurred when EF and LF were added to same side as PA<sub>63</sub> (the *cis*-side of the membrane), substrate given to the *trans*-side did not show any effect indicating that the PA pore only possesses one binding site within the mushroom body (Neumeyer *et al.*, 2006a; Neumeyer *et al.*, 2006b). The conductance decreased in a dose-dependent manner. The affinity to the PA pore is in the low nanomolar range and it could be shown that the block of PA is a single hit process. As the binding is ionic strength-dependent the  $K_d$  values increase by a factor of about 500 from 50 mM to 1000 mM KCl electrolyte concentration.

#### 6.3.1.2 EF<sub>N</sub> and LF<sub>N</sub>

EF's and LF's N-terminal fragments called EF<sub>N</sub> and LF<sub>N</sub> as well as fusion proteins are able to bind to PA channels, e.g. LF<sub>N</sub>-DTA, and are translocated through the pore into the cytosol of target cells (Blanke *et al.*, 1996). Therefore, the truncated components EF<sub>N</sub> and LF<sub>N</sub> were supposed to have similar binding properties as full length EF and LF. However, the affinity of the truncated proteins is tenfold weaker compared to full length EF and LF indicating that

further interactions of the C-terminal region of EF and LF are involved in the binding process (Leuber *et al.*, 2008).

### 6.3.1.3 His-tagged proteins

Several studies elucidated that an N-terminal His<sub>6</sub>-tag attached to EF or LF increases the binding affinity to the PA channel (Blanke *et al.*, 1996; Neumeyer *et al.*, 2006a; Neumeyer *et al.*, 2006b). As the binding is due to interactions between negative charges of the PA pore and positive charges of the enzymatic components, additional positive charges of the His<sub>6</sub>-tag enhance the binding of the truncated EF<sub>N</sub> and LF<sub>N</sub> to the PA channel as well by a factor of about 10 (Leuber *et al.*, 2008).

## 6.3.2 Cross-reactivity of Anthrax and C2 toxin

### 6.3.2.1 Binding of close related proteins

Another prominent member of the AB<sub>7</sub> toxin family is the C2 toxin of *Clostridium botulinum*. It performs a very similar mode of intoxication and the channel forming components C2II and PA exhibit about 35% amino acid homology. To test if these two toxins are also functionally interchangeable, cross-reaction experiments were performed by combining the channel forming component of one toxin with the respective enzymatic component of the other toxin (Kronhardt *et al.*, 2011b). In lipid bilayer experiments binding could be observed for each combination, however, Anthrax EF and LF had higher binding affinities to the C2II-channel than C2I to the PA channel. *In vitro* experiments revealed that PA is not only able to bind but also to translocate the enzymatic component C2I of C2 toxin resulting in intoxication and cell death. The combination of C2II and EF or LF, respectively, merely led to toxic effects when exposed to HUVEC cells (Kronhardt *et al.*, 2011b). Due to this high flexibility PA is an extremely interesting protein for a general transport system across membranes.

### 6.3.2.2 Binding of unrelated proteins is enabled by His<sub>6</sub>-tag

It was shown before that polycationic peptides fused to diphtheria toxin (DTA) enhances the uptake of this protein via PA pores (Blanke *et al.*, 1996). This work focused on different, charged tags, which exhibited either no change in affinity for Glu<sub>6</sub>-tag and random sequence (compared to untagged DTA) or increased binding for His<sub>6</sub>-, Arg<sub>6</sub>- and Lys-tags of different length. With the knowledge of the binding properties of his-tagged native effectors, the DTA experiments and cross-reactivity of C2I, the next step was to check for His<sub>6</sub>-C2I. The affinity to PA *in vivo* and *in vitro* was strongly increased as expected (Beitzinger *et al.*, 2011). Following this set of experiments

a protein fragment of Lambda phage protein (gpJ) not related to any toxins was tested. Whereas gpJ was not able to bind to PA, its affinity towards the PA channel was in the range of EF and LF when it was coupled to a His<sub>6</sub>-tag (Beitzinger *et al.*, 2011). Finally, the authors could show similar results for EDIN of *Staphylococcus aureus*, which ADP-ribosylates and inactivates Rho GTP binding proteins. His<sub>6</sub>-EDIN binds to the PA channel in titration experiments and is transported through the PA channel in intoxication assays. Additionally, it has been found that the process is highly voltage-dependent. This means that PA pores may be used as molecular syringes, which deliver His<sub>6</sub>-tagged target proteins into cells possessing the known receptors for PA (Lang *et al.*, 2010).

### 6.3.3 Small molecule inhibitors

#### 6.3.3.1 Chloroquine and other 4-aminoquinolones block protective antigen

Anthrax toxin is one of the most potent bacterial toxins and could be used as a biological weapon or for terroristic activities by spreading spores of multi resistant *B. anthracis* bacteria (Keim *et al.*, 2001; Inglesby *et al.*, 2002; Jernigan *et al.*, 2002). This threat could be handled by introducing small molecules which are able to block PA pores and efficiently prohibit translocation of the effectors, therefore buying time to deal with the bacterial infection. First results were found for chloroquine and other 4-aminoquinolones formerly used as antibiotics (Lewis *et al.*, 1973; Vedy, 1975). These substrates depicted high affinity binding in titration experiments to PA (Orlik 2005a). Additionally, it is well known, that chloroquine acquires positive charges under acidic condition and accumulates in endosomes (Neumeyer *et al.*, 2008). Both effects would enhance the blockage of PA *in vivo*. Concerning the side effects of chloroquine and related substances on humans, there is the urge for blocker-molecules with homologous structure which do not exhibit cell toxicity.

#### 6.3.3.2 Cyclodextrin-complexes form a plug for the PA pore

Cyclodextrins have been found to bind to CymA porin of *Klebsiella oxytoca* (Pajatsch *et al.*, 1999; Orlik *et al.*, 2003). The ring-shaped complex of seven glucose units in  $\beta$ -cyclodextrin happens to be in a perfect size for the blockage of binary toxin channels and is itself not toxic at all. Additionally,  $\beta$ -cyclodextrin and PA share a sevenfold symmetry, which offers one side chain of  $\beta$ -cyclodextrin for each PA<sub>63</sub> monomer. Therefore,  $\beta$ -cyclodextrin has been tested as a basis drug for PA blockage (Nestorovich *et al.*, 2010). Recently, experiments with  $\beta$ -cyclodextrin and C2II – a very homologous AB<sub>7</sub> toxin-channel as described before – were performed in a trial of modern, literature based drug design. In this study, changes in the outward facing part of the rings



functional groups led to enhanced binding stabilities. Interestingly, the introduction of a positive charge and some aromatic residues were found to be responsible for this effect (Nestorovich *et al.*, 2011). The possible seven charges in the  $\beta$ -cyclodextrin structure seem to match with the PA binding pocket. Even though the authors could show blockage of intoxication in cell-based assays, the seven permanent charges could avoid specificity or passage through membranes *in vivo*, which reasons in the necessity of further pharmacological studies.

#### 6.3.4 Binding of divalent and trivalent cations to protective antigen

The PA channel is known to be highly cation selective (Blaustein *et al.*, 1989) and additional positive charges of His<sub>6</sub>-tags increase the binding properties of several proteins (Blanke *et al.*, 1996; Neumeyer *et al.*, 2006a; Neumeyer *et al.*, 2006b; Leuber *et al.*, 2008; Beitzinger *et al.*, 2011). Therefore, we addressed the question if also divalent and trivalent cations are able to bind and to block the PA<sub>63</sub> channel.

The binding of CuSO<sub>4</sub>, ZnCl<sub>2</sub> and NiCl<sub>2</sub> LaCl<sub>3</sub> to the PA<sub>63</sub> channel was investigated by performing titration experiments similar to those described for binding of EF and LF (Boquet and Lemichez, 2003; Neumeyer *et al.*, 2006a; Neumeyer *et al.*, 2006b). After reconstitution of the PA channels into the *cis*-side of a lipid bilayer membrane, the rate of insertions became very small. Then, concentrated solutions of divalent or trivalent cations were added to the *cis*- or the *trans*-side of the membrane, respectively, while stirring to allow equilibration. The membrane conductance decreased in a dose-dependent manner meaning that the cations bound to the PA channel and thereby reduced the conductance. Analysis of the titration experiments by Lineweaver-Burke plots according to equation [6.1] indicated that the interaction between the cations and the PA channel represents a single hit binding process. The results shown in Table 6.1 reveal that there are considerable differences concerning the stability constants of the respective cations to the PA pore. Highest binding affinity was observed for Cu<sup>2+</sup>, followed by La<sup>3+</sup>, which was in the micromolar range, whereas the binding affinity of Ni<sup>2+</sup> and Zn<sup>2+</sup> were in the millimolar range. The binding constants of the divalent and trivalent cations to the PA channel decreased in the series  $K_{Cu} > K_{La} > K_{Zn} > K_{Ni}$  from about 10,000 1/M to about 100 1/M in 150 mM KCl (see Table 6.1).

Binding to the PA channel is generally supposed to rely on ion-ion interaction. Therefore, we performed titration experiments for binding of Cu<sup>2+</sup> in various electrolyte concentrations to check if this was also true for the binding of the divalent cations. The stability constants  $K$  for Cu<sup>2+</sup> binding to the PA channel decreased with increasing electrolyte concentration from about 80,000 1/M at 50 mM KCl to about 1,500 mM 1/M at 1 M KCl (see Table 6.2). That means that

the stability constant of copper ion binding to the PA channel is strongly ionic-strength dependent.

**Table 6.1. Stability constants  $K$  of  $\text{Cu}^{2+}$  to  $\text{PA}_{63}$  channels in lipid bilayer membranes.**

$\text{PA}_{63}$ with		$K [\text{M}^{-1}]$	$K_s [\text{mM}]$
$\text{Cu}^{2+}$	cis +10mV	9240	0.11
	cis -10mV	7240	0.22
	trans +10mV	5250	0.21
$\text{Ni}^{2+}$	cis +10mV	122	8.6
	cis -10mV	47	22.9
	trans +10mV	65	17.8
$\text{Zn}^{2+}$	cis +10mV	1250	1.1
	cis -10mV	307	3.3
	trans +10mV	244	4.9
$\text{La}^{3+}$	cis +10mV	1330	0.8
	cis -10mV	654	1.6

The membranes were formed from diphytanoyl phosphatidylcholine/n-decane. The aqueous phase contained four different KCl-concentrations, 10 mM MES-KOH pH 6.0;  $T = 20^\circ\text{C}$ . The data represent means of at least three titration experiments.  $K_s$  is the half saturation constant, calculated as  $1/K$ . Note that the ionic strength had a considerable influence on the stability constant of binding of copper ions to the  $\text{PA}_{63}$  channel.

Interestingly, the binding of the cations was barely influenced by the side of addition. Irrespective of the side of addition, the stability constants were nearly stable. Additionally, the binding affinities of the cations to the PA channel were not changed when negative voltage in the physiological range was applied. This indicates that the cations were able to equilibrate rapidly across the PA channel irrespective of the applied voltage.

The results of the titration experiments suggested that the PA channel either contains two different binding sites for divalent and trivalent cations, one at the *cis*- and one at the *trans*-side of the channel, or just one binding site which is accessible from both sides of the channel. This could be the case, as the small cations are able to cross the channel rapidly and equilibrate in the aqueous solution. Titration experiments with copper ions on both sides of the membrane led to subsequent decrease of PA-induced conductance. Then, 5 mM EDTA was added to the *trans*-side

of the membrane. No effect on the conductance could be observed. However, addition of EDTA to the *cis*-side of the membrane resulted in increasing conductance. The copper induced blockage of the PA channels could be fully restored meaning that the PA pore only contains one binding site for copper ions which is localized at the *cis*-side of the channel.

**Table 6.2. Stability constants  $K$  of  $\text{Cu}^{2+}$ ,  $\text{Ni}^{2+}$ ,  $\text{Zn}^{2+}$  and  $\text{La}^{3+}$  to  $\text{PA}_{63}$  channels in lipid bilayer membranes.**

$\text{PA}_{63}$ with		$K [\text{M}^{-1}]$	$K_s [\text{mM}]$
$\text{Cu}^{2+}$	50 mM	87935	0.01
	150 mM	9237	0.11
	300 mM	3638	0.31
	1 M	1626	0.66

The membranes were formed from diphytanoyl phosphatidylcholine/n-decane. The aqueous phase contained 150 mM KCl, 10 mM MES-KOH pH 6.0;  $T=20^\circ\text{C}$ . The voltage was applied as indicated. The data represent the means of at least three individual experiments.  $K_s$  is the half saturation constant, calculated as  $1/K$ .

## 6.4 DISCUSSION

### 6.4.1 Binding substrates of protective antigen share common motives

#### 6.4.1.1 Positive charges play a crucial role in binding to PA<sub>63</sub> channels

It is well known that PA pores are strongly cation selective up to a factor of  $20 p_c/p_a$  (Blaustein *et al.*, 1989). Additionally, recent studies found proof, that negatively charged amino acids in the vestibule of PA-channels play a crucial role in the binding of EF and LF (Orlik *et al.*, 2005; Leuber *et al.*, 2008). These findings already indicate the importance of ion-ion interaction for binding and translocation events to PA. The data presented here underline this assumption by depicting the existence of positive charges in high affinity substrates ranging from simple ions, over small inhibitor molecules and molecule complexes as well as peptides, to related proteins and finally protein effectors only containing chargeable tags.

First time evidence that different cationic electrolytes serve as a binding partner to PA channels is presented in this work. This is of special interest, as the ions themselves seem to be too small to block the channel conductance. The sevenfold symmetry of the pore provides seven possible negative charges for each acidic amino acid facing the lumen of PA<sub>63</sub>. On top of that, the constriction site of PA, the so called  $\Phi$ -clamp is surrounded by these rings of negative charges. Therefore, a plug consisting of more and more cations may form around this site explaining the results. Additional support for this theory is provided by the studies with sevenfold charged  $\beta$ -cyclodextrin and the length dependent binding of positive charged tags (Blanke *et al.*, 1996; Nestorovich *et al.*, 2010). Binding of cations could be possible from both sides of PA channels out of two reasons: First, multiple rings of acidic amino acids exist in the lumen of the channel, which are accessible from both sides. Second, ions might be small enough to pass the  $\Phi$ -clamp and bind from the opposite side. It has been shown, that this is not the case as for all substrates starting with simple molecules only one binding site could be verified.

#### 6.4.1.2 Aromatic residues enhance affinities towards PA pores

Another important function is represented by aromatic ring-systems. Especially when the affinity of blocker-substrates is discussed, it becomes obvious that the existence of aromatic residues strengthens the binding to toxin channels (Nestorovich *et al.*, 2011). This could be found on the existence of the  $\Phi$ -clamp, too. As the on-rate derived by current noise analysis is in the range of diffusion for molecules like chloroquine, the off-rate contributes to a larger extent to the stability constant (Orlik *et al.*, 2005). That means, that molecules which are directed directly to the constriction site and settle there should form the most stable block. Considering the  $\Phi$ -clamps

composition out of seven phenylalanine residues, it is easy to understand, that aromatic side-chains serve this purpose best (Orlik *et al.*, 2005). Taken the pharmacological use of those substrates into consideration, the aromatic residues could provide a further purpose in enabling these molecules to cross membranes and reach the endosome, where they are charged due to acidic pH. This trapping effect known from chloroquine and other 4-aminoquinolones further increases blockage of PA channels.

#### **6.4.2 Binding of charged substrates is voltage-dependent**

Recently a change in voltage-dependency of the PA channel after His<sub>6</sub>-EDIN titration has been found (Beitzinger *et al.*, 2011). The stability constants for binding are influenced when positive voltages are applied. It seems to be the case, that the force of the electric field pulls the tagged N-terminus of the protein deeper into the pore, thereby increasing the stability constant for binding of these His<sub>6</sub>-tagged polypeptides. This finding partially serves as an explanation for the translocation of foreign substrates *in vivo*, which possess positively charged tags, as the acidic endosome exhibits this field direction. Further studies are necessary to fully elucidate this voltage-dependent binding and translocation process of all charged substrates to the PA pore mentioned here.

#### **6.4.3 Conclusion**

Considering the data provided and summed up here, it is obvious, that binding and translocation concerning PA is of special interest. Not only for understanding one of the most potent bacterial toxins in more detail, but in order to cure anthrax intoxication in the context of biological terrorism and the potential usage of PA as a versatile molecular syringe for various purposes, further work has to be done in this vital field of studies.



---

---

## CLOSTRIDIUM DIFFICILE CDT TOXIN FORMS TWO DIFFERENT TYPES OF CHANNELS \*

### 7.1 INTRODUCTION

*Clostridium difficile* is an anaerobic, Gram-positive bacterium able to form highly resistant spores. Nowadays, a severe increase of *Clostridium difficile* infection has been reported in North America and Europe (McDonald *et al.*, 2006; Rupnik *et al.*, 2009; Viswanathan *et al.*, 2010). The pathogenicity is due to the secretion of various toxins. The major virulence factors are Toxin A and Toxin B (TcdA and TcdB) which are exotoxins of the large clostridial toxin family (LCTs). They are known as nosocomial pathogens inducing mucosal inflammation and diarrhea after treatment with antibiotics in hospitals. Hypervirulent strains also produce the binary toxin *Clostridium difficile* transferase (CDT). It belongs to the family of binary actin-ADP-ribosylating toxins and is closely related to *Clostridium perfringens* iota toxin or *Clostridium spiroforme* binary toxin.

Binary toxins of the AB<sub>7</sub> type consist of an enzymatic component A and a separate, non linked binding and translocation component B. After bacterial secretion, the binding component is activated by proteolytic cleavage. Activated monomers oligomerize and form prepores which bind to a cellular receptor as well as to the enzymatic component. Following endocytosis, acidification of the endosome leads to a conformational change of the prepore into a functional, membrane spanning pore which translocates the enzymatic component into the cell cytosol.

*Clostridium difficile* CDT toxin's enzymatic subunit CDTa acts as an actin-ADP-ribosyltransferase modifying G-actin at position Arginine-177 (Vandekerckhove *et al.*, 1987; Barth *et al.*, 2004) leading to depolymerization of the actin cytoskeleton and hence to cell rounding and death (Wieggers *et al.*, 1991; Perelle *et al.*, 1997; Hilger *et al.*, 2009). In low concentration, CDTa induces the formation of microtubule-based protrusions on the cell surface facilitating an increased bacterial adherence and colonization (Schwan *et al.*, 2009).

\* This work resulted from a collaboration of Angelika Kronhardt, Michel R. Popoff and Roland Benz and is included in this thesis in agreement with all authors.

The binding components of *C. difficile* CDTb, *C. spiroforme* Sb and *C. perfringens* Ib share about 80% amino acid homology and are known to be interchangeable (Popoff and Boquet, 1988). This means that they are able to translocate the enzymatic component of the respective other toxins into target cells leading to intoxication and cell death. However, the mechanism of cell intoxication is still largely unknown yet.

Here we report that there are two different channels formed by *Clostridium difficile* CDTb depending on the presence of cholesterol which differ considerably in their biophysical properties. Our study reveals so far unknown features of oligomerization and channel formation by a binary toxin's B component.



## 7.2 MATERIALS AND METHODS

### 7.2.1 CDTa and CDTb production and purification

CDT genes were amplified from *C. difficile* strain CD196 and cloned into the expression plasmid pMRP384 (Gibert *et al.*, 2000) and checked by sequencing. The recombinant plasmids were transformed for propagation into *Escherichia coli* strain TOP10 and thereafter transferred via electroporation into *C. perfringens* strain 667 (lecithinase-, enterotoxin-, beta-, epsilon-, and Iota-negative strain) for expression.

Recombinant *C. perfringens* strain harboring *cdtb* gene was grown in broth containing 30 g of Trypticase, 20 g of yeast extract, 5 g of glucose, and 0.5 g of cysteine-HCl/l (7.2) under anaerobic conditions. The supernatant from overnight culture was subjected to precipitation with ammonium sulfate (70% saturation), dialyzed against 10 mM Tris pH 7.5, and dissolved in the same buffer. The proteins were loaded onto a DEAE-Sephacel column (1.5 by 10 cm; Pharmacia, Orsay, France) equilibrated with 10 mM Tris pH 7.5, and the column was washed with 0.1 M NaCl in 10 mM Tris pH 7.5 and eluted with 0.2 M NaCl in the same buffer. The eluate was dialyzed against 10 mM sodium citrate (pH 5.5) and loaded onto a DEAE-Sephacel column (1.5 by 10 cm; Pharmacia, Orsay, France) equilibrated with the citrate buffer. Proteins were eluted with a linear gradient from 0 to 0.1 M in the citrate buffer. The CDTb-containing fractions, as tested by measuring the cytopathic activity in the presence of CDTa, were combined and concentrated by ammonium sulfate precipitation. Afterwards proteins were activated with 0.2 µg of  $\alpha$ -chymotrypsin /µg of protein for 30 min at 37 °C and separated by gel filtration on a Superdex 200 column (2.6 by 60 cm; Pharmacia, Orsay, France).

Culture supernatant of recombinant *C. perfringens* harboring *cdta* gene was prepared from the overnight cultures by centrifugation at 5000 x g for 10 min. Proteins in the supernatant were precipitated with ammonium sulfate (70% saturation). The precipitate was dissolved in 10 mM Tris-HCl, pH 7.5, and then dialyzed against the same buffer. The dialysate was loaded to a DEAE-Sephacel column (1.5 x 10 cm; Pharmacia, Orsay, France) equilibrated with the same buffer. Proteins were eluted with a linear gradient of 0 to 0.1 M NaCl in the same buffer. Fractions containing CDTa as tested by cytopathic activity in the presence of CDTb, were combined, and concentrated by precipitation with ammonium sulfate (70% saturation). Proteins were separated by gel filtration on a Superdex 200 column (2.6 x 60 cm; Pharmacia) equilibrated with Tris-HCl pH 7.5 buffer. The CDTa containing fraction was stored at -80° C.

### 7.2.2 Lipid bilayer experiments

Black lipid bilayer measurements were performed as described previously (Benz *et al.*, 1978). The instrumentation consisted of a Teflon chamber with two aqueous compartments connected by a small circular hole. The hole had a surface area of about 0.4 mm<sup>2</sup>. Membranes were formed by painting a 1% solution of diphytanoyl phosphatidylcholine (Avanti Polar Lipids, Alabaster, AL) in n-decane onto the hole. The aqueous salt solutions (Merck, Darmstadt, Germany) were buffered with 10 mM MES to pH 5.5 to pH 6. Control experiments revealed that the pH was stable during the time course of the experiments. The binding components of the binary toxins were reconstituted into the lipid bilayer membranes by adding concentrated solutions to the aqueous phase to one side (the *cis*-side) of a black membrane. The temperature was kept at 20°C throughout. Membrane conductance was measured after application of a fixed membrane potential with a pair of silver/silver chloride electrodes inserted into the aqueous solutions on both sides of the membrane. The potentials applied to the membranes throughout the study refer always to those applied to the *cis* side, the side of addition of PA. Similarly, positive currents were caused by positive potentials at the *cis* side and negative ones by negative potentials at the same side. Membrane current was measured using a homemade current-to-voltage converter made with a Burr Brown operational amplifier. The amplified signal was monitored on a storage oscilloscope and recorded on a strip chart recorder. Zero-current membrane potentials were measured by establishing a salt gradient across membranes containing 100–1000 channels, as described earlier (Benz *et al.*, 1985).

#### 7.2.2.1 Selectivity

For the selectivity measurements, the membranes were formed in a 100-mM KCl solution. CDTb was added to the *cis*-sides of the membrane and the increase of the membrane conductance due to insertion of pores was observed with an electrometer. After incorporation of 100–1000 pores into a membrane the instrumentation was switched to the measurement of the zero-current potential and a KCl gradient was established by adding 3 M KCl solution to the *cis*-side of the membrane. To adjust the volume 0.15 mM KCl was added to the *trans*-side at the same time. Analysis of the zero current membrane potential was performed using the Goldman–Hodgkin–Katz equation (Benz *et al.*, 1979a).

### 7.2.2.2 Binding experiments

The binding of EF and LF to the C2II channel and the binding of C2I to the PA<sub>63</sub> and to the C2II channel was investigated performing titration experiments similar to those used previously to study the binding of 4-aminoquinolones to the PA<sub>63</sub> and C2II channels and LF to the PA<sub>63</sub>-channel in single- or multi-channel experiments (Bachmeyer *et al.*, 2003; Orlik *et al.*, 2005; Neumeyer *et al.*, 2006b). The PA<sub>63</sub> and C2II channels were reconstituted into lipid bilayers. About 60 minutes after the addition of either activated PA<sub>63</sub> or C2II to the *cis*-side of the membrane, the rate of channel insertion in the membranes was very small. Then concentrated solutions of EF, LF or C2I were added to the *cis*-side of the membranes while stirring to allow equilibration. The results of the titration experiments, i.e. the blockage of the channels, were analyzed using Langmuir adsorption isotherms (see eqn. [1]) (Benz *et al.*, 1987; Neumeyer *et al.*, 2006a).

$$G(c) = G_{\max} \frac{1}{(K \cdot c + 1)} \quad [7.1]$$

$G(c)$  is the conductance of the channels at a given concentration  $c$  of the enzymatic components and  $G_{\max}$  is their conductance before the start of the titration experiment (at  $c = 0$ ).  $K$  is the stability constant for binding of the enzymatic components of the binary toxins to the PA<sub>63</sub> or C2II channels. The half saturation constant  $K_s$  of binding is given by the inverse stability constant  $1/K$ . The percentage of blocked channels is given by:

$$\% \text{ closed channels} = \frac{100 \cdot K \cdot c}{K \cdot c + 1} \quad [7.2]$$

## 7.3 RESULTS

### 7.3.1 Single channel measurements

#### 7.3.1.1 Channel formation by activated CDTb

In the first experimental setup we studied the ability of CDTb to form pores in lipid bilayer membranes made of diphytanoyl phosphatidylcholine/*n*-decane. Channel insertion was observed in low frequency when activated CDTb was added to the aqueous phase. The pores were stable and had a lifetime of at least 10 minutes in the membrane (Figure 7.1A). The single channel conductance was on average 380 pS in 1 M KCl with an applied voltage of 50 mV. Figure 7.2A shows the distribution of channel conductance which was fairly homogenous. The observed single channel conductance was dependent on the salt concentration in the bulk aqueous phase resulting in a linear function indicating that there is no binding site for chloride or potassium ions. The conductance was also measured in 1 M LiCl and in 1 M K<sup>+</sup>acetate. Compared to measurements in 1 M KCl the conductance was reduced in both salts, in LiCl the conductance of CDTb channels was 280 pS whereas in K<sup>+</sup>acetate it was 160 pS (Table 7.1).

**Table 7.1. Single channel conductance of CDTb and Ib channels in different electrolyte solutions.**

Electrolyte	Concentration <i>c</i> [M]	Single channel conductance <i>G</i> [pS]		
		CDTb	CDTb <i>G/C</i>	Ib <sup>1</sup>
KCl	0.15	60	30	n.m.*
	1	380	160	85
	3	1300	n.m.*	180
LiCl	1	280	n.m.*	35
KCH <sub>3</sub> COO	1	160	n.m.*	55

Average single channel conductance (*G*) of the channels formed by the activated binding component CDTb untreated (left column) or after preincubation with cholesterol dissolved in 1% genapol (*G/C*) (middle column) in different salt solutions. Membranes were formed from 1% diphytanoyl phosphatidylcholine dissolved in *n*-decane. The aqueous solutions were unbuffered and had a pH of 6. The applied voltage was 50 mV, the temperature was kept at 20°C throughout. The average single channel conductance was calculated from at least 100 single events. *c* is the concentration of the aqueous salt solution. The single channel conductance of Ib of *C. perfringens* iota toxin is given for comparison. (\*n.m., not measured; <sup>1</sup> taken from Knapp *et al*, 2002)

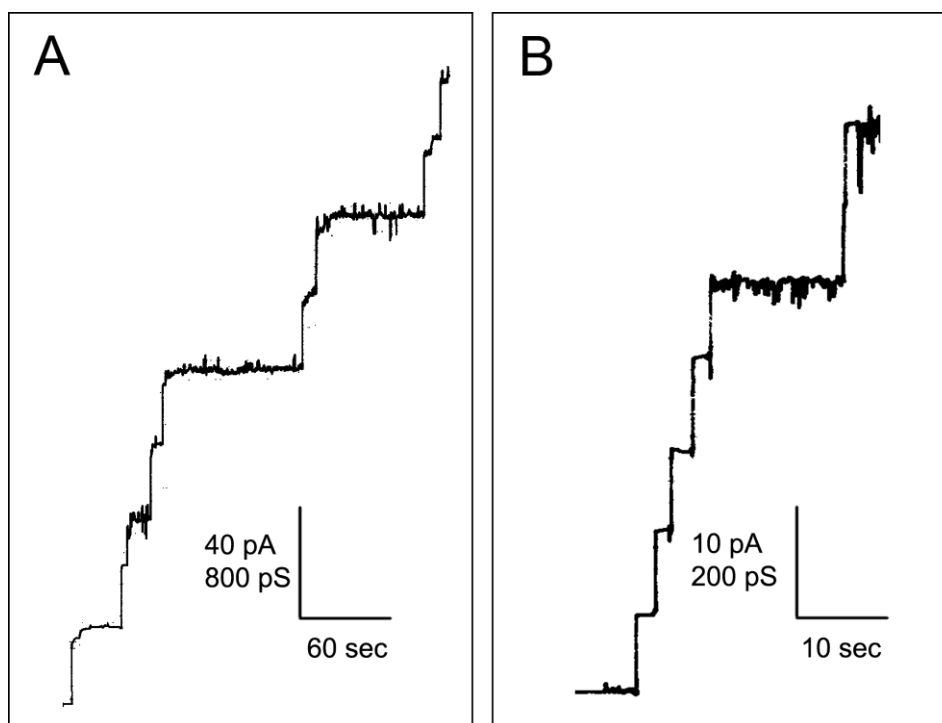


**Figure 7.1. Single channel recordings of CDTb.** (A) Activated CDTb ( $c = 35\text{nM}$ ) was added to the *cis*-side of a membranes formed of diphytanoyl phosphatidylcholine/*n*-decane. The aqueous phase contained 1 M KCl, applied membrane potential 50 mV,  $T=20^\circ\text{C}$ . (B) Activated CDTb ( $c = 1\text{nM}$ ) preincubated with cholesterol in 1% genapol was added to the *cis*-side of a membrane formed of diphytanoyl phosphatidylcholine/*n*-decane. The aqueous phase contained 1 M KCl, applied membrane potential was 50 mV,  $T=20^\circ\text{C}$ .

### 7.3.1.2 Channel formation by CDTb with cholesterol

Because of the low frequency of channel insertion we preincubated activated CDTb with cholesterol dissolved in 1% Genapol overnight in a volume ratio of 1:1. Under same experimental conditions (1 M KCl, 50 mV applied voltage) the rate of channel insertion was considerably increased (Figure 7.1B). Furthermore, the single channel conductance decreased and only few channels of the original conductance could be detected. The majority of the channels had a conductance of 160 pS (Figure 7.2B). Pores were stable for minutes in the membrane but became slightly noisy after insertion of several channels. In 0.15 M KCl the average single channel conductance dropped likewise from 60 to 30 pS (Table 7.1). Note that this effect was clearly due to the addition of cholesterol as the incubation with 1% Genapol only did not lead to the insertion of smaller channels.

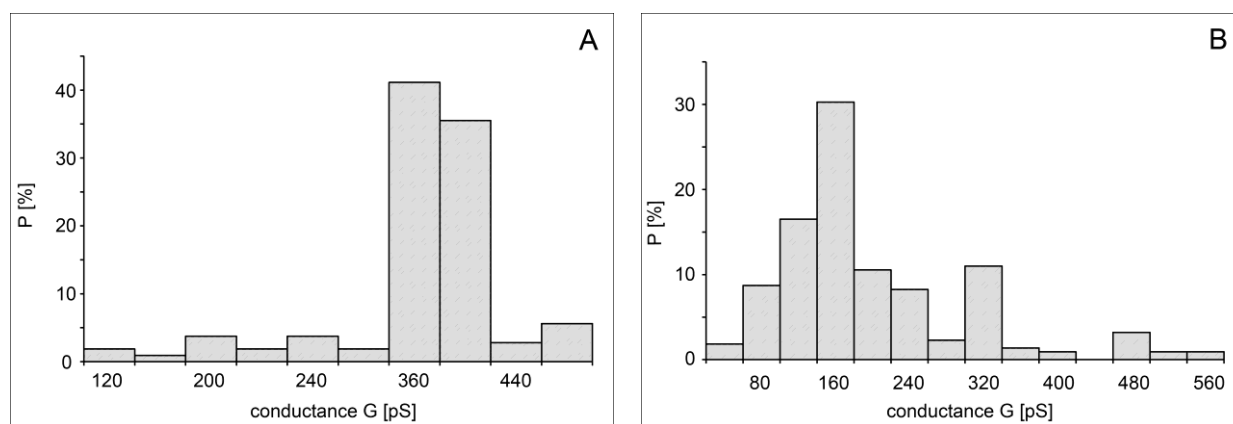


**Figure 7.2. Histograms of the probability of the occurrence of certain conductivity units observed with membranes in the presence of activated CDTb from *C. difficile*.** (A) The aqueous phase contained 1 M KCl and activated, untreated CDTb. The applied membrane potential was 50 mV;  $T = 20^{\circ}\text{C}$ . The average single channel conductance was 380 pS for 107 single channel events. (B) The aqueous phase contained 1 M KCl and activated CDTb incubated with cholesterol in 1% genapol. The applied membrane potential was 50 mV;  $T = 20^{\circ}\text{C}$ . The average single channel conductance was 160 pS for 212 single channel events.

### 7.3.2 Selectivity

#### 7.3.2.1 Untreated CDTb channels are anion selective

The selectivity of CDTb channels was measured in zero-current membrane potential measurements. After insertion of least 100 channels to the *cis*-side of a black lipid bilayer membrane with an aqueous phase containing 0.15 M KCl, a salt gradient was created over the membrane by addition of 3 M KCl to the *cis*-side of the membrane. Simultaneously, the same amount of 0.15 M KCl was added to the *trans*-side of the membrane to adjust the volume. Addition was performed stepwise with 100  $\mu\text{l}$  salt solution. After each addition the *trans*-side of the membrane, which was the more diluted, became negative. This indicates a preferential movement of anions over cations through the lumen of the CDTb channel. Analysis using the Goldman-Hodgkin-Katz equation (Benz *et al.*, 1979a) revealed a ratio  $P_{\text{cations}}/P_{\text{anions}}$  of 0.5 which means that for every cation two anions passed the channel (Table 7.2).

#### 7.3.2.2 CDTb channels preincubated with cholesterol are cation selective

In order to check if the CDTb pores incubated with cholesterol had the same biophysical properties as the untreated channels, we performed selectivity measurements using the zero-current membrane potential method performed as described above. The smaller CDTb channels turned out to be slightly cation selective as after each addition the *trans*-side, which was more diluted, became positive. The ratio of  $P_{\text{cations}}/P_{\text{anions}}$  calculated using the Goldman-Hodgkin-Katz

equation was 1.3 meaning that for every anion 1.3 cations were able to pass the channel (Table 7.2).

**Table 7.2. Selectivity of untreated CDTb and CDTb preincubated with cholesterol in 1% genapol (C/G) in comparison with Ib channels.**

	$P_c / P_a$
CDTb untreated	0.5
CDTb C/G	1.3
Ib*	5.5

Membranes were formed from 1% diphytanoyl phosphadylcholine dissolved in n-decane. The aqueous solutions were unbuffered, pH 6, T=20°C. The permeability ratio  $P_{\text{cation}}/P_{\text{anion}}$  ( $P_c/P_a$ ) was calculated with the Goldman-Hodgkin-Katz equation (Benz *et al.*, 1979b) from at least 3 individual experiments. The selectivity of Ib channels is given for comparison (\*taken from Knapp *et al.*, 2002).

### 7.3.3 Voltage-dependency

#### 7.3.3.1 Untreated CDTb channels are highly voltage-dependent

Activated CDTb was added to the *cis*-side of a black lipid bilayer membrane and the conductance increased in defined steps. When channel insertion became considerably low we applied different positive and negative potentials with respect to the *cis*-side starting with 10 mV. We repeated the experiment in 10 mV steps up to 120 mV positive and negative potential, respectively. The membrane conductance (G) was measured as a function of the applied voltage ( $V_m$ ) when the opening and the closing of CDTb channels reached equilibrium. (G) was divided by the initial value of the conductance ( $G_0$ ) which was obtained right after the onset of the voltage. CDTb channels showed voltage-dependent behavior in an asymmetric manner (Figure 7.3). Only for negative potentials applied to the *cis*-side the membrane current decreased in an exponential manner, at -110 mV the channels closed almost completely, whereas positive potentials at the *cis*-side only led to minor effects. The different channel properties at positive and negative potentials indicate an asymmetric insertion of the CDTb channels and that the channels are fully orientated in the membrane.

#### 7.3.3.2 CDTb channels preincubated with cholesterol are less voltage-dependent

We repeated the experiment with CDTb channels which were preincubated with cholesterol as described above. The obtained result differed considerably. The voltage-dependency was

decreased, however, the asymmetric behavior could still be observed indicating that also the CDTb channels with small single channel conductance insert fully orientated in the membrane (Figure 7.3).

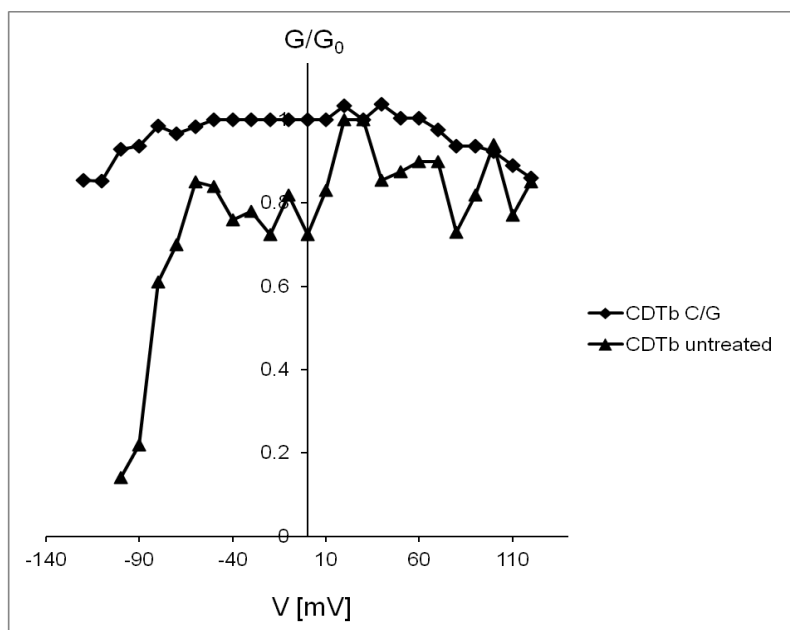


**Figure 7.3. Voltage-dependency of CDTb channels untreated and preincubated with cholesterol in 1% genapol.** The ratio of the conductance ( $G$ ) at an applied voltage ( $V$ ) was measured and divided by the initial value of the conductance ( $G_0$ ) immediately after the turning-on of the voltage. Either untreated CDTb (triangles) or CDTb incubated with cholesterol dissolved in 1% genapol (squares) were added to the *cis*-side of a membrane formed of diphtanoyl phosphatidylcholine/*n*-decane. After reconstitution of approximately 100 pores the different potentials were applied. The aqueous phase contained 1 M KCl,  $T=20^\circ\text{C}$ .

### 7.3.4 Binding of CDTb channels to CDTa

#### 7.3.4.1 Untreated CDTb does not bind CDTa

To study the interaction of CDTb channels with the enzymatic component CDTa we performed multi-channel experiments with black lipid bilayer membranes as described previously (Neumeyer *et al.*, 2006b). About 2 hours after addition of activated CDTb the rate of channel insertion had slowed down to equilibrium. At that time increasing concentrations of CDTa were added to the *cis*-side of the membrane (the side of the applied voltage). Even at high concentrations of CDTa (11.5 mM) no CDTa-induced blockage could be observed meaning that there was no reduction of the bulk conductance. To rule out the possibility that binding and blockage of the CDTb channel was pH-dependent we tested various pH values ranging from 5.2 to 7.0, but no CDTa-induced decrease of conductance could be detected.



### 7.3.4.2 CDTb preincubated with cholesterol binds CDTa

In contrast to these findings, CDTb channels incubated with cholesterol were able to bind CDTa with very high affinity leading to a substantial decrease of membrane conductance in a dose-dependent manner. Figure 7.4 shows an example for a titration experiment with an applied voltage of 50 mV in 1 M KCl in which increasing concentrations of CDTa (arrows) were added to the *cis*-side of a membrane which contained about 150 CDTb channels.

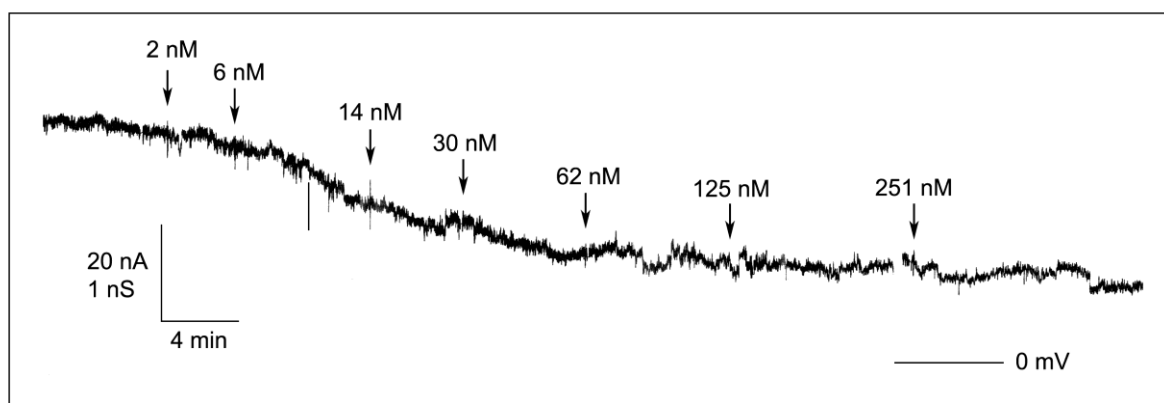


**Figure 7.4. Interaction of CDTa with CDTb channels.** Titration of CDTb-induced membrane conductance with CDTa. The membrane was formed from diphytanoyl phosphatidylcholine/*n*-decane, containing about 150 channels. CDTa was added in the concentrations indicated at the top of the panel. The aqueous phase contained activated CDTb preincubated with cholesterol in 1% genapol (added only to the *cis*-side of the membrane), 1 M KCl, 50 mV applied voltage. The temperature was 20°C.

The membrane conductance decreased as a function of the CDTa concentration within a few minutes after addition (the aqueous phase contained 1 M KCl, 10 mM MES, pH 6.0) (Figure 7.4). The data of Figure 7.4 and of similar experiments were analyzed using equation [7.2] as described previously (Orlik *et al.*, 2005; Neumeyer *et al.*, 2006b). The stability constant  $K$  of the binding of CDTb to CDTa was averaged out of at least three individual experiments resulting in  $K$   $(38 \pm 9) \times 10^6 \text{ M}^{-1}$ . The half-saturation constant  $K_s$  was 26 nM (Table 7.3).

### 7.3.4.3 CDTa blocks CDTb channels in a single hit process

The blockage and binding properties of CDTb channels with CDTa were studied on single channel level. Therefore, only small amounts of CDTb/Cholesterol stock solution were added to the *cis*-side of the membrane. After about 10 minutes 5 CDTb channels were. At that time, CDTa was added to the *cis*-side to a final concentration of 12 nM causing a step-wise closure of the

CDTb channels. The channels closed almost completely after some time demonstrating that binding of CDTa to CDTb is a single hit process (see Figure 7.5).

**Table 7.3.** Stability constants  $K$  for the binding of CDTb to CDTa and the cross reaction of Ib with CDTa.

	$K [M^{-1}]$	$K_s [nM]$
CDTb C/G with CDTa	38198505	26

Stability constants  $K$  for the binding of CDTa to CDTb (preincubated with cholesterol in 1% genapol) (C/G) reconstituted in lipid bilayer membranes. The membranes were formed from diphytanoyl phosphatidylcholine/*n*-decane. The aqueous phase contained 1 M KCl,  $T = 20^\circ\text{C}$ . Measurements were performed at a membrane potential of 50 mV. The data represent the means of at least three individual titration experiments.  $K_s$  is the half saturation constant, i.e.  $1/K$ .

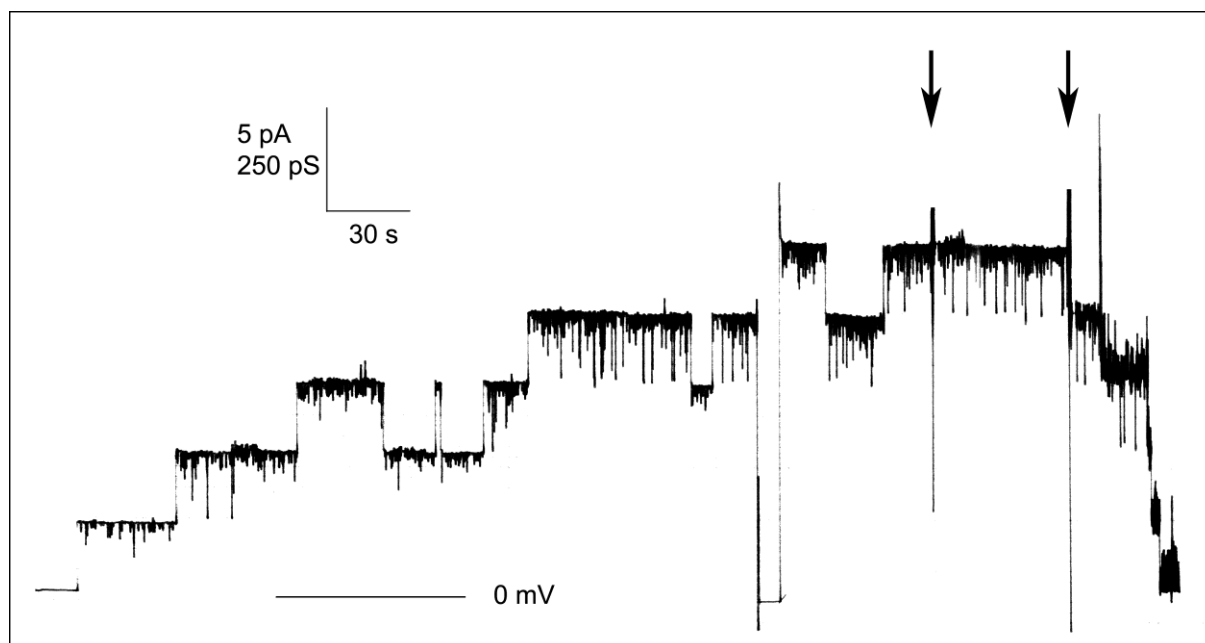


**Figure 7.5.** Block of CDTb channels by CDTa observed on the single channel level. 50 mV were applied to the *cis*-side of a diphytanoyl phosphatidylcholine/*n*-decane membrane containing approximately 5 CDTb channels. CDTa was added in a final concentration of 12 nM to the *cis*-side of the membrane (arrows). All CDTb channels were subsequently blocked caused by binding of CDTa to the channels (1 M KCl, 10 mM MES, pH 6.0,  $T=20^\circ\text{C}$ ).

## 7.4 DISCUSSION

In this study we investigated the ability of *Clostridium difficile* binary toxin B component (CDTb) to form pores in artificial membranes. CDTb was activated with  $\alpha$ -chymotrypsin that cleaves an N-terminal fragment of the protein as it is known for many toxins of the AB<sub>7</sub>-type, i.e. Anthrax toxin, C2 toxin or iota toxin (Barth *et al.*, 2000; Knapp *et al.*, 2002; Collier, 2009). We could show that there are two different types of channels formed by CDTb which possess different biophysical properties, concerning single channel conductance, ion selectivity, voltage-dependency and binding affinity to the enzymatic subunit CDTa.

The untreated CDTb channels formed in black lipid bilayer membranes revealed a single channel conductance of 380 pS in 1 M KCl which is rather high for a binary toxin's channel. Compared to the structurally closely related Ib from *Clostridium perfringens* the conductance is more than 4-fold increased (Knapp *et al.*, 2002). As the frequency of channel insertion was low, we incubated the activated CDTb with cholesterol dissolved in 1% Genapol overnight. To our surprise, not only the rate of insertion was increased, we also found that the conductance of CDTb channels was changed. Only few channels of the original conductance were present but most channels had a reduced conductance of 160 pS. This effect was clearly an effect caused by cholesterol, the addition of Genapol only did not have any impact on channel conductance.

In accordance with these findings, the channels showed different properties in voltage-dependency. Untreated CDTb channels were strongly voltage-dependent in the negative range, whereas the small CDTb channels showed nearly no voltage-dependency. Recent studies revealed that many binary toxin channels are voltage-dependent in the high negative range, i.e. *Bacillus anthracis* Anthrax toxin or *Clostridium perfringens* iota toxin (Blaustein *et al.*, 1989; Knapp *et al.*, 2002). Why this is not the case for the small CDTb channels requires further investigation.

In general channels formed by binary toxins' B components are cation selective. Anthrax toxin's protective antigen is highly cation selective with a value  $P_{\text{cation}}/P_{\text{anion}}$  of about 20 (Blaustein *et al.*, 1989), whereas iota toxin's Ib is moderately cation selective ( $P_c/P_a = 5.5$ ) (Knapp *et al.*, 2002). Due to the high amino acid homology to Ib, we expected the CDTb channel to be cation selective as well. We found the large channel formed by untreated CDTb to be slightly anion selective ( $P_c/P_a = 0.5$ ) meaning that for two anions only one cation is passing the channel. In contrast, the small CDTb channel was slightly cation selective ( $P_c/P_a = 1.32$ ). The small CDTb channel itself might be even more cation selective, as we cannot exclude that some of the large channels were inserted in the membrane.

The channel forming component of binary toxins of the AB<sub>7</sub> type is essential for the translocation of the enzymatic component into target cells. Initiating the process of translocation,

binding to the enzymatic subunit is prerequisite. To investigate the binding properties of CDTb we performed titration experiments by adding the enzymatic component CDTa to the *cis*-side of the membrane which was saturated with CDTb channels. In the case of the untreated large CDTb channels we could not detect any decrease in conductance. This could be out of two reasons. Either, the enzymatic subunit bound to the CDTb channel on the channel surface but did not enter the channel, or CDTa did not bind to CDTb at all.

Repeating the experiment under the same conditions with the CDTb channel incubated with cholesterol, the binding affinity of CDTb to CDTa was in the low nanomolar range. The half saturation constants are in the range of other binary toxins (Neumeyer *et al.*, 2006a; Kronhardt *et al.*, 2011b). Even when we applied CDTa in high concentration (up to 250 nM) the block of the channels was not completely and a residual conductance remained. This could be due to the insertion of some of the large channels which could not be blocked by CDTa. In single channel titration experiments the conductance induced by the small CDTb channels decreased to a minimum indicating that CDTa blocks the channels entirely and in a single-hit process.

A possible explanation for the availability of the large CDTb pore is that a complex consisting out of two or more heptameric CDTb channels is formed. Addition of cholesterol might lead to a disaggregation of these complexes. Taking into consideration that not only the single channel conductance but also the selectivity, voltage-dependency and binding properties are considerably changed, this seems to be not the case. Instead, we propose that there are two entirely different pores are formed by the same monomeric subunits. As the small channel is able to bind to the enzymatic subunit CDTa, the single channel conductance and the selectivity are similar to those of iota toxin's B component; this kind of channel seems to be responsible for cell intoxication via endosomes to release the enzymatic component into the cell cytosol.

Single channel data of iota toxin's Ib channel revealed that Ib forms aside from the dominant pore with a conductance of 85 pS in 1 M KCl also larger pores of about double size and even more (Knapp *et al.*, 2002). It was indicated that these pores might be dimers of the Ib channel. Considering the results presented in this work it might be the case that Ib monomers have the capability to form a different kind of pore as well, although in a lower extent.

Various toxins are known to be cholesterol-dependent, i.e. the family of CDCs (cholesterol-dependent toxins). These toxins bind to cholesterol rich regions and oligomerize to prepores. *Streptococcus intermedius* intermediolysin does not require cholesterol for oligomerization and binding to the cell surface, but for pore formation and membrane insertion (Heuck *et al.*, 2007). Interestingly, the pore forming toxin listeriolysin O produced by *Listeria monocytogenes* has been shown to facilitate bacterial internalization by inducing and endocytosis of the bacteria/toxin

complex (Vadia *et al.*, 2011). If this is also the pathogenic role of the large CDTb channel, we can only speculate. The channel does not bind the enzymatic subunit indicating that it is not involved in the intoxication pathway by translocation of CDTa into the cell cytosol. However, it may possess another functionality concerning membrane damaging or bacterial internalization, finally leading to an extended flexibility of *Clostridium difficile* pathogenicity.

Here we present first-time evidence that a B component of a binary AB<sub>7</sub> type of toxin is able to form two different types of channels differing dramatically in their biophysical properties. To understand the mechanism and the function of the flexibility of pore formation further has to be investigated in future.



## CONCLUSION

Binary toxins are among the most potent toxins in the world. Therefore, a main goal of research is to investigate how these toxins work in detail to understand their sophisticated mode of intoxication. In particular, Anthrax toxin is in the focus of public interest because of its usage as a bioterroristic weapon for centuries. As treating the infection with antibiotics is in general quite late due to delayed symptoms new ways to inhibit the infection are required. One possibility to deal with the infection is to find substrates which block the PA channel efficiently. In this work we studied different substrates, molecules and enzymatic components of related binary toxins which are able not only to block PA pores but also to be translocated into cells and we could define general features improving the binding affinity.

The B components PA of Anthrax toxin and C2II of C2 toxin are closely related and exhibit high amino acid homology. Nevertheless, the process of translocation is different as positive charges enhance the binding for PA drastically but they do not in the case of C2II. Additionally, it is known that only C2II requires cellular chaperons for the translocation of the enzymatic component. The PA channel possesses high flexibility concerning both the binding and the translocation process as the enzymatic component C2I binds to the PA channel with high affinity and is translocated *in vivo* experiments. However, C2II is indeed able to bind Anthrax toxin's enzymatic components EF and LF but not able to translocate them into the cytosol of target cells leading to different perspectives concerning the treatment of infections.

The complex mode of intoxication provides new possibilities to use of these toxins partially for medical applications. We could show that the binding and translocation moiety PA of Anthrax toxin is able to transport various proteins which are not related to AB<sub>7</sub> toxins into the cytosol of target cells and that positive charges increase this effect in a voltage-dependent manner. The interesting question of future studies will be how to use this molecular syringe specifically and target-orientated in different contexts, e.g. targeting exclusively cancer cells by modifying the receptor PA binds to in order to transport effector molecules into the cytosol.

At present, nosocomial infections become an increasing problem especially in connection with multi-resistant bacterial strains. One of these toxins causing more and more severe infections in hospitals is the binary AB toxin CDT produced by *Clostridium difficile*. In this work we studied the ability of the binding and translocation component CDTb in artificial membranes and found a so far unknown feature to produce two different kinds of pores. One pore seems to be responsible for binding and translocation of the enzymatic component. The single channel conductance and the selectivity and the binding affinities to CDTa are in favor of this suggestion. The other reveals an exceptionally high single channel conductance and does not exhibit any binding to the enzymatic moiety and therefore has to be involved in different processes concerning the infection. Although the functional role of this capacity to form two different pores is not understood so far this feature through up various questions illustrating how much investigation is still necessary to conceive the complex mechanism of these fascinating toxins.







## REFERENCES

- Abrami L, Lindsay M, Parton RG, Leppla SH, van der Goot FG (2004) Membrane insertion of anthrax protective antigen and cytoplasmic delivery of lethal factor occur at different stages of the endocytic pathway. *J Cell Biol* **166**: 645-651
- Abrami L, Reig N, van der Goot FG (2005) Anthrax toxin: the long and winding road that leads to the kill. *Trends Microbiol* **13**: 72-78
- Agrawal A, Lingappa J, Leppla SH, Agrawal S, Jabbar A, Quinn C, Pulendran B (2003) Impairment of dendritic cells and adaptive immunity by anthrax lethal toxin. *Nature* **424**: 329-334
- Aktories K, Ankenbauer T, Schering B, Jakobs KH (1986a) ADP-ribosylation of platelet actin by botulinum C2 toxin. *Eur J Biochem* **161**: 155-162
- Aktories K, Barmann M, Ohishi I, Tsuyama S, Jakobs KH, Habermann E (1986b) Botulinum C2 toxin ADP-ribosylates actin. *Nature* **322**: 390-392
- Aktories K, Barth H (2004) The actin-ADP-ribosylating *Clostridium botulinum* C2 toxin. *Anaerobe* **10**: 101-105
- Aktories K, Weller U, Chhatwal GS (1987) *Clostridium botulinum* type C produces a novel ADP-ribosyltransferase distinct from botulinum C2 toxin. *FEBS Lett* **212**: 109-113
- Aktories K, Wilde C, Vogelsang M (2004) Rho-modifying C3-like ADP-ribosyltransferases. *Rev Physiol Biochem Pharmacol* **152**: 1-22
- Allured VS, Collier RJ, Carroll SF, McKay DB (1986) Structure of exotoxin A of *Pseudomonas aeruginosa* at 3.0-Angstrom resolution. *Proc Natl Acad Sci U S A* **83**: 1320-1324
- Andersen C, Jordy M, Benz R (1995) Evaluation of the rate constants of sugar transport through maltoporin (LamB) of *Escherichia coli* from the sugar-induced current noise. *J Gen Physiol* **105**: 385-401
- Arora N, Leppla SH (1993) Residues 1-254 of anthrax toxin lethal factor are sufficient to cause cellular uptake of fused polypeptides. *J Biol Chem* **268**: 3334-3341
- Ascenzi P, Visca P, Ippolito G, Spallarossa A, Bolognesi M, Montecucco C (2002) Anthrax toxin: a tripartite lethal combination. *FEBS Lett* **531**: 384-388
- Bachmeyer C, Orlik F, Barth H, Aktories K, Benz R (2003) Mechanism of C2-toxin inhibition by fluphenazine and related compounds: investigation of their binding kinetics to the C2II-channel using the current noise analysis. *J Mol Biol* **333**: 527-540
- Barth H, Aktories K, Popoff MR, Stiles BG (2004) Binary bacterial toxins: biochemistry, biology, and applications of common *Clostridium* and *Bacillus* proteins. *Microbiol Mol Biol Rev* **68**: 373-402, table of contents
- Barth H, Blocker D, Aktories K (2002a) The uptake machinery of clostridial actin ADP-ribosylating toxins--a cell delivery system for fusion proteins and polypeptide drugs. *Naunyn Schmiedeberg's Arch Pharmacol* **366**: 501-512
- Barth H, Blocker D, Behlke J, Bergsma-Schutter W, Brisson A, Benz R, Aktories K (2000) Cellular uptake of *Clostridium botulinum* C2 toxin requires oligomerization and acidification. *J Biol Chem* **275**: 18704-18711

- Barth H, Roebeling R, Fritz M, Aktories K (2002b) The binary Clostridium botulinum C2 toxin as a protein delivery system: identification of the minimal protein region necessary for interaction of toxin components. *J Biol Chem* **277**: 5074-5081
- Beitzinger C, Rolando M, Kronhardt A, Flatau G, Popoff MR, Lemichez E, Benz R (2011) Anthrax toxin protective antigen up-take of N-terminal His-tagged proteins into cells is voltage-dependent. (*Manuscript*)
- Benson EL, Huynh PD, Finkelstein A, Collier RJ (1998) Identification of residues lining the anthrax protective antigen channel. *Biochemistry (Mosc)* **37**: 3941-3948
- Benz R, Hancock RE (1987) Mechanism of ion transport through the anion-selective channel of the Pseudomonas aeruginosa outer membrane. *J Gen Physiol* **89**: 275-295
- Benz R, Janko K, Boos W, Lauger P (1978) Formation of large, ion-permeable membrane channels by the matrix protein (porin) of Escherichia coli. *Biochim Biophys Acta* **511**: 305-319
- Benz R, Janko K, Lauger P (1979a) Ionic selectivity of pores formed by the matrix protein (porin) of Escherichia coli. *Biochim Biophys Acta* **551**: 238-247
- Benz R, Janko K, Lauger P (1979b) Ionic selectivity of pores formed by the matrix protein (porin) of Escherichia coli. *Biochim Biophys Acta* **551**: 238-247
- Benz R, Schmid A, Hancock RE (1985) Ion selectivity of gram-negative bacterial porins. *J Bacteriol* **162**: 722-727
- Benz R, Schmid A, Nakae T, Vos-Scheperkeuter GH (1986) Pore formation by LamB of Escherichia coli in lipid bilayer membranes. *J Bacteriol* **165**: 978-986
- Benz R, Schmid A, Vos-Scheperkeuter GH (1987) Mechanism of sugar transport through the sugar-specific LamB channel of Escherichia coli outer membrane. *J Membr Biol* **100**: 21-29
- Berkane E, Orlik F, Stegmeier JF, Charbit A, Winterhalter M, Benz R (2006) Interaction of bacteriophage lambda with its cell surface receptor: an in vitro study of binding of the viral tail protein gpJ to LamB (Maltoporin). *Biochemistry (Mosc)* **45**: 2708-2720
- Bezrukov SM, Winterhalter M (2000) Examining noise sources at the single-molecule level: 1/f noise of an open maltoporin channel. *Phys Rev Lett* **85**: 202-205
- Blanke SR, Milne JC, Benson EL, Collier RJ (1996) Fused polycationic peptide mediates delivery of diphtheria toxin A chain to the cytosol in the presence of anthrax protective antigen. *Proc Natl Acad Sci U S A* **93**: 8437-8442
- Blaustein RO, Koehler TM, Collier RJ, Finkelstein A (1989) Anthrax toxin: channel-forming activity of protective antigen in planar phospholipid bilayers. *Proc Natl Acad Sci U S A* **86**: 2209-2213
- Blaustein RO, Lea EJ, Finkelstein A (1990) Voltage-dependent block of anthrax toxin channels in planar phospholipid bilayer membranes by symmetric tetraalkylammonium ions. Single-channel analysis. *J Gen Physiol* **96**: 921-942
- Blocker D, Bachmeyer C, Benz R, Aktories K, Barth H (2003a) Channel formation by the binding component of Clostridium botulinum C2 toxin: glutamate 307 of C2II affects channel properties in vitro and pH-dependent C2I translocation in vivo. *Biochemistry (Mosc)* **42**: 5368-5377
- Blocker D, Barth H, Maier E, Benz R, Barbieri JT, Aktories K (2000) The C terminus of component C2II of Clostridium botulinum C2 toxin is essential for receptor binding. *Infect Immun* **68**: 4566-4573
- Blocker D, Pohlmann K, Haug G, Bachmeyer C, Benz R, Aktories K, Barth H (2003b) Clostridium botulinum C2 toxin: low pH-induced pore formation is required for translocation of the enzyme component C2I into the cytosol of host cells. *J Biol Chem* **278**: 37360-37367
- Boonserm P, Davis P, Ellar DJ, Li J (2005) Crystal structure of the mosquito-larvicidal toxin Cry4Ba and its biological implications. *J Mol Biol* **348**: 363-382
- Boquet P, Lemichez E (2003) Bacterial virulence factors targeting Rho GTPases: parasitism or symbiosis? *Trends Cell Biol* **13**: 238-246
- Boyer L, Doye A, Rolando M, Flatau G, Munro P, Gounon P, Clement R, Pulcini C, Popoff MR, Mettouchi A, Landraud L, Dussurget O, Lemichez E (2006) Induction of transient

- macroapertures in endothelial cells through RhoA inhibition by *Staphylococcus aureus* factors. *J Cell Biol* **173**: 809-819
- Bradley KA, Mogridge J, Mourez M, Collier RJ, Young JA (2001) Identification of the cellular receptor for anthrax toxin. *Nature* **414**: 225-229
- Carson-Walter EB, Watkins DN, Nanda A, Vogelstein B, Kinzler KW, St Croix B (2001) Cell surface tumor endothelial markers are conserved in mice and humans. *Cancer Res* **61**: 6649-6655
- Cataldi A, Labruyere E, Mock M (1990) Construction and characterization of a protective antigen-deficient *Bacillus anthracis* strain. *Mol Microbiol* **4**: 1111-1117
- Chvyrkova I, Zhang XC, Terzyan S (2007) Lethal factor of anthrax toxin binds monomeric form of protective antigen. *Biochem Biophys Res Commun* **360**: 690-695
- Collier RJ (2009) Membrane translocation by anthrax toxin. *Mol Aspects Med* **30**: 413-422
- Collier RJ, Young JA (2003) Anthrax toxin. *Annu Rev Cell Dev Biol* **19**: 45-70
- Considine RV, Simpson LL (1991) Cellular and molecular actions of binary toxins possessing ADP-ribosyltransferase activity. *Toxicon* **29**: 913-936
- Conti F, Wanke E (1975) Channel noise in nerve membranes and lipid bilayers. *Q Rev Biophys* **8**: 451-506
- Cunningham K, Lacy DB, Mogridge J, Collier RJ (2002) Mapping the lethal factor and edema factor binding sites on oligomeric anthrax protective antigen. *Proc Natl Acad Sci U S A* **99**: 7049-7053
- Dal Molin F, Tonello F, Ladant D, Zornetta I, Zamparo I, Di Benedetto G, Zaccolo M, Montecucco C (2006) Cell entry and cAMP imaging of anthrax edema toxin. *EMBO J* **25**: 5405-5413
- Dixon TC, Meselson M, Guillemin J, Hanna PC (1999) Anthrax. *N Engl J Med* **341**: 815-826
- Doye A, Boyer L, Mettouchi A, Lemichez E (2006) Ubiquitin-mediated proteasomal degradation of Rho proteins by the CNF1 toxin. *Methods Enzymol* **406**: 447-456
- Egerer M, Giesemann T, Jank T, Satchell KJ, Aktories K (2007) Auto-catalytic cleavage of *Clostridium difficile* toxins A and B depends on cysteine protease activity. *J Biol Chem* **282**: 25314-25321
- Elliott JL, Mogridge J, Collier RJ (2000) A quantitative study of the interactions of *Bacillus anthracis* edema factor and lethal factor with activated protective antigen. *Biochemistry (Mosc)* **39**: 6706-6713
- Escuyer V, Collier RJ (1991) Anthrax protective antigen interacts with a specific receptor on the surface of CHO-K1 cells. *Infect Immun* **59**: 3381-3386
- Ezzell JW, Jr., Abshire TG (1992) Serum protease cleavage of *Bacillus anthracis* protective antigen. *J Gen Microbiol* **138**: 543-549
- Fang H, Xu L, Chen TY, Cyr JM, Frucht DM (2006) Anthrax lethal toxin has direct and potent inhibitory effects on B cell proliferation and immunoglobulin production. *J Immunol* **176**: 6155-6161
- Feld GK, Thoren KL, Kintzer AF, Sterling HJ, Tang, II, Greenberg SG, Williams ER, Krantz BA (2010) Structural basis for the unfolding of anthrax lethal factor by protective antigen oligomers. *Nat Struct Mol Biol* **17**: 1383-1390
- Finkelstein A (1994) The channel formed in planar lipid bilayers by the protective antigen component of anthrax toxin. *Toxicology* **87**: 29-41
- Friedlander AM (1986) Macrophages are sensitive to anthrax lethal toxin through an acid-dependent process. *J Biol Chem* **261**: 7123-7126
- Fujii N, Kubota T, Shirakawa S, Kimura K, Ohishi I, Moriishi K, Isogai E, Isogai H (1996) Characterization of component-I gene of botulinum C2 toxin and PCR detection of its gene in clostridial species. *Biochem Biophys Res Commun* **220**: 353-359
- Gibert M, Petit L, Raffestin S, Okabe A, Popoff MR (2000) *Clostridium perfringens* iota-toxin requires activation of both binding and enzymatic components for cytopathic activity. *Infect Immun* **68**: 3848-3853
- Grabe M, Oster G (2001) Regulation of organelle acidity. *J Gen Physiol* **117**: 329-344
- Halverson KM, Panchal RG, Nguyen TL, Gussio R, Little SF, Misakian M, Bavari S, Kasianowicz JJ (2005) Anthrax biosensor, protective antigen ion channel asymmetric blockade. *J Biol Chem* **280**: 34056-34062

- Han S, Craig JA, Putnam CD, Carozzi NB, Tainer JA (1999) Evolution and mechanism from structures of an ADP-ribosylating toxin and NAD complex. *Nat Struct Biol* **6**: 932-936
- Hanna PC, Acosta D, Collier RJ (1993) On the role of macrophages in anthrax. *Proc Natl Acad Sci U S A* **90**: 10198-10201
- Haug G, Leemhuis J, Tiemann D, Meyer DK, Aktories K, Barth H (2003) The host cell chaperone Hsp90 is essential for translocation of the binary Clostridium botulinum C2 toxin into the cytosol. *J Biol Chem* **278**: 32266-32274
- Heuck AP, Savva CG, Holzenburg A, Johnson AE (2007) Conformational changes that effect oligomerization and initiate pore formation are triggered throughout perfringolysin O upon binding to cholesterol. *J Biol Chem* **282**: 22629-22637
- Hilger H, Pust S, von Figura G, Kaiser E, Stiles BG, Popoff MR, Barth H (2009) The long-lived nature of clostridium perfringens iota toxin in mammalian cells induces delayed apoptosis. *Infect Immun* **77**: 5593-5601
- Inglesby TV, O'Toole T, Henderson DA, Bartlett JG, Ascher MS, Eitzen E, Friedlander AM, Gerberding J, Hauer J, Hughes J, McDade J, Osterholm MT, Parker G, Perl TM, Russell PK, Tonat K (2002) Anthrax as a biological weapon, 2002: updated recommendations for management. *JAMA* **287**: 2236-2252
- Jernigan DB, Raghunathan PL, Bell BP, Brechner R, Bresnitz EA, Butler JC, Cetron M, Cohen M, Doyle T, Fischer M, Greene C, Griffith KS, Guarner J, Hadler JL, Hayslett JA, Meyer R, Petersen LR, Phillips M, Pinner R, Popovic T, Quinn CP, Reefhuis J, Reissman D, Rosenstein N, Schuchat A, Shieh WJ, Siegal L, Swerdlow DL, Tenover FC, Traeger M, Ward JW, Weisfuse I, Wiersma S, Yeskey K, Zaki S, Ashford DA, Perkins BA, Ostroff S, Hughes J, Fleming D, Koplan JP, Gerberding JL (2002) Investigation of bioterrorism-related anthrax, United States, 2001: epidemiologic findings. *Emerg Infect Dis* **8**: 1019-1028
- Johnson EA (1999) Clostridial toxins as therapeutic agents: benefits of nature's most toxic proteins. *Annu Rev Microbiol* **53**: 551-575
- Jordy M, Andersen C, Schulein K, Ferenci T, Benz R (1996) Rate constants of sugar transport through two LamB mutants of Escherichia coli: comparison with wild-type maltoporin and LamB of Salmonella typhimurium. *J Mol Biol* **259**: 666-678
- Katayama H, Wang J, Tama F, Chollet L, Gogol EP, Collier RJ, Fisher MT (2010) Three-dimensional structure of the anthrax toxin pore inserted into lipid nanodiscs and lipid vesicles. *Proc Natl Acad Sci U S A* **107**: 3453-3457
- Keim P, Smith KL, Keys C, Takahashi H, Kurata T, Kaufmann A (2001) Molecular investigation of the Aum Shinrikyo anthrax release in Kameido, Japan. *J Clin Microbiol* **39**: 4566-4567
- Kintzer AF, Thoren KL, Sterling HJ, Dong KC, Feld GK, Tang, II, Zhang TT, Williams ER, Berger JM, Krantz BA (2009) The protective antigen component of anthrax toxin forms functional octameric complexes. *J Mol Biol* **392**: 614-629
- Knapp O, Benz R, Gibert M, Marvaud JC, Popoff MR (2002) Interaction of Clostridium perfringens iota-toxin with lipid bilayer membranes. Demonstration of channel formation by the activated binding component Ib and channel block by the enzyme component Ia. *J Biol Chem* **277**: 6143-6152
- Krantz BA, Finkelstein A, Collier RJ (2006) Protein translocation through the anthrax toxin transmembrane pore is driven by a proton gradient. *J Mol Biol* **355**: 968-979
- Krantz BA, Melnyk RA, Zhang S, Juris SJ, Lacy DB, Wu Z, Finkelstein A, Collier RJ (2005) A phenylalanine clamp catalyzes protein translocation through the anthrax toxin pore. *Science* **309**: 777-781
- Krantz BA, Trivedi AD, Cunningham K, Christensen KA, Collier RJ (2004) Acid-induced unfolding of the amino-terminal domains of the lethal and edema factors of anthrax toxin. *J Mol Biol* **344**: 739-756
- Kronhardt A, Beitzinger C, Duscha K, Hajos G, Barth H, Benz R (2011a) Interaction of Chloroquine-like Blocker-substrates with Anthrax toxin's Protective Antigen (PA) in vitro and in vivo. *Manuscript*

- Kronhardt A, Rolando M, Beitzinger C, Stefani C, Leuber M, Flatau G, Popoff MR, Benz R, Lemichez E (2011b) Cross-Reactivity of Anthrax and C2 Toxin: Protective Antigen Promotes the Uptake of Botulinum C2I Toxin into Human Endothelial Cells. *PLoS One* **6**: e23133
- Lacy DB, Collier RJ (2002) Structure and function of anthrax toxin. *Curr Top Microbiol Immunol* **271**: 61-85
- Lacy DB, Lin HC, Melnyk RA, Schueler-Furman O, Reither L, Cunningham K, Baker D, Collier RJ (2005) A model of anthrax toxin lethal factor bound to protective antigen. *Proc Natl Acad Sci U S A* **102**: 16409-16414
- Lang AE, Schmidt G, Schlosser A, Hey TD, Larrinua IM, Sheets JJ, Mannherz HG, Aktories K (2010) Phototransduction toxins ADP-ribosylate actin and RhoA to force actin clustering. *Science* **327**: 1139-1142
- Lemichez E, Boquet P (2003) To be helped or not helped, that is the question. *J Cell Biol* **160**: 991-992
- Leppla SH, Arora N, Varughese M (1999) Anthrax toxin fusion proteins for intracellular delivery of macromolecules. *J Appl Microbiol* **87**: 284
- Leuber M (2007) Anthrax, C2 and Vip Toxin: Comparison of the Mode of Translocation, Biophysical Properties and Possible Cross Reactivity of the Binary AB Components. *Würzburg*
- Leuber M, Kronhardt A, Tonello F, Dal Molin F, Benz R (2008) Binding of N-terminal fragments of anthrax edema factor (EF(N)) and lethal factor (LF(N)) to the protective antigen pore. *Biochim Biophys Acta* **1778**: 1436-1443
- Lewis AN, Dondero TJ, Jr., Ponnampalam JT (1973) Letter: Falciparum malaria resistant to chloroquine suppression but sensitive to chloroquine treatment in West Malaysia. *Trans R Soc Trop Med Hyg* **67**: 310-312
- Lindemann B, DeFelice LJ (1981) On the use of general network functions in the evaluation of noise spectra obtained from epithelia. *Soc Gen Physiol Ser* **36**: 1-13
- Liu S, Leppla SH (2003) Cell surface tumor endothelium marker 8 cytoplasmic tail-independent anthrax toxin binding, proteolytic processing, oligomer formation, and internalization. *J Biol Chem* **278**: 5227-5234
- McDonald LC, Owings M, Jernigan DB (2006) Clostridium difficile infection in patients discharged from US short-stay hospitals, 1996-2003. *Emerg Infect Dis* **12**: 409-415
- Melnyk RA, Collier RJ (2006) A loop network within the anthrax toxin pore positions the phenylalanine clamp in an active conformation. *Proc Natl Acad Sci U S A* **103**: 9802-9807
- Menard A, Altendorf K, Breves D, Mock M, Montecucco C (1996) The vacuolar ATPase proton pump is required for the cytotoxicity of Bacillus anthracis lethal toxin. *FEBS Lett* **386**: 161-164
- Miller CJ, Elliott JL, Collier RJ (1999) Anthrax protective antigen: prepore-to-pore conversion. *Biochemistry (Mosc)* **38**: 10432-10441
- Mock M, Fouet A (2001) Anthrax. *Annu Rev Microbiol* **55**: 647-671
- Mogridge J, Cunningham K, Collier RJ (2002) Stoichiometry of anthrax toxin complexes. *Biochemistry (Mosc)* **41**: 1079-1082
- Nassi S, Collier RJ, Finkelstein A (2002) PA63 channel of anthrax toxin: an extended beta-barrel. *Biochemistry (Mosc)* **41**: 1445-1450
- Nekolla S, Andersen C, Benz R (1994) Noise analysis of ion current through the open and the sugar-induced closed state of the LamB channel of Escherichia coli outer membrane: evaluation of the sugar binding kinetics to the channel interior. *Biophys J* **66**: 1388-1397
- Nestorovich EM, Karginov VA, Berezhkovskii AM, Bezrukov SM (2010) Blockage of anthrax PA63 pore by a multicharged high-affinity toxin inhibitor. *Biophys J* **99**: 134-143
- Nestorovich EM, Karginov VA, Popoff MR, Bezrukov SM, Barth H (2011) Tailored ss-cyclodextrin blocks the translocation pores of binary exotoxins from C. Botulinum and C. Perfringens and protects cells from intoxication. *PLoS One* **6**: e23927
- Neumeyer T, Schiffler B, Maier E, Lang AE, Aktories K, Benz R (2008) Clostridium botulinum C2 toxin. Identification of the binding site for chloroquine and related compounds and influence of the binding site on properties of the C2II channel. *J Biol Chem* **283**: 3904-3914

- Neumeyer T, Tonello F, Dal Molin F, Schiffler B, Benz R (2006a) Anthrax edema factor, voltage-dependent binding to the protective antigen ion channel and comparison to LF binding. *J Biol Chem* **281**: 32335-32343
- Neumeyer T, Tonello F, Dal Molin F, Schiffler B, Orlik F, Benz R (2006b) Anthrax lethal factor (LF) mediated block of the anthrax protective antigen (PA) ion channel: effect of ionic strength and voltage. *Biochemistry (Mosc)* **45**: 3060-3068
- Nguyen TL (2004) Three-dimensional model of the pore form of anthrax protective antigen. Structure and biological implications. *J Biomol Struct Dyn* **22**: 253-265
- Orlik F, Andersen C, Benz R (2002a) Site-directed mutagenesis of tyrosine 118 within the central constriction site of the LamB (Maltoporin) channel of Escherichia coli. I. Effect on ion transport. *Biophys J* **82**: 2466-2475
- Orlik F, Andersen C, Benz R (2002b) Site-directed mutagenesis of tyrosine 118 within the central constriction site of the LamB (maltoporin) channel of Escherichia coli. II. Effect on maltose and maltooligosaccharide binding kinetics. *Biophys J* **83**: 309-321
- Orlik F, Andersen C, Danelon C, Winterhalter M, Pajatsch M, Bock A, Benz R (2003) CymA of Klebsiella oxytoca outer membrane: binding of cyclodextrins and study of the current noise of the open channel. *Biophys J* **85**: 876-885
- Orlik F, Schiffler B, Benz R (2005) Anthrax toxin protective antigen: inhibition of channel function by chloroquine and related compounds and study of binding kinetics using the current noise analysis. *Biophys J* **88**: 1715-1724
- Paccani SR, Tonello F, Ghittoni R, Natale M, Muraro L, D'Elis MM, Tang WJ, Montecucco C, Baldari CT (2005) Anthrax toxins suppress T lymphocyte activation by disrupting antigen receptor signaling. *J Exp Med* **201**: 325-331
- Pajatsch M, Andersen C, Mathes A, Bock A, Benz R, Engelhardt H (1999) Properties of a cyclodextrin-specific, unusual porin from Klebsiella oxytoca. *J Biol Chem* **274**: 25159-25166
- Pannifer AD, Wong TY, Schwarzenbacher R, Renatus M, Petosa C, Bienkowska J, Lacy DB, Collier RJ, Park S, Leppla SH, Hanna P, Liddington RC (2001) Crystal structure of the anthrax lethal factor. *Nature* **414**: 229-233
- Papatheodorou P, Carette JE, Bell GW, Schwan C, Guttenberg G, Brummelkamp TR, Aktories K (2011) Lipolysis-stimulated lipoprotein receptor (LSR) is the host receptor for the binary toxin Clostridium difficile transferase (CDT). *Proc Natl Acad Sci U S A* **108**: 16422-16427
- Pellizzari R, Guidi-Rontani C, Vitale G, Mock M, Montecucco C (1999) Anthrax lethal factor cleaves MKK3 in macrophages and inhibits the LPS/IFN $\gamma$ -induced release of NO and TNF $\alpha$ . *FEBS Lett* **462**: 199-204
- Perelle S, Gibert M, Bourlioux P, Corthier G, Popoff MR (1997) Production of a complete binary toxin (actin-specific ADP-ribosyltransferase) by Clostridium difficile CD196. *Infect Immun* **65**: 1402-1407
- Petosa C, Collier RJ, Klimpel KR, Leppla SH, Liddington RC (1997) Crystal structure of the anthrax toxin protective antigen. *Nature* **385**: 833-838
- Pimental RA, Christensen KA, Krantz BA, Collier RJ (2004) Anthrax toxin complexes: heptameric protective antigen can bind lethal factor and edema factor simultaneously. *Biochem Biophys Res Commun* **322**: 258-262
- Popoff MR, Boquet P (1988) Clostridium spiroforme toxin is a binary toxin which ADP-ribosylates cellular actin. *Biochem Biophys Res Commun* **152**: 1361-1368
- Rainey GJ, Young JA (2004) Antitoxins: novel strategies to target agents of bioterrorism. *Nat Rev Microbiol* **2**: 721-726
- Rappuoli R, Montecucco C (1997) Guidebook to protein toxins and their use in cell biology. *Oxford University Press, New York* pp.preface XV-XVIII
- Rolando M, Munro P, Stefani C, Auberger P, Flatau G, Lemichez E (2009) Injection of Staphylococcus aureus EDIN by the Bacillus anthracis protective antigen machinery induces vascular permeability. *Infect Immun* **77**: 3596-3601



- Rolando M, Stefani C, Flatau G, Auberger P, Mettouchi A, Mhlanga M, Rapp U, Galmiche A, Lemichez E (2010) Transcriptome dysregulation by anthrax lethal toxin plays a key role in induction of human endothelial cell cytotoxicity. *Cell Microbiol* **12**: 891-905
- Rossi Paccani S, Tonello F, Patrussi L, Capitani N, Simonato M, Montecucco C, Baldari CT (2007) Anthrax toxins inhibit immune cell chemotaxis by perturbing chemokine receptor signalling. *Cell Microbiol* **9**: 924-929
- Roux E, Yersin A (1888) Contribution a l'etude de la diphtherie. *Annales de l'Institut Pasteur* **2**: 629-661
- Rupnik M, Wilcox MH, Gerding DN (2009) Clostridium difficile infection: new developments in epidemiology and pathogenesis. *Nat Rev Microbiol* **7**: 526-536
- Santelli E, Bankston LA, Leppla SH, Liddington RC (2004) Crystal structure of a complex between anthrax toxin and its host cell receptor. *Nature* **430**: 905-908
- Schleberger C, Hochmann H, Barth H, Aktories K, Schulz GE (2006) Structure and action of the binary C2 toxin from Clostridium botulinum. *J Mol Biol* **364**: 705-715
- Schmid A, Benz R, Just I, Aktories K (1994) Interaction of Clostridium botulinum C2 toxin with lipid bilayer membranes. Formation of cation-selective channels and inhibition of channel function by chloroquine. *J Biol Chem* **269**: 16706-16711
- Schmitt CK, Meysick KC, O'Brien AD (1999) Bacterial toxins: friends or foes? *Emerg Infect Dis* **5**: 224-234
- Schwan C, Stecher B, Tzivelekidis T, van Ham M, Rohde M, Hardt WD, Wehland J, Aktories K (2009) Clostridium difficile toxin CDT induces formation of microtubule-based protrusions and increases adherence of bacteria. *PLoS Pathog* **5**: e1000626
- Scobie HM, Young JA (2005) Interactions between anthrax toxin receptors and protective antigen. *Curr Opin Microbiol* **8**: 106-112
- Sellman BR, Nassi S, Collier RJ (2001) Point mutations in anthrax protective antigen that block translocation. *J Biol Chem* **276**: 8371-8376
- Shen Y, Zhukovskaya NL, Guo Q, Florian J, Tang WJ (2005) Calcium-independent calmodulin binding and two-metal-ion catalytic mechanism of anthrax edema factor. *EMBO J* **24**: 929-941
- Simpson LL (1984) Molecular basis for the pharmacological actions of Clostridium botulinum type C2 toxin. *J Pharmacol Exp Ther* **230**: 665-669
- Simpson LL, Zepeda H, Ohishi I (1988) Partial characterization of the enzymatic activity associated with the binary toxin (type C2) produced by Clostridium botulinum. *Infect Immun* **56**: 24-27
- Song L, Hobaugh MR, Shustak C, Cheley S, Bayley H, Gouaux JE (1996) Structure of staphylococcal alpha-hemolysin, a heptameric transmembrane pore. *Science* **274**: 1859-1866
- Sun J, Lang AE, Aktories K, Collier RJ (2008) Phenylalanine-427 of anthrax protective antigen functions in both pore formation and protein translocation. *Proc Natl Acad Sci U S A* **105**: 4346-4351
- Sundriyal A, Roberts AK, Shone CC, Acharya KR (2009) Structural basis for substrate recognition in the enzymatic component of ADP-ribosyltransferase toxin CDTa from Clostridium difficile. *J Biol Chem* **284**: 28713-28719
- Szule JA, Coorsen JR (2003) Revisiting the role of SNAREs in exocytosis and membrane fusion. *Biochim Biophys Acta* **1641**: 121-135
- Tonello F, Naletto L, Romanello V, Dal Molin F, Montecucco C (2004) Tyrosine-728 and glutamic acid-735 are essential for the metalloproteolytic activity of the lethal factor of Bacillus anthracis. *Biochem Biophys Res Commun* **313**: 496-502
- Trent MS, Stead CM, Tran AX, Hankins JV (2006) Diversity of endotoxin and its impact on pathogenesis. *J Endotoxin Res* **12**: 205-223
- Turk BE (2007) Manipulation of host signalling pathways by anthrax toxins. *Biochem J* **402**: 405-417
- Vadia S, Arnett E, Haghghat AC, Wilson-Kubalek EM, Tweten RK, Seveau S (2011) The pore-forming toxin listeriolysin O mediates a novel entry pathway of L. monocytogenes into human hepatocytes. *PLoS Pathog* **7**: e1002356
- Vandekerckhove J, Schering B, Barmann M, Aktories K (1987) Clostridium perfringens iota toxin ADP-ribosylates skeletal muscle actin in Arg-177. *FEBS Lett* **225**: 48-52

- Vedy MJ (1975) [Retinopathy caused by chloroquine in the prevention of malaria in children]. *Bull Soc Ophthalmol Fr* **75**: 609-611
- Verveen AA, DeFelice LJ (1974) Membrane noise. *Prog Biophys Mol Biol* **28**: 189-265
- Viswanathan VK, Mallozzi MJ, Vedantam G (2010) Clostridium difficile infection: An overview of the disease and its pathogenesis, epidemiology and interventions. *Gut Microbes* **1**: 234-242
- Vitale G, Pellizzari R, Recchi C, Napolitani G, Mock M, Montecucco C (1998) Anthrax lethal factor cleaves the N-terminus of MAPKKs and induces tyrosine/threonine phosphorylation of MAPKKs in cultured macrophages. *Biochem Biophys Res Commun* **248**: 706-711
- Wang J, Hofnung M, Charbit A (2000) The C-terminal portion of the tail fiber protein of bacteriophage lambda is responsible for binding to Lamb, its receptor at the surface of Escherichia coli K-12. *J Bacteriol* **182**: 508-512
- Ward CA, Bazzazi H, Clark RB, Nygren A, Giles WR (2006) Actions of emigrated neutrophils on Na(+) and K(+) currents in rat ventricular myocytes. *Prog Biophys Mol Biol* **90**: 249-269
- Wegner A, Aktories K (1988) ADP-ribosylated actin caps the barbed ends of actin filaments. *J Biol Chem* **263**: 13739-13742
- Wei W, Lu Q, Chaudry GJ, Leppla SH, Cohen SN (2006) The LDL receptor-related protein LRP6 mediates internalization and lethality of anthrax toxin. *Cell* **124**: 1141-1154
- Wieggers W, Just I, Muller H, Hellwig A, Traub P, Aktories K (1991) Alteration of the cytoskeleton of mammalian cells cultured in vitro by Clostridium botulinum C2 toxin and C3 ADP-ribosyltransferase. *Eur J Cell Biol* **54**: 237-245
- Wohnsland F, Benz R (1997) 1/f-Noise of open bacterial porin channels. *J Membr Biol* **158**: 77-85
- Young JA, Collier RJ (2007) Anthrax toxin: receptor binding, internalization, pore formation, and translocation. *Annu Rev Biochem* **76**: 243-265
- Zakharov SD, Kotova EA, Antonenko YN, Cramer WA (2004) On the role of lipid in colicin pore formation. *Biochim Biophys Acta* **1666**: 239-249
- Zhang S, Cunningham K, Collier RJ (2004a) Anthrax protective antigen: efficiency of translocation is independent of the number of ligands bound to the prepore. *Biochemistry (Mosc)* **43**: 6339-6343
- Zhang S, Finkelstein A, Collier RJ (2004b) Evidence that translocation of anthrax toxin's lethal factor is initiated by entry of its N terminus into the protective antigen channel. *Proc Natl Acad Sci U S A* **101**: 16756-16761
- Zhang S, Udho E, Wu Z, Collier RJ, Finkelstein A (2004c) Protein translocation through anthrax toxin channels formed in planar lipid bilayers. *Biophys J* **87**: 3842-3849